

**IDENTIFICATION AND CHARACTERIZATION OF MICRORNAS
INVOLVED IN THE INVASION AND MIGRATION PROPERTIES
OF LUNG, PROSTATE AND BREAST CANCER CELLS**

YAP SEOW HUI

**FACULTY OF SCIENCE
UNIVERSITY OF MALAYA
KUALA LUMPUR**

2012

**IDENTIFICATION AND CHARACTERIZATION OF MICRORNAS
INVOLVED IN THE INVASION AND MIGRATION PROPERTIES
OF LUNG, PROSTATE AND BREAST CANCER CELLS**

YAP SEOW HUI

**DISSERTATION SUBMITTED IN FULFILLMENT OF
THE REQUIREMENTS FOR THE DEGREE OF
MASTER OF SCIENCE**

**INSTITUTE OF BIOLOGICAL SCIENCES
FACULTY OF SCIENCE
UNIVERSITY OF MALAYA
KUALA LUMPUR**

2012

UNIVERSITI MALAYA

ORIGINAL LITERARY WORK DECLARATION

Name of Candidate: Yap Seow Hui

(I.C/Passport No:861222-38-5052)

Registration/Matric No: SGR090095

Name of Degree: Master of Science

Title of Project Paper/Research Report/"Dissertation"/Thesis ("this Work"):

IDENTIFICATION AND CHARACTERIZATION OF MICRORNAS INVOLVED IN THE
INVASION AND MIGRATION PROPERTIES OF LUNG, PROSTATE AND BREAST
CANCER CELL LINES

Field of Study: Molecular Oncology

I do solemnly and sincerely declare that:

- 1) I am sole author/writer of this Work;
- 2) This Work is original;
- 3) Any use of any work in which copyright exist was done by way of fair dealing and for permitted purposes and any excerpt or extract from, or reference to or reproduction of any copyright work has been disclosed expressly and sufficiently and the title of the Work and its authorship have been acknowledge in this Work;
- 4) I do not have any actual knowledge nor do I ought reasonably to know that the making of this work constitutes an infringement of any copyright work;
- 5) I hereby assign all and every rights in the copyright to this Work to the University of Malaya ("UM"), who henceforth shall be owner of the copyright in this Work and that any reproduction or use in any form or by any means whatsoever is prohibited without the written consent of UM having been first had and obtained;
- 6) I am fully aware that if in the course of making this Work I have infringed any copyright whether intentionally or otherwise, I may be subjected to legal action or any other action as may be determined by UM

Candidate's Signature

Date 16.08.2012

Subscribed and solemnly declare before,

Witness's Signature

Date 16.08.2012

Name:

Designation:

Noor Hasima Bt. Nagoor PhD
Associate Professor
Division of Genetics & Molecular Biology
Institute of Biological Sciences
Faculty of Science
University of Malaya
50603 Kuala Lumpur, Malaysia

ABSTRACT

Primary cancer is often treatable by radiation therapy, chemotherapy or surgery, but tumour invasion and metastasis still remains the most challenging problem to cancer patients, causing death through organ damage or treatment complications. Past researches have focused on these issues, but no major breakthroughs have been achieved to prevent tumour metastasis. Dysregulation in the expression of short non-protein coding microRNAs (miRNAs) found contributes toward the initiation and progression of cancer through their capability to regulate multiple target genes. In this study, four pairs of high and low invasiveness sub-cell lines distinct in invasion and migration properties were established from their heterogeneous parental lung cancer cell line of A549, prostate cancer cell line of PC-3, breast cancer cell lines of MDA-MB-231 and MCF7 using serial transwell invasion approach. To gain insight into the molecular mechanisms that contribute to cancer migration and invasion, miRNA microarray was conducted on the three paired-sub cell lines of A549, PC-3 and MCF7. Lists of significant differentially expressed miRNAs between the three paired cell lines were identified and a subset of miRNAs from A549 was validated by Real-Time PCR. Through pathway enrichment analysis, a hypothetical pathway model describing A549 lung cancer metastasis was generated highlighting the network interaction of miRNAs and their gene targets. All these miRNAs act in concert in modulating three main pathways which were the non-canonical Wnt/planar cell polarity (PCP), transforming growth factor- β (TGF- β) and integrin signalling cascade to promote lung cancer migration and invasion. These results provide potential candidate metastatic markers for non-small cell lung cancer classification, prognosis and a possible therapeutic effect through targeting these miRNAs to control lung tumour invasion and metastasis.

ABSTRAK

Kanser primer selalunya boleh dirawat dengan terapi radiasi, kemoterapi atau pembedahan, namun invasif dan metastatik tumor tetap menjadi masalah yang paling mencabar untuk pesakit kanser, iaitu menyebabkan kematian melalui kerosakan organ atau komplikasi rawatan. Kajian-kajian terdahulu telah memberi tumpuan kepada isu-isu ini, tetapi tiada penemuan utama telah dicapai bagi mencegah berlakunya metastatik tumor. Deregulasi dalam ekspresi microRNAs (miRNAs), RNA yang tidak mengekod protein telah menyumbang kepada permulaan dan perkembangan kanser melalui keupayaan mereka untuk mengawal pelbagai gen sasaran. Dalam kajian ini, empat pasang sub-sel yang berbeza dalam tinggi dan rendah ciri invasif dan migrasi telah dihasilkan daripada induk heterogenus sel kanser paru-paru A549, sel kanser prostat PC-3, sel kanser payudara MDA-MB-231 dan MCF7 dengan menggunakan kaedah “serial transwell invasion”. Bagi mendapatkan maklumat tentang mekanisme molekul yang menyumbang kepada migrasi dan invasif kanser, “miRNA microarray” telah dijalankan ke atas tiga pasang sub sel iaitu A549, PC-3 dan MCF7. Senarai miRNAs yang jelas menyatakan perbezaan miRNAs di antara pasang sel dari tiga jenis kanser tersebut telah dikenalpasti dan subset miRNAs dari A549 telah disahkan oleh “Real-Time PCR”. Melalui analisis “enrichment pathway”, satu model laluan hipotesis yang menerangkan A549 metastatik kanser paru-paru dengan menunjukkan interaksi rangkaian miRNAs dan gen sasarannya telah dicadangkan. Semua miRNAs ini bertindak secara bersama dalam modulasi tiga laluan utama iaitu “non-canonical Wnt/planar cell polarity (PCP), transforming growth factor- β (TGF- β) and integrin signalling cascade” untuk menggalakkan migrasi dan invasif kanser paru-paru. Keputusan ini menunjukkan petanda calon metastatik yang berpotensi untuk mengklasifikasikan “non-small” kanser paru-paru, prognosis dan kemungkinan nilai

terapeutik dengan mensasarkan miRNA untuk mengkawal invasif tumor paru-paru dan berlakunya metastatik.

ACKNOWLEDGEMENT

This study was supported by the University of Malaya Postgraduate Research Grant (PPP - PS261-2010A and PV044-2011B) and the University of Malaya Research Grant (UMRG -RG037-10BIO). I would like to acknowledge Skim Biasiswa Universiti Malaya (SBUM) for financing two years of my living hood in Kuala Lumpur, allowing me to have no worries on any financial matters and be able to concentrate on my research.

First and foremost, I would like to take this opportunity to express my highest appreciation and gratitude to my supervisor, Associated Professor Dr Noor Hasima Nagoor for her continuous guidance and valuable advice throughout the study. I would also like to thank to the Postdoctoral research fellow, Dr. Lionel In Lian Aun, whose provided important guidance and knowledge in troubleshooting and data analysis.

I also like to express my deepest appreciation to all my labmates, Norahayu bt Othman, Phuah Neoh Hun, Yap Lim Hui, Mohammad Tasyriq Che Omar, Norhafiza bt Mohd Arshad, Noor Shahirah binti Suparji, Norain binti Ab Latif and Norliza bt. Shah Jehan Muttiah. They provided maximum guidance, sense of direction and sharing their valuable research experiences with me.

Besides that, I would like to take this opportunity to thank the Oral Cancer Research and Coordinating Centre (OCRCC) for provision of the Partek® Genomics Suite™ software for microarray analysis.

Lastly, I cannot finish without saying how grateful I am to my family who has given me a loving environment to develop and I wish to thank my parents for their constant support and encouragement in the past three years.

TABLE OF CONTENTS

Contents	Page No
Abstract	ii
Abstrak	iii
Acknowledgement	v
Table of contents	vi
List of Figures	xii
List of Tables	xvi
List of Abbreviation	xvii
Chapter 1: Introduction	1
1.1 Research Question	4
1.2 Hypothesis	4
1.3 Study Objectives	4
Chapter 2: Literature Review	5
2.1 Cancer Overview	5
2.2 Cancer Metastasis Overview	6
2.3 Cancer Metastasis Progression	8
2.3.1 Cancer Invasion and Epithelial-Mesenchymal Transition	9
2.3.2 Cancer Migration	11
2.3.3 Cancer Angiogenesis	13
2.4 Cancer Metastasis-Related Signalling Pathways	14
2.4.1 TGF- β Signalling Pathway	14
2.4.2 Wnt Signalling Pathway	17

	Contents	Page No
	2.4.2.1 Canonical Wnt Signalling Pathway	17
	2.4.2.2 Non-Canonical Wnt Signalling Pathway	19
	2.4.3 Integrin-FAK-Src Signalling Transduction	20
2.5	MicroRNA (miRNA)	24
	2.5.1 miRNA Biogenesis	25
2.6	MiRNAs and Cancer	26
2.7	MiRNAs and Cancer Metastasis	28
	2.7.1 Pro-Metastatic MiRNAs	29
	2.7.2 Anti-Metastatic MiRNAs	32
	2.7.3 MiRNAs and Epithelial-Mesenchymal Transition	33
	2.7.4 MiRNAs Modulate Cancer Angiogenesis	35
	Chapter 3: Methodology	37
3.1	Cancer Cell Cultures	37
	3.1.1 Cultivation of Cell Lines	37
	3.1.2 Preparation of Frozen Stocks	38
	3.1.3 Thawing of Cryopreserved Cells	38
	3.1.4 Trypan Blue Dye Exclusion Assay	39
3.2	Serial Selection of High and Low Invasiveness Sub-Cell Lines	39
3.3	Transwell Invasion Assay	40
3.4	Wound Healing Assay	41
3.5	Cell Proliferation Assay	42
3.6	Total RNA Extraction	42
3.7	RNA Quality Control	43
	3.7.1 Nanodrop Spectrophotometry	43

	Contents	Page No
	3.7.2 Agilent Bioanalyzer	44
3.8	MiRNA Microarray	45
	3.8.1 RNA Poly (A) Tailing and Labelling	45
	3.8.2 ELOSA QC Assay	46
	3.8.3 Hybridization of GeneChip® miRNA Arrays	48
	3.8.4 Array Washing, Staining and Scanning	49
	3.8.5 MiRNAs Expression Analysis	49
3.9	Quantitative Real-Time PCR (qPCR)	50
	3.9.1 Reverse Transcription	50
	3.9.2 Real-Time PCR Amplification	51
3.10	Pathway Enrichment Analysis	52
3.11	Statistical Analysis	53
	CHAPTER 4: RESULTS	54
4.1	Establishment of High and Low Invasiveness Cancer Sub-Cell Lines with Similar Proliferation Properties and Distinctly Different Invasion and Migration Attributes	54
	4.1.1 Serial Selection of High and Low Invasiveness Sub-Cell Lines	54
	4.1.2 Transwell Invasion Assay	55
	4.1.2.1 Transwell Invasion Assay of A549	56
	4.1.2.2 Transwell Invasion Assay of PC-3	57
	4.1.2.3 Transwell Invasion Assay of MCF7	58
	4.1.2.4 Transwell Invasion Assay of MDA-MB-231	59
	4.1.3 Wound Healing Assay	61
	4.1.3.1 Wound Healing Assay of A549	61

Contents		Page No
4.1.3.2	Wound Healing Assay of PC-3	62
4.1.3.3	Wound Healing Assay of MCF7	63
4.1.3.4	Wound Healing Assay of MDA-MB-231	65
4.1.4	Cell Proliferation Assay	67
4.1.4.1	Cell Proliferation Assay of A549	67
4.1.4.2	Cell Proliferation Assay of PC-3	68
4.1.4.3	Cell Proliferation Assay of MCF7	70
4.1.4.4	Cell Proliferation Assay of MDA-MB-231	71
4.2	Identification and Validation of Differentially Expressed Metastasis-Related MiRNAs	73
4.2.1	Total RNA Quality Control Using Agilent Bioanalyzer	73
4.2.2	MiRNA Microarray Analysis	76
4.2.2.1	MiRNA Microarray Analysis of A549	77
4.2.2.2	MiRNA Microarray Analysis of PC-3	79
4.2.2.3	MiRNA Microarray Analysis of MCF7	82
4.2.3	Quantitative Real-Time RT-PCR	85
4.2.3.1	Nanodrop Spectrophotometer	85
4.2.3.2	Pearson Correlation Plot	86
4.3	Predicted Targets of A549 Metastasis-Related MiRNAs Enriched in Metastasis-Related Signalling Pathways	87
4.3.1	Pathways Enrichment Analyses	87

Contents		Page No
CHAPTER 5: DISCUSSION		91
5.1	Hypothetical A549 Lung Cancer Metastasis Signalling Network Model	92
5.1.1	Metastasis-Related MiRNAs in Relation To Wnt/PCP Signalling Pathway	95
5.1.2	Metastasis-Related MiRNAs in Relation To TGF- β Signalling Pathway	99
5.1.3	Metastasis-Related MiRNAs in Relation To Integrin Signalling Pathway	102
5.1.4	Metastasis-Related MiRNAs in Relation To MAPK and mTOR Signalling Pathways	106
5.2	Future Perspectives	109
CHAPTER 6: CONCLUSION		112
REFERENCES		113
APPENDICES		129
Appendix 1	Solutions and Formulations	129
Appendix 1.1	Cell Culture	129
Appendix 1.2	Transwell Invasion Assay	130
Appendix 1.3	Wound Healing Assay	131
Appendix 1.4	MiRNA Microarray	131
Appendix 2	Commercial Kits	132
Appendix 3	Transwell Invasion Assay Data	133
Appendix 4	Wound Healing Assay Data	134

Contents		Page No
Appendix 5	Cell Proliferation Assay Data	136
	Appendix 5.1 Number of Viable Cells Data	136
	Appendix 5.2 Doubling Time Data	140
Appendix 6	Agilent Bioanalyzer Data	142
Appendix 7	MiRNA Microarray Data	143
Appendix 8	Real-Time PCR Data	147
Appendix 9	Target Prediction Data	150

LIST OF FIGURES

		Page No
Figure 2.1	Steps in the metastatic process.	8
Figure 2.2	Overview of the role of EMT in tumour metastasis.	9
Figure 2.3	Schematic diagram represented the major structures of the actin cytoskeleton in most of the migrating cell without a specific cell type.	11
Figure 2.4	A schematic of the cell migration.	12
Figure 2.5	Schematic diagram of canonical Smad-mediated TGF- β signalling pathway.	15
Figure 2.6	A schematic representation of the canonical Wnt signalling pathway.	17
Figure 2.7	A schematic representation of (A) the planar cell polarity (PCP) and (B) Wnt/Ca ²⁺ transduction cascade.	19
Figure 2.8	An illusion of the integrin-FAK-Src signal transduction cascade in regulating actin cytoskeletal reorganization and focal adhesion complex for cell migration and cell elongation.	21
Figure 2.9	Schematic representation of the formation of lamellipodia and filopodia.	22
Figure 2.10	Biogenesis and function of miRNAs.	25
Figure 3.1	An illustration of high and low invasiveness sub-cell line selection using serial transwell invasion assay	40
Figure 4.1	Diagram showing high (A549-I7, PC-3-I7, MCF7-I7 and MDA-MB-231-I7) and low (A549-NI7, PC-3-NI7, MCF7-NI7 and MDA-MB-231-NI7) invasiveness sub-cell lines were established from each parental cell lines of A549, PC-3, MCF7 and MDA-MB-231 using serial transwell invasion approach.	55
Figure 4.2	Representative cell fields of methylene blue stained invaded cells on the bottom membranes of Matrigel transwell invasion insert for A549-I7 and A549-NI7 at 200X magnification.	56
Figure 4.3	A bar graph represented the average invaded cells per field of A549-I7 and A549-NI7 with data presented as mean + SEM of three independent experiments with p-value <0.05.	56

Figure 4.4	Representative cell fields of methylene blue stained invaded cells on the bottom membranes of Matrigel transwell invasion insert for PC-3-I7 and PC-3-NI7 at 200X magnification.	57
Figure 4.5	A bar graph represents the average invaded cells per field of PC-3-I7 and PC-3-NI7 with data presented as mean \pm SEM from three independent experiments with p -value <0.05 .	57
Figure 4.6	Representative cell fields of methylene blue stained invaded cells on the bottom membranes of Matrigel transwell invasion insert for MCF7-I7 and MCF7-NI7 at 200X magnification.	58
Figure 4.7	A bar graph represents the average invaded cells per field of MCF7-I7 and MCF7-NI7 with data presented as mean \pm SEM from three independent experiments with p -value <0.05 .	59
Figure 4.8	Representative cell fields of methylene blue stained invaded cells on the bottom membranes of Matrigel transwell invasion insert for MDA-MB-231-I7 and MDA-MB-231-NI7 at 200X magnification.	59
Figure 4.9	A bar graph represents the average invaded cells per field of MDA-MB-231-I7 and MDA-MB-231-NI7 with data presented as mean \pm SEM from three independent experiments with p -value <0.05 .	60
Figure 4.10	Migration of A549-I7 and A549-NI7 cells into the wound were captured at 0 h and 28 h time at 100X magnification.	61
Figure 4.11	A bar chart represents the percentage of wound healing for A549-I7 and A549-NI7 with data presented as mean \pm SEM from four independent experiments.	62
Figure 4.12	Migrations of PC-3-I7 and PC-3-NI7 cells into the wound were captured at 0 h and 28 h time at 100X magnification.	62
Figure 4.13	A bar chart represents the percentage of wound healing for PC-3-I7 and PC-3-NI7 with data presented as mean \pm SEM from four independent experiments.	63
Figure 4.14	Migrations of MCF7-I7 and MCF7-NI7 cells into the wound were captured at 0 h and 23 h time at 100X magnification.	64
Figure 4.15	A bar chart represents the percentage of wound healing for MCF7-I7 and MCF7-NI7 with data presented as mean \pm SEM from four independent experiments.	64

Figure 4.16	Migrations of MDA-MB-231-I7 and MDA-MB-231-NI7 cells into the wound were captured at 0 h and 23 h time at 100X magnification.	65
Figure 4.17	A bar chart represents the percentage of wound healing for MDA-MB-231-I7 and MDA-MB-231-NI7 with data presented as mean \pm SEM from four independent experiments.	66
Figure 4.18	Cell proliferation curve for A549-I7, A549-NI7 and A549 over 7 days with number of viable cells on each day presented as mean + SEM from the three individual experiments.	67
Figure 4.19	A bar chart representing the doubling time (h) for A549-I7, A549-NI7 and A549 are presented as mean \pm SEM from the three individual experiments.	68
Figure 4.20	Cell proliferation curve for PC-3-I7, PC-3-NI7 and PC-3 over 7 days with number of viable cells on each day presented as mean + SEM from the three individual experiments.	69
Figure 4.21	A bar chart representing the doubling time (h) for PC-3-I7, PC-3-NI7 and PC-3 are presented as mean \pm SEM from the three individual experiments.	69
Figure 4.22	Cell proliferation curve for MCF7-I7, MCF7-NI7 and MCF7 over 7 days with number of viable cells on each day presented as mean \pm SEM from the three individual experiments.	70
Figure 4.23	A bar chart representing the doubling time (h) for MCF7-I7, MCF7-NI7 and MCF7 presented as mean \pm SEM from the three individual experiments.	71
Figure 4.24	Cell proliferation curve for MDA-MB-231-I7, MDA-MB-231-NI7 and MDA-MB-231 over 7 days with number of viable cells on each day presented as mean + SEM from the three individual experiments.	72
Figure 4.25	A bar chart representing the doubling time (h) for MDA-MB-231-I7, MDA-MB-231-NI7 and MDA-MB-231 are presented as mean + SEM from the three individual experiments.	72
Figure 4.26	Bioanalyzer analysis of extracted total RNA of four samples from high and low invasiveness sub-cell lines of PC-3, A549 and MCF7.	75

Figure 4.27	Three different plane views of PCA of A549-I7 (red) and A549-NI7 (blue) displayed the distribution of microarray data replicates.	78
Figure 4.28	Three different plane views of PCA of PC3-I7 (red) and PC3-NI7 (blue) displayed the distribution of microarray data replicates.	80
Figure 4.29	Three different plane views of PCA of MDA-MB-231-I7 (red) and MDA-MB-231-NI7 (blue) displayed the distribution of microarray data replicates.	83
Figure 4.30	Four differentially expressed miRNAs (miR-92b, miR-378, miR-671-5p and miR-1827) between A549-I7 and A549-NI7 validated using Real-Time PCR.	86
Figure 4.31	A pearson's correlation plot between miRNA microarray and Real-Time PCR data.	87
Figure 4.32	A hypothetical signalling network showing the interaction of miRNAs and their putative targets in regulating A549 lung cancer metastasis.	90
Figure 5.1	Illustration of hypothetical Wnt/PCP signalling pathway as regulated by a list of significantly expressed miRNAs.	95
Figure 5.2	Illustration of hypothetical TGF- β signalling pathway as regulated by a list of significantly expressed miRNAs.	99
Figure 5.3	Illustration of hypothetical integrin signalling pathway as regulated by a list of significantly expressed miRNAs.	102
Figure 5.4	Illustration of hypothetical MAPK and mTOR signalling pathways as regulated by a list of significantly expressed miRNAs.	106

LIST OF TABLES

		Page No
Table 3.1	Temperature and time for program for reverse transcription run.	51
Table 3.2	Thermal cycling condition for Real-Time PCR amplification step.	51
Table 4.1	RIN range (0.0 min. to 10.0 max.) of total RNAs extracted from high and low invasiveness sub-cell lines of PC-3, A549 and MCF7 using Agilent Bioanalyzer 2100 RNA 6000 Nano kit.	75
Table 4.2	Differentially expressed metastasis-related miRNAs between A549-I7 and A549-NI7 with p -value ≤ 0.05 and fold change ≥ 2.0 filtering using Partek [®] Genomics Suite [™] software.	79
Table 4.3	Differentially expressed metastasis-related miRNAs between PC-3-I7 and PC-3-NI7 with p -value ≤ 0.05 and fold change ≥ 2.0 filtering using Partek [®] Genomics Suite [™] software.	80
Table 4.4	Differentially expressed metastasis-related miRNAs between MCF7-I7 and MCF7-NI7 with p -value ≤ 0.05 and fold change ≥ 2.0 filtering using Partek [®] Genomics Suite [™] software.	84
Table 4.5	RNA concentration, absorbance and absorbance ratio of both A549-I7 and A549-NI7 using Nanodrop Spectrophotometer 2000 in three replicates.	85
Table 4.6	Top eight descending list of metastasis-related KEGG pathways that were predicted to be contribute in A549 cancer metastasis using the DIANA-mirPath algorithm employing DIANA-microT-4.0 as a prediction software with a $-\ln(p$ -value) threshold of ≥ 3.00 .	89

LIST OF ABBREVIATION

3' UTR	3' Untranslated Region
β -Pix	p21-Activated Kinase-Interacting Exchange Factor
Arp2/3	Actin-Related Protein-2/3
ATCC	American Type Culture Collection
Avg	Average
BCL2	B-Cell CLL/Lmphoma 2.
B-CLL	B-Cell Chronic Lymphocytic Leukaemia
bHLH	Basic Helix-Loop-Helix
BMP	Bone Morphogenetic Proteins
BRMS1	Breast Cancer Metastasis Suppressor 1
CaMKII	Calmodulin-Dependent Protein Kinase II
CO ₂	Carbon Dioxide
co-Smad	Common Mediated Smad
CTGF	Connective Tissue Growth Factor
Daam	Dishevelled-Associated Activator of Morphogenesis
DEPC	Diethyl Pyrocarbonate
DMEM	Dulbeco's Modified Eagle Medium
DMSO	Dimethyl Sulfoxide
Dvl	Disheveled
E-cadherin	Epithelial Cadherin
ECM	Extracellular Matrix
EDTA	Ethylenediaminetetraacetic acid
EGFR	Epidermal Growth Factor Receptor
EMT	Epithelial To Mesenchymal Transition
eNOS	Endothelial Nitric Oxide Synthase
Ezh2	Enhancer of Zeste Homolog 2
FBS	Fetal Bovine Serum
FOXO3	Forkhead Box O3
Fzd	Frizzled
GEF	Guanine Nucleotide Exchange Factor
GSK3- β	Glycogen Synthase Kinase 3 β
HCC	Hepatocellular Carcinomas
HER2	Human Epidermal Growth Factor Receptor 2
HGS	Hepatocyte Growth Factor-Regulated Tyrosine Kinase Substrate
HIF-1 α	Hypoxia-Inducible Factor 1 α
HMGA2	High Mobility Group A2
HOXD10	Homeobox 10
IRAK1	Interleukin 1 Receptor-Associated Kinase 1
IRSp53	Insulin-Receptor Substrate p53
I-Smad	Inhibitory Smads
JNK	C-Jun N-Terminal Kinases
KEGG	Kyoto Encyclopedia of Genes and Genomes
KITENIN	KAI1 C-Terminal Interacting Tetraspanin
Kny	Knypek

Lef	Lymphocyte Enhancer Factors
LIMK	LIM Kinase
LRP	Lipoprotein Receptor-Related Protein
MAPK	Mitogen-Activated Protein Kinase
mDia2	Formin Mammalian Diaphanous-2
MERTK	C-Mer Tyrosine Kinase
MET	Mesenchymal To Epithelial transition
MiRNA	MicroRNA
MITF	microphthalmia-associated transcription factor-M
MLCK	Myosin Light-Chain Kinase
MMP	Matrix Metalloproteinases
mRNA	Messenger RNAs
mTOR	Mammalian Target of Rapamycin
N-cadherin	Neural Cadherin
NCR	National Cancer Registry
NF- κ B	Nuclear Factor- κ B
NSCLC	Non-Small Cell Lung Cancer
N-WASP	Neural Wiskott-Aldrich Syndrome Protein
Pak	p21-Activated Kinase
PBS	Phosphate Buffered Saline
PCP	Planar Cell Polarity
PDCD4	Programmed Cell Death 4
PDGFR- β	Platelet-Derived Growth Factor Receptor β
PI3K	Phosphatidylinositol 3-Kinase
PIK3R2	Phosphoinositol-3 Kinase Regulatory Subunits 2
PKC	Protein Kinase C
pre-miRNA	Precursor microRNA
pri-miRNA	Primary microRNAs
PSA	Prostate Specific Antigen
PTEN	Phosphatase and Tensin Homolog
PTPRN2	Receptor Type Tyrosine Protein Phosphatase
qRT-PCR	Quantitative Real-Time RT-PCR
RhoA	Ras Homolog Gene Family, Member A
RISC	RNA-Inducing Silencing Complex
ROCK	Rho-Associated Protein Kinase
RPMI 1640	Roswell Park Memorial Institute 1640
R-Smad	Receptor-Regulated SMAD.
SCF	Stem Cell Factor
SCLC	Small Cell Lung Cancer
SDS	Sodium Dodecyl Sulfate Polyacrylamide
SEM	Standard Error Mean
SFK	Src Family Kinase
sFRP	Secreted Frizzled-Related Proteins
siRNA	Small-Interfering RNA
Smurf1	Smad Ubiquitin Regulatory Factors 1
SOX4	SRY-Box Containing Transcription Factor

SPRED1	Sprouty-Related Protein 1
SuFu	Suppressor of Fused Homolog
Std Dev	Standard Deviation
Tcf	T-Cell Factor
TGF- β	Transforming Growth Factor- β
TGF- β -RI	Transforming Growth Factor- β Type I Receptor
TGF- β -RII	Transforming Growth Factor- β Type II Receptor
TIMP3	Tropomyosin 1 and Tissue Inhibitor of Metalloprotease-3
TNC	Tenascin C
TRAF6	Tumor Necrosis Factor Receptor-Associated Factor 6
Tsp1	Adhesive Glycoprotein Thrombospondin 1
uPA	Urokinase Plasminogen Activator
VANGL1	Vangl1 (Van Gogh, Drosophila)-Like 1
VEGF-A	Vascular Endothelial Growth Factor A
VEGFR2	Vascular Endothelial Growth Factor Receptor 2
WASP	Wiskott-Aldrich Syndrome Protein
WAVE	Wiskott-Aldrich Syndrome Protein Family Verprolin-Homologous Protein
ZEB	Zinc Finger E-box Binding Homeobox

CHAPTER 1: INTRODUCTION

The three cancer types focused in this study are lung, breast and prostate as worldwide, lung cancer is the leading cause of cancer-related-deaths in males and second in females. Additionally breast cancer is the most common cancer type among females and prostate cancer is second among males (Kamangar *et al.*, 2006; Jemal *et al.*, 2011). Cancer metastasis is a complex, multiple-step processes that involved tumour cells to dislodge, spread and proliferate at distant sites from the primary tumour. The major cause of cancer related deaths in cancer patients is commonly attributed to its ability to metastasize to distant organs that causes organ damage or treatment complications. To date, the mechanism in which cancer metastasizes and relapses is still poorly understood (Bracken *et al.*, 2009; Xia and Hu, 2010).

The process of migration, a hallmark of cell invasion, involves a complex interaction between proteins from transmembrane receptors to transcription factors, which triggers multiple-step cellular signalling events ranging from morphological changes to focal adhesion dynamics, actomyosin polymerization and contraction (Friedl and Bröcker, 2000). Among the signalling events commonly involved in cancer cell migration includes the integrin-FAK-Src signalling complex which regulates metastatic cells to loosen its extracellular matrix (ECM) adhesion and Rho-GTPases superfamily signalling proteins that play a significant role in the re-organization of the actin cytoskeleton to form filopodia, lamellipodia and stress fibers (Nobes and Hall, 1995; Hood and Cheresch, 2002). The epithelial to mesenchymal transition (EMT) is another essential in promoting tumour metastasis by causing the disruption of cell-cell adherence, matrix remodelling, increased motility and invasiveness. These process is regulated by signalling pathways of transforming growth factor- β (TGF- β), Wnt,

integrin, nuclear factor- κ B (NF- κ B), phosphatidylinositol 3-kinase (PI3K)/AKT and Notch pathway (Jing *et al.*, 2011).

MicroRNAs (miRNAs) are short non-protein-coding RNAs of approximately 18 to 24 nucleotides that post-transcriptionally regulate gene expression involved in various biological processes, including development, cell proliferation, differentiation and apoptosis (Hwang and Mendell, 2006). MiRNAs are particularly attractive candidates as upstream regulators of tumorigenesis and metastasis because they post-transcriptionally regulate numerous target genes, thereby potentially enabling their intervention at multiple steps of the invasion-metastasis cascade (Bracken *et al.*, 2009; Valastyan *et al.*, 2009). Past studies have shown that dysregulation in miRNA expression is associated with cancer which contributes toward tumour development including malignant transformation, angiogenesis and tumour metastasis (Du and Pertsemidid, 2010). Recently, numerous studies have demonstrated that miRNAs such as miR-10b, miR-335, miR-126, miR-206, miR-373, miR-520c and miR-21 all play an important role in cancer cell invasion, migration and metastasis, where miR-10b acts as a pro-metastatic miRNA, while miR-335, miR-126 and miR-206 acts as anti-metastatic miRNAs (Ma *et al.*, 2007; Tavazoie *et al.*, 2008; Huang *et al.*, 2008; Zhu *et al.*, 2008).

Even though past studies have focused on issues revolving cancer metastasis, no major breakthroughs have been reported to prevent tumour metastasis. In order to elucidate the miRNAs required for the migration and invasion of metastatic cancers, comparative studies on the biological characteristics and genetic profiles between cancer cell variants possessing different degrees of migration and invasion properties were conducted. Malignant tumours are typically composed of heterogeneous cells with different phenotypic properties, with only a sub-population of cells possessing invasive and metastatic properties (Spremluli and Dexter, 1983; Gupta and Massagué, 2006). In this study, serial transwell invasion approach were employed to establish four pairs of

high and low invasiveness sub-cell lines that varies in invasion and migration properties from A549 lung cancer cell line, PC-3 prostate cancer cell line and MCF7 and MDA-MB-231 breast cancer cell lines from each heterogeneous parental cancer cell lines. This was followed by miRNA microarray, quantitative Real-Time PCR validation and pathway enrichment analysis to highlight how the differentially expressed miRNA between sub-cell lines act in concert in modulating metastasis-related pathways for invasion and migration of cancer metastasis.

1.1 Research Question

Since molecular mechanisms of common cancer types like lung, prostate and breast cancer metastasis still remain poorly understood, it is important to investigate on the miRNAs that contribute to the invasion and migration properties of these cancer types.

1.2 Hypothesis

The differentially expressed miRNAs between the high and low invasiveness sub-cell lines have potential in regulating migration and invasion for cancer metastasis.

1.3 Study Objectives

- 1) To investigate the miRNA(s) involved in the invasive and migration properties of lung, prostate and breast cancer.
- 2) To establish high and low invasiveness sub-cell lines from each heterogeneous parental cell lines of A549, PC-3, MCF7 and MDA-MB-231 using serial transwell invasion approach.
- 3) To identify the differences in miRNAs expression profile between high and low invasiveness sub-cell lines using microRNA microarrays and validated using quantitative Real-Time PCR approach.
- 4) To highlight the mechanism of differentially expressed miRNAs that act in concert in modulating metastasis-related pathways for the process of invasion and migration of cancer metastasis.
- 5) To propose candidate cancer metastatic markers.

CHAPTER 2: LITERATURE REVIEW

2.1 Cancer Overview

Cancer is featured by uncontrolled cell proliferation and inappropriate survival of damaged cells or mutated cells resulting in tumour formation and able to gain ability to develop progressively and metastasize to other parts of the body through the blood and lymph (Yu *et al.*, 2007; Tlsty and Coussens, 2006). Cancer can affect everybody and is the second highest killer after cardiovascular diseases in Malaysia (Chuah *et al.*, 2006).

Cancer is the leading cause of death worldwide. Kamangar *et al.* (2006) reported that an estimated 11 million cancer incidences and 7 million cancer deaths occur worldwide, and about 25 million individuals were living with cancer (Kamangar *et al.*, 2006). A total of 21,773 cancer cases comprising of 9,974 males and 11,799 females were diagnosed among Malaysians in Peninsular Malaysia according to the National Cancer Registry (NCR) in 2006. Cancer is a rising health problem and can occur at all ages. Breast, colorectal, lung, cervix and nasopharynx cancer are the five most common cancer among the population in 2006 (Zainal *et al.*, 2006). In this study, three cancer types of lung, prostate, breast cancer were focused and reviewed in this literature review.

Lung cancer. Globally, lung cancer is the most commonly diagnosed cancer and is the leading cause of cancer-related-death, accounting for 1,179,074 cancer deaths per year (Kamangar *et al.*, 2006). In year 2002, it was estimated that 1.35 million new cases of lung cancer occurred in the world and 1.18 million deaths (Parkin *et al.*, 2005). In Peninsular Malaysia, lung cancer is the second most frequent cancer type among males and the third most common cancer among populations. In year 2006, a total of 2,048 new cases of lung cancer were registered with NCR in Peninsular Malaysia with 1,445 being males and 603 females (Zainal *et al.*, 2006).

Prostate cancer. In worldwide, prostate cancer is second most common cancer type in men and fifth most common cancer type among populations. It was estimated that 679,000 new prostate cancer cases was diagnosed and 221,000 deaths in the year 2002 (Parkin *et al.*, 2005). In Peninsular Malaysia, prostate cancer is the fourth most common cancer among male where 735 new cases of prostate cancer were reported by NCR in year 2006 (Zainal *et al.*, 2006).

Breast cancer. Worldwide, breast cancer is the most common cancer type among females, with an estimated 1,152,161 new cases and 411,093 deaths per year (Kamangar *et al.*, 2006). NCR reported that breast cancer is the most common diagnosed cancer type among women in Peninsular Malaysia. 3,525 female breast cancer cases was registered in the year 2006 and accounted for 16.5% of all cancer cases registered (Zainal *et al.*, 2006).

2.2 Cancer Metastasis Overview

Metastasis is the most common cause of death for cancer patients and may occur through organ damage or treatment complications (Bracken *et al.*, 2009).

Lung Cancer. Lung cancer can be classified histologically into small cell lung cancer (SCLC) and non-small cell lung cancer (NSCLC). NSCLC accounts for 85% of lung cancer patients and two-third of these patients were diagnosed at late stages when the cancer has undergone local or distant metastasis, hence reducing the likelihood of curative surgery (Berghmans, 2011). Lung cancer are commonly metastasize to brain, bone, and adrenals. Patient with untreated brain metastases have a median survival of 1 month and this can be prolonged by another 1 month if treated with steroid and 3-8 months with radiotherapy (Lagerwaard *et al.*, 1999). The fact that metastasis accounted for high lung cancer mortality rates was further supported in a recent study indicating an overall poor prognosis in 313 patients with NSCLC and concurrent distant metastasis

with 45%, 48%, 12% 4% and 0% for 1-, 2-, 3-, 4- and 5- year survival rates respectively (Ma *et al.*, 2006).

Prostate Cancer. Despite advancement of early prostate cancer detection via prostate specific antigen (PSA) based screening, about 20% of patient presented with metastatic at the time of diagnoses and metastasis is the major contributor of morbidity and mortality (Moul, 2000; Siddiqui *et al.*, 2004). An autopsy study of 1,589 patients with prostate cancer done by Bubendorf *et al.* (2000) found 35% of patients detected with hematogeneous metastases where bone was most frequent organ detected with metastases, followed by liver, pleura and adrenals. Bone metastatic prostate is associated with various complications such as marrow failure, spinal cord compression and skeletal morbidity which later reduce the patient mobility and ultimately cause death (Saad *et al.*, 2006). Prostate cancer treatment by blocking androgen receptors offers a temporary regression of advance prostate cancer, but it often progress into androgen independent metastatic stage in an approximately 18–36 months later (Baldi *et al.*, 2003).

Breast Cancer. Primary breast cancers are often treatable by surgery or radiotherapy, but relapse and metastatic spread can still occur at distant sites that leads to fatal disease (Bracken *et al.*, 2009). Breast cancer often first spreads through the lymphatics involving the regional lymph nodes such as the axillary nodes and commonly metastasized to lung, liver and bones for advance breast cancer. Regional lymph node status is one of the most important prognostic factors in breast cancer where the prognosis of breast cancer decrease as the number of tumour-positive lymph nodes increases (Cunnick *et al.*, 2008). The prognosis of patients with liver metastasis is poor with only 16-25 months with chemotherapy (Pentheroudakis *et al.*, 2006; Er *et al.*, 2008).

2.3 Cancer Metastasis Progression

Uncontrolled cell proliferation and angiogenesis are hallmarks of the initiation and early growth of primary cancers (Kalluri and Weinberg, 2009).

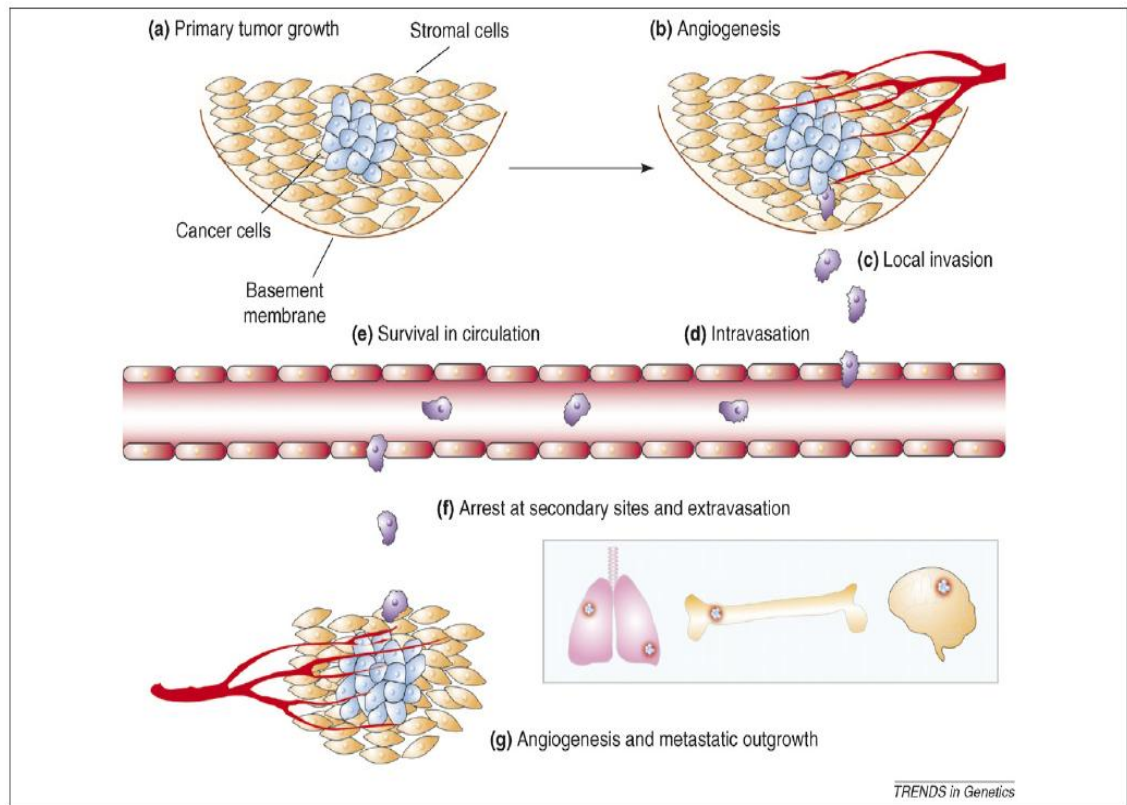


Figure 2.1: Steps in the metastatic process (adapted from Ma and Weinberg, 2008).

Cancer metastasis is a complex sequential process by which primary tumour cells spread and grow at a secondary site. Cancer metastasis initially occurs with detachment of cancer cells from their neighbour cells. Cells then migrate and undergo local invasion through the basement membrane. Subsequently, metastatic cells intravasate to the blood circulation either directly or via the lymphatic system and survive in the circulatory system. Size constraints the cells attached to the vascular endothelium at a distant organ site (e.g. the lungs, bone or brain) or to the subendothelial basement membrane, tumour cells can then extravasate into the foreign tissue microenvironment. These cells may remain dormant or may proliferate and

stimulate blood vessel growth stimulation (angiogenesis) to allow micrometastases growth into macroscopic secondary tumours that are clinically detectable (Figure 2.1) (Ma and Weinberg, 2008; Bracken *et al.*, 2009).

2.3.1 Cancer Invasion and Epithelial-Mesenchymal Transition

Cancer cells changing its adhesive ability, gain migratory and invasive capabilities by involving dynamic reorganization of actin cytoskeleton through formation of membrane protrusions, leading to the mesenchymal phenotype (Yilmaz and Christofi, 2009).

Cadherins, a transmembrane glycoprotein regulate the interactions between cells through extracellular domain, whilst its intracellular domain mediates signalling to the actin cytoskeleton (Halbleib and Nelson, 2006). Epithelial (E)-cadherin is expressed on epithelial cells and is important in mediating cell-cell and cell-matrix adhesion. While the expression of Neural (N)-cadherin on cancer cells form contact between cancer cell-endothelial wall, this activates Src-kinases activity to promote transendothelial migration (Ramis-Conde *et al.*, 2009).

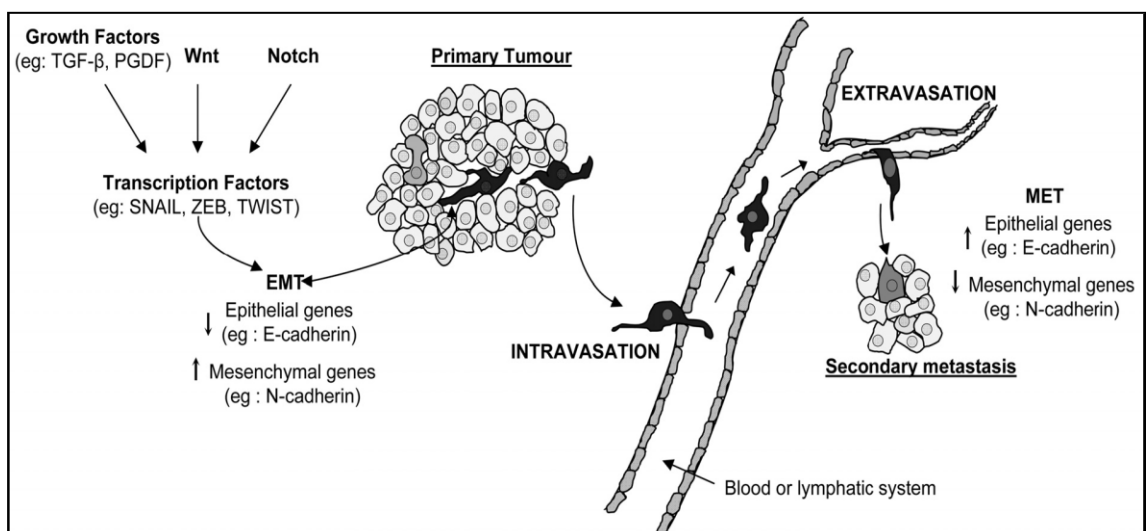


Figure 2.2: Overview of the role of EMT in tumour metastasis (adapted from Bracken *et al.*, 2009).

Cell invasion is the initial step of cancer metastasis where tumour cells lose contact with the neighboring cells in primary tumour and migration through the ECM and basement membrane. EMT program has been proposed as the vital mechanism for epithelial cancer cells acquire invasion and migration of malignant phenotypes (Yilmaz and Christofi, 2009). Loss of cell-cell adherence by EMT program is characterized by reduced E-cadherin and up-regulated N-cadherin, which also known as “cadherin switch” (Araki *et al.*, 2011). The sequential event of EMT can be triggered by many transcription factors such as snail1, zinc finger E-box binding homeobox (ZEB) and TWIST families that regulate actin cytoskeletal remodelling and ECM protein degradation by ECM-degrading proteases for examples matrix metalloproteinases (MMPs) and urokinase plasminogen activator (uPA). Actin cytoskeleton remodelling together with ECM degradation allow cell invasion into surrounding stroma and intravasation into the blood or lymphatic circulation. The cell is being carried away and extravasation to regional lymph nodes or distant organs. Later, a reversal event known as mesenchymal-epithelial transition (MET) with increased in expression of epithelial-specific gene and repressed expression of mesenchymal-specific gene, thus leading to the formation of macroscopic metastases with epithelial characteristic at secondary site (Figure 2.2) (Bracken *et al.*, 2009; Dykxhoorn *et al.*, 2009; Baranwal and Alahari, 2010).

2.3.2 Cancer Migration

Cell migration is vital during tumour invasion and metastasis progression (Stetler-Stevenson *et al.*, 1993).

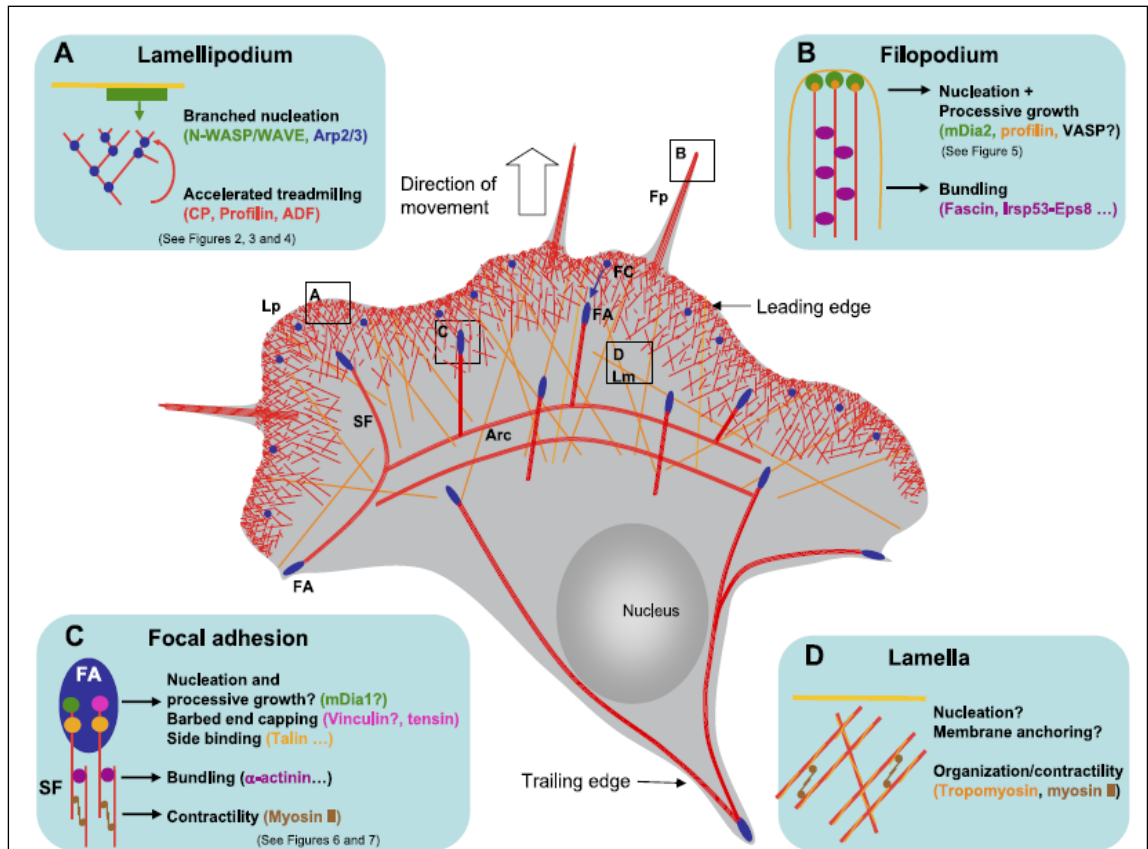


Figure 2.3: Schematic diagram represented the major structures of the actin cytoskeleton in most of the migrating cell without a specific cell type (adapted from Le Clainche and Carlier, 2008).

In Figure 2.3, a schematic diagram represented the major structures (A) lamellipodium, (B) filopodium, (C) focal adhesion and (D) lamella of the actin cytoskeleton of a migrating cell (Le Clainche and Carlier, 2008). The migration mechanisms of tumour cells employ for spreading are similar to migration processes of normal cells such as embryonic morphogenesis, inflammatory immune responses, wound healing, and angiogenesis (Friedl and Bröcker, 2000).

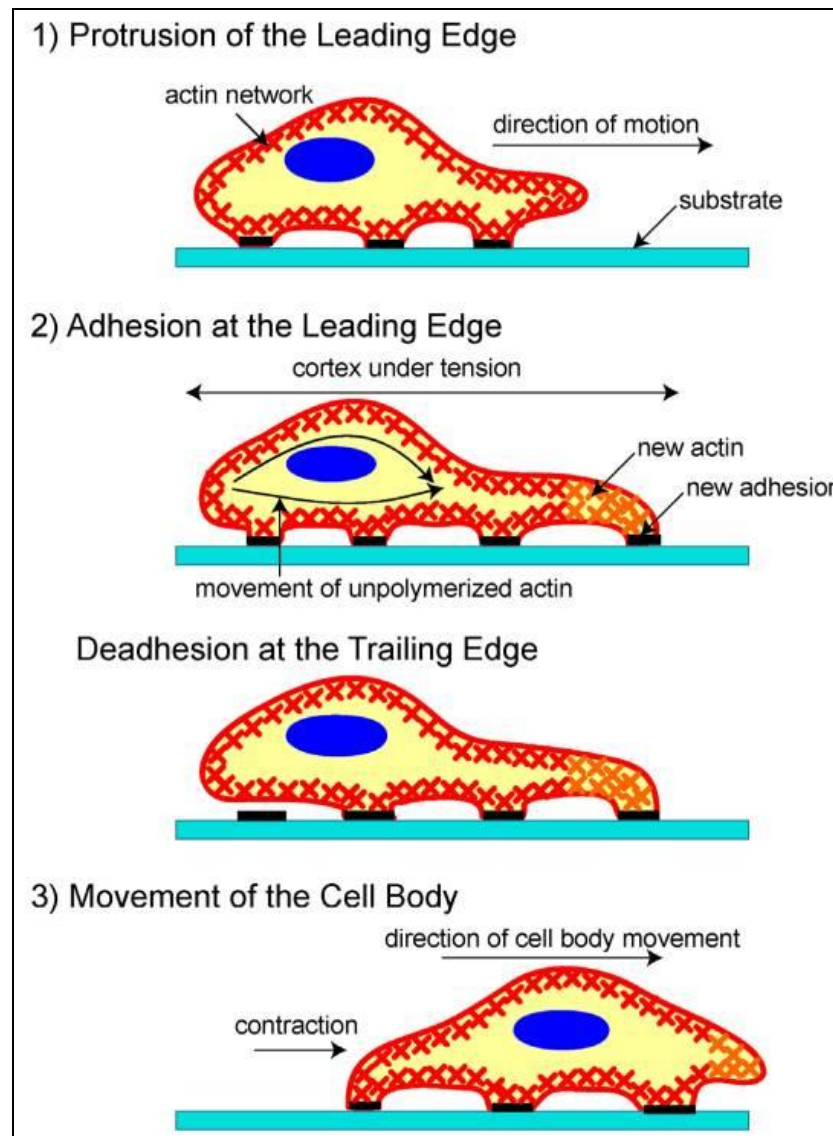


Figure 2.4: A schematic diagram of cell migration (adapted from Ananthakrishnan and Ehrlincher, 2007).

In Figure 2.4, a combination of cellular events lead to dynamic actin cytoskeleton reorganization for a cell to migrate. First, cell polarized and elongated with extending protrusions in the direction of migration (also known as leading edge) in respond to migration-promoting agent. The spike-like filopodia or large and broad lamellipodia protrusions at leading edge are driven by actin polymerization and stabilized by adhering to extracellular matrix or adjacent cells via transmembrane receptors that linked to actin cytoskeleton. Subsequently, forward extension of lamellipodium by adhering to the surface of leading edge, while de-adhesion at the cell body and retraction of the rear end (also known as trailing edge) resulting in a net

translocation of the cell in the direction of the movement. In addition, actin filaments must be disassembled at the rear end, so that actin monomers can be replenished for further polymerization at the leading edge (Ridley *et al.*, 2003; Pollard and Borisy, 2003; Ananthakrishnan and Ehrlicher, 2007; Ding *et al.*, 2008).

2.3.3 Cancer Angiogenesis

Tumour cell must arrest within the blood or lymphatic system through breaking local cell-cell adhesion and invasion into the surrounding stroma to metastasize. This process is further enhanced by angiogenesis which allows tumour continued growth at primary site, thus providing access to the blood or lymphatic circulation. After intravasation into circulation, tumour cells must withstand the mechanical stress in the dynamic circulation and some are able to arrest in capillary bed of distant organs by adhering to the endothelial cell surfaces or exposed subendothelial basement membrane and then extravasate into the tissue at the secondary site. These small metastasized cells are called micrometastases. These cells need to induce angiogenesis for vessel formation to get enough oxygen, nutrient and growth factor supply in order to survive and grow at secondary site (Bracken *et al.*, 2009).

2.4 Cancer Metastasis-Related Signalling Pathways

Multiple signalling molecules such as adhesion receptors, tyrosine kinases, cytoskeleton proteins, adapters and downstream signalling protein molecules interaction in signal transduction to regulate cancer migration and invasion (Bozzuto *et al.*, 2010). Multiple signalling pathways including TGF- β , Wnt, integrin, NF- κ B, PI3K/AKT, Notch and others were reported to regulate EMT in tumour microenvironment (Larue and Bellacosa, 2005; Jing *et al.*, 2011). Recently, Scheel and colleagues demonstrated TGF- β , canonical and noncanonical Wnt signalling interaction to induce activation of the EMT program and thereafter function in an autocrine fashion to maintain cells in mesenchymal state (Scheel *et al.*, 2011). Only the three signalling pathways of TGF- β , Wnt and integrin signalling pathways are discussed in the following literature review.

2.4.1 TGF- β Signalling Pathway

TGF- β signalling pathway plays dual role in tumour progression. TGF- β exerts anti-proliferative effects on normal cells and early stage of tumour. As tumour develop or during late tumour stage, cancer cells start to promote cancer invasion and metastasis through regulating EMT, neoangiogenesis and escaping from immune surveillance (Jeon and Jen, 2010). Inhibition of TGF- β and TGF- β receptor has been shown to suppress metastasis, which indicates the involvement of TGF- β signalling pathway in cancer metastasis (Bandyopadhyay *et al.*, 2006; Biswas *et al.*, 2007).

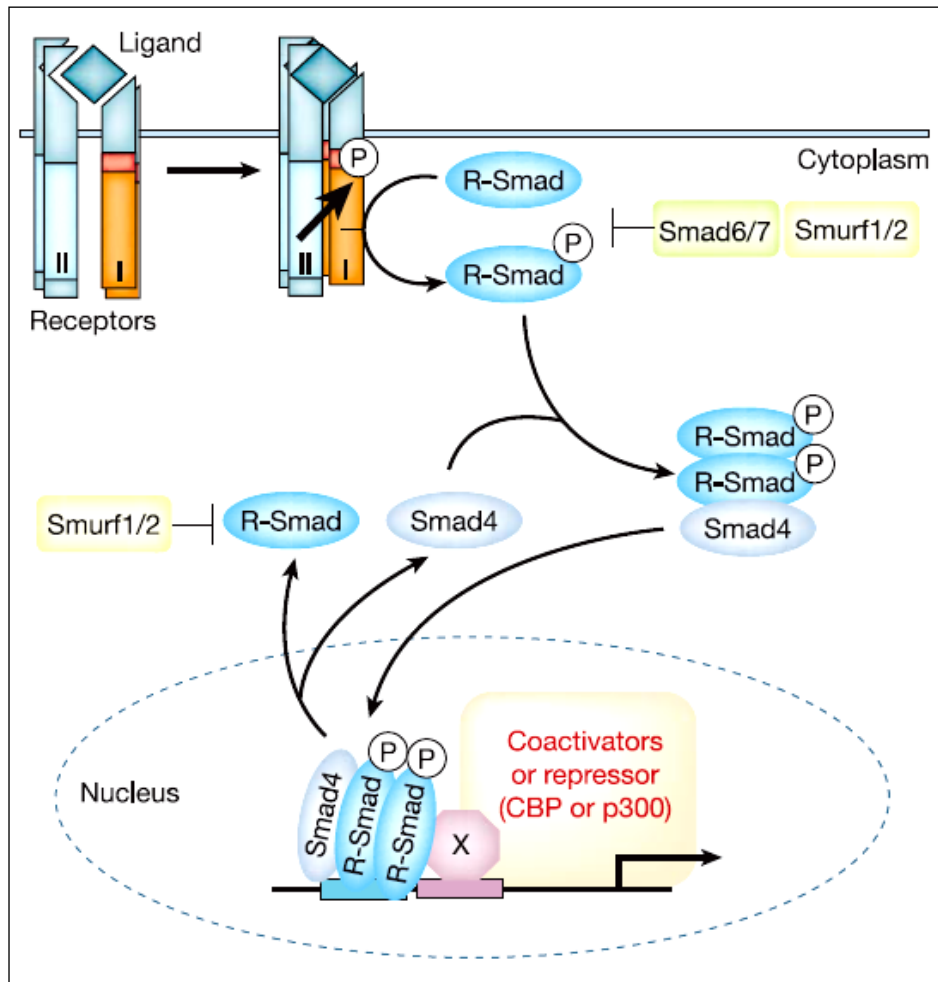


Figure 2.5: Schematic diagram of canonical Smad-mediated TGF- β signalling pathway (adapted from Derynck and Zhang, 2003).

TGF- β ligands superfamily of TGF- β , activins, nodals, and bone morphogenetic proteins (BMP) play role in regulate tissue homeostasis and tumour proliferation, differentiation, and survival (Kato *et al.*, 2002). In Figure 2.5, canonical Smad-mediated TGF- β signalling pathway is initiated when TGF- β ligand binding to TGF- β type II receptor (TGF- β -RII) leads to type I receptor (TGF- β -RI) employment and phosphorylation. This lead to activation of TGF- β -RII kinase domain in the cytoplasm which can then phosphorylates receptor-regulated Smad proteins (R-Smad), Smad2 and Smad3. Activated phosphorylated Smad2 and Smad3 form heteromeric complexes with Smad4, the common mediated Smad (co-Smad), then translocate into the nucleus to regulate a diverse array of genes transcription (Derynck and Zhang, 2003; Jeon and Jen, 2010).

Since TGF- β play an important role in regulate normal cellular homoeostasis, therefore a number of feedback mechanisms to maintain appropriate TGF- β signalling activation. TGF- β signalling is subjected to negative feedback by two inhibitory Smads (I-Smad), Smad6 and Smad7 which can inhibit Smad2/3 phosphorylation by interaction with TGF- β receptor (Hayashi *et al.*, 1997; Imamura *et al.*, 1997; Jeon and Jen, 2010). Smad7 also inhibits the Smad-mediated TGF- β signalling through the recruitment of Smad ubiquitin regulatory factors 1 (Smurf1) and 2 (Smurf2). Smurf1 and Smurf2 induce ubiquitination and degradation of Smad2 and TGF- β family receptors (Ebisawa *et al.*, 2001; Zhang *et al.*, 2001; Jeon and Jen, 2010). In addition, TGF- β ligands also activate non-Smad mediated TGF- β signalling pathways including MAP kinase (MAPK) pathways, Rho-like GTPase signalling pathways and phosphatidylinositol-3-kinase (PI3K)/AKT pathways (Zhang, 2009).

Levy and Hill (2006) reviewed that altered expression of TGF- β components such as ligands, TGF- β -RI, TGF- β -RII, Smad and antagonists of the Smad-mediated TGF- β signalling pathway were associated with various type of cancer tumourigenesis and metastasis (Levy and Hill, 2006). For example, inhibition of TGF- β signalling suppressing cancer metastasis was observed when Smad3 expression down-regulated or defective TGF- β -RI. This suggest an involvement of the canonical Smad-mediated TGF- β signalling pathway in tumour invasion and metastatic spreading (Tian *et al.*, 2003; Tian *et al.*, 2004). Also, constitutive activation of TGF- β or TGF- β -RII were reported to promote EMT and cancer metastasis (Muraoka-Cook *et al.*, 2004; Siegel *et al.*, 2003).

2.4.2 Wnt Signalling Pathway

Wnt signalling pathway plays important role in cell fate specification, cell migration, cell polarity, neural patterning and organogenesis during embryonic development. There are three intra-cellular signal transduction cascades can be activated by extracellular Wnt ligands: (i) canonical pathway and non-canonical pathways consist of (ii) planar cell polarity (PCP) and (iii) Wnt/Ca²⁺ pathway (Habas and Dawid, 2005; Komiya and Habas, 2008).

2.4.2.1 Canonical Wnt Signalling Pathway

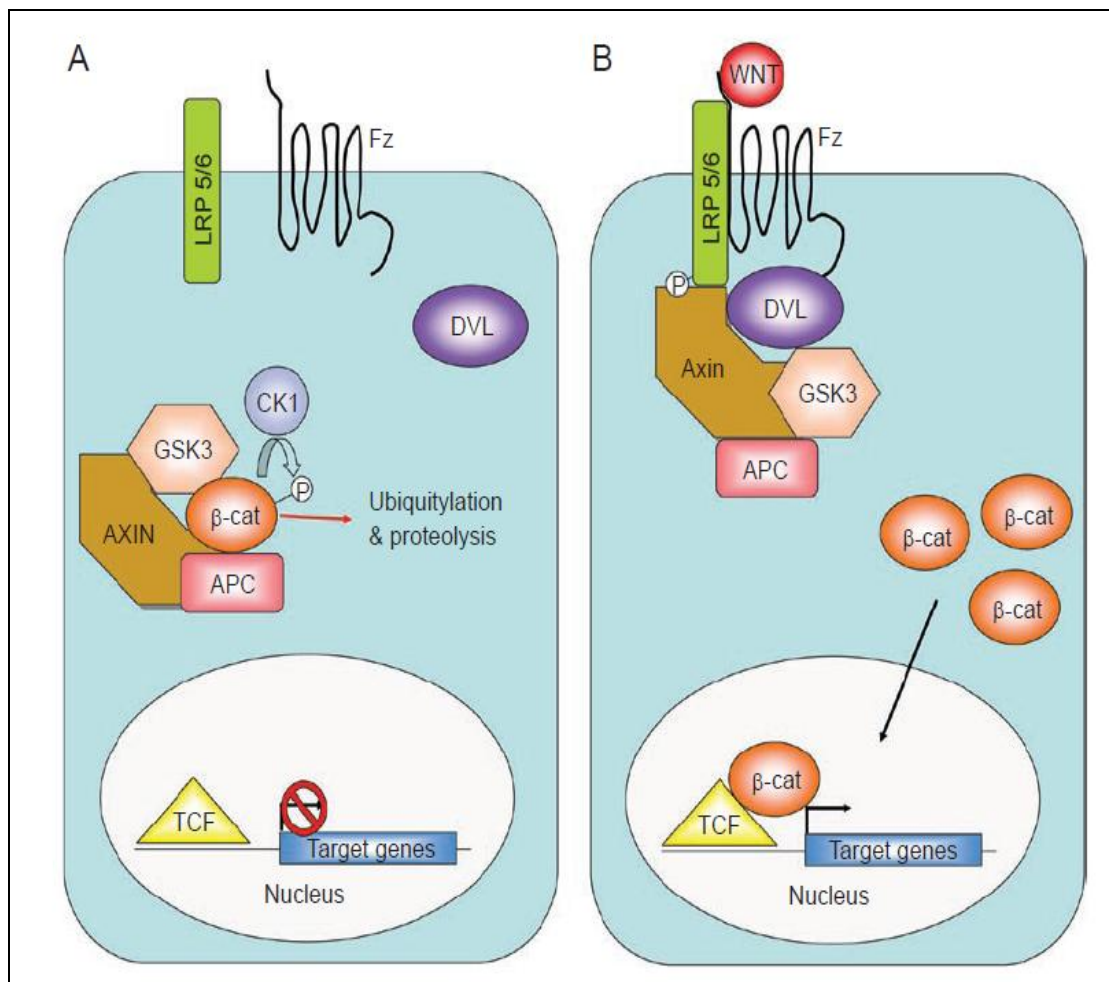


Figure 2.6: A schematic representation of the canonical Wnt signalling pathway (adapted from Lai *et al.*, 2009).

The canonical or Wnt/ β -catenin dependent signalling pathway regulates cell fate and proliferation. β -catenin gets phosphorylated and targeted for ubiquitination and degradation by the proteasome when complexed with APC, axin and glycogen synthase kinase 3 β (GSK3- β) in the absence of Wnt ligands binding (Figure 2.6A). In Figure 2.6B, disheveled (Dvl for vertebrate/DSH for fly) activated upon Wnt ligand binding to transmembrane frizzled (Fz or Fzd) receptor and co-receptors lipoprotein receptor-related protein 5 and 6 (LRP5/6). This prevents β -catenin from degraded by the destruction complex. β -catenin subsequently translocates into the nucleus and associates with T-cell factor/lymphocyte enhancer factors (Tcf/Lef) to form a transcriptional complex to activate downstream target genes expression (Komiya and Habas, 2008; Lai *et al.*, 2009). Previous research found that involvement of Wnt canonical pathway in regulating proliferation and invasion of lung cancer cells when axin down-regulates TCF-4 transcription via β -catenin (Yang *et al.*, 2010).

2.4.2.2 Non-Canonical Wnt Signalling Pathway

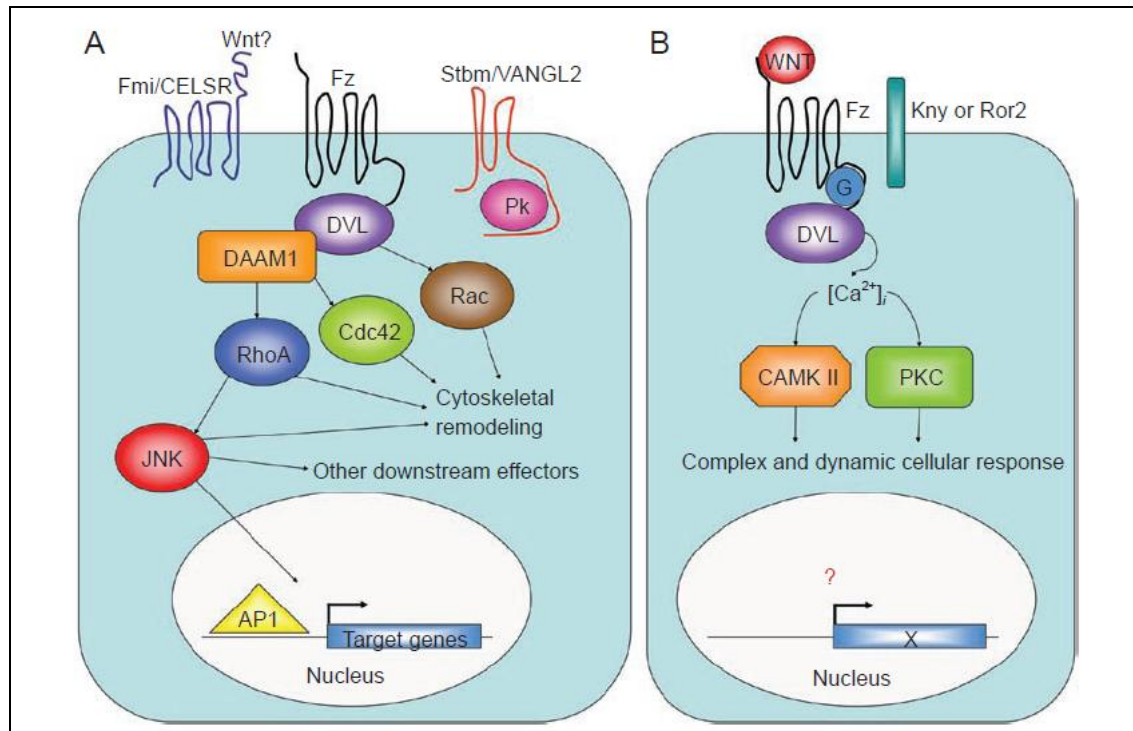


Figure 2.7: A schematic representation of (A) the PCP and (B) Wnt/Ca²⁺ transduction cascade (adapted from Lai *et al.*, 2009).

Figure 2.7A, the PCP signalling pathway is transduced when non-canonical-Wnt ligand (Wnt-5a, Wnt-5b and Wnt-11) bind to Frizzled receptor (Fzd3 or Fzd6) leading to the recruitment of cytoplasmic scaffold protein of Dvl to the plasma membrane. Dishevelled-associated activator of morphogenesis 1 (Daam1) binds with Dvl and mediates activation of ras homolog gene family, member A (RhoA) which in turn activates Rho-associated protein kinase (ROCK). Daam1 also interact with Profilin to mediate actin polymerization in response to Wnt signal. In addition, Dvl mediates activation of Rac, which in turn activates c-Jun N-terminal kinases (JNK). Collectively, signal transduction cascade from ROCK, JNK and Profilin promote dynamic cytoskeleton alteration for cell polarization and migration (Komiya and Habas, 2008; Lai *et al.*, 2009).

In Figure 2.7B, activation of the Wnt/Ca²⁺ transduction cascade when interaction of Wnt ligand with Fzd and co-receptor Knypek (Kny) or Ror2 increases intracellular calcium level and subsequently activates calcium/calmodulin-dependent protein kinase II (CaMKII) and protein kinase C (PKC). Wnt/Ca²⁺ pathway has also been reported to play a crucial role in cell adhesion and mobility during gastrulation (Lai *et al.*, 2009).

Numerous studies have shown that aberrant activation of the canonical and non-canonical Wnt pathway promote cancer development and metastasis progression (Lee *et al.*, 2008; Wang, 2009). For example, the non-canonical Wnt ligand, Wnt-5A, is involved in cancer progression and Wnt-5A over-expression has been found to be associated with aggressive tumour biology, increases cancer invasiveness and migration (Weeraratna *et al.*, 2002; Kurayoshi *et al.*, 2006; Pukrop and Binder, 2008).

2.4.3 Integrin-FAK-Src Signalling Transduction

A complex interaction between extracellular matrix, transmembrane receptors, kinases, adapter proteins and other downstream signalling molecules triggers cell morphological changes to regulate cell migration (Friedl and Brocker, 2000). Integrin-focal adhesion kinase (FAK)-Src signalling transduction plays a role in regulating cancer metastatic cells by loosen cell-ECM adhesion and promoting cell invasion and migration (Hood and Cheresch, 2002).

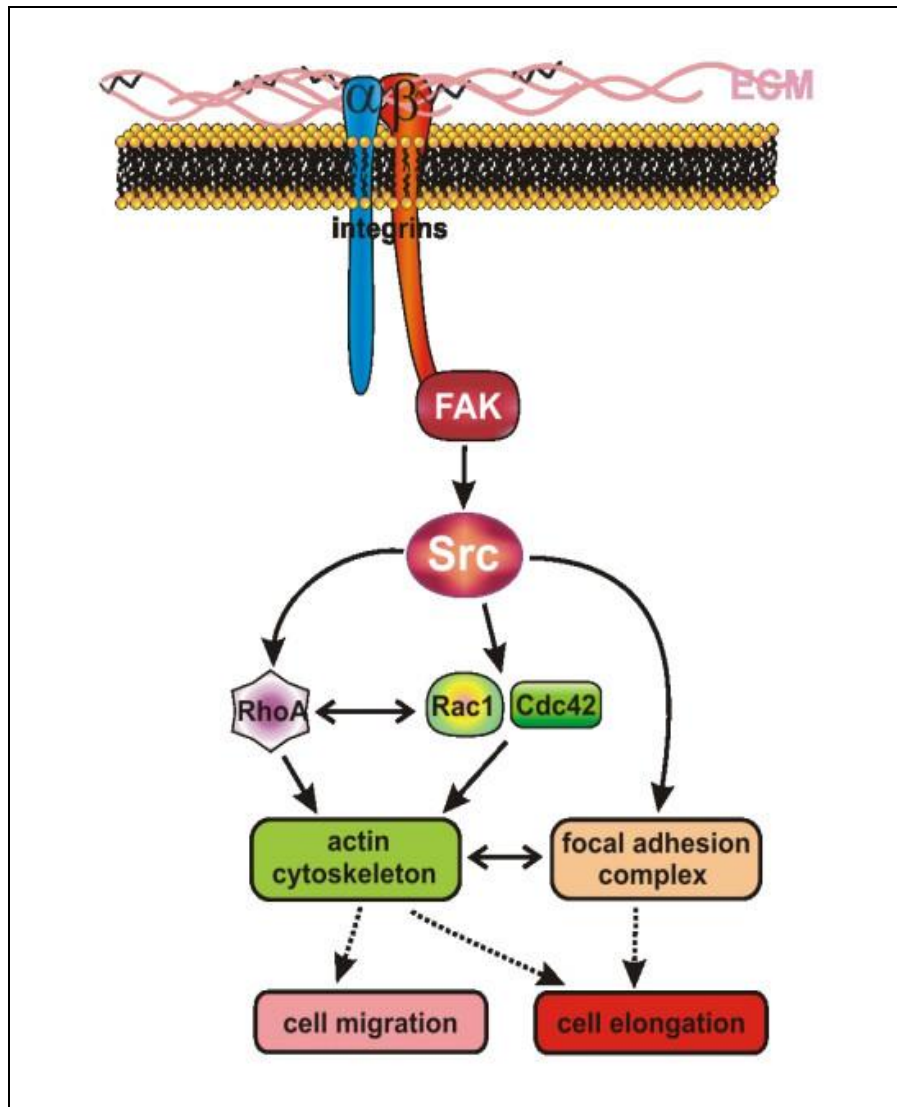


Figure 2.8: An illustration of the integrin-FAK-Src signal transduction cascade in regulating actin cytoskeletal reorganization and focal adhesion complex for cell migration and cell elongation (adapted from Schneider *et al.*, 2008).

Integrin function in tethering cell to the ECM, but activation of integrin induces recruitment of FAK and Src protein tyrosine kinase to trigger integrin-FAK-Src intracellular transduction cascades via multiple downstream proteins including the Rho GTPases superfamily proteins (such as Cdc42, Rac and RhoA) that play a significant role in the reorganization of the actin cytoskeleton to acquire a migratory and invasive phenotype (Figure 2.8) (Hood and Cheresch, 2002; Schneider *et al.*, 2008). During cell movement, Cdc42 mediates formation of long, thin, actin-containing extensions called filopodia; Rac mediates formation of curtain-like extensions called lamellipodia and ruffles; whereas RhoA activation regulates formation of stress fibers (also known as

acto-myosin filaments) and focal adhesion of cells to induce retraction of the trailing edge (Nobes and Hall, 1995).

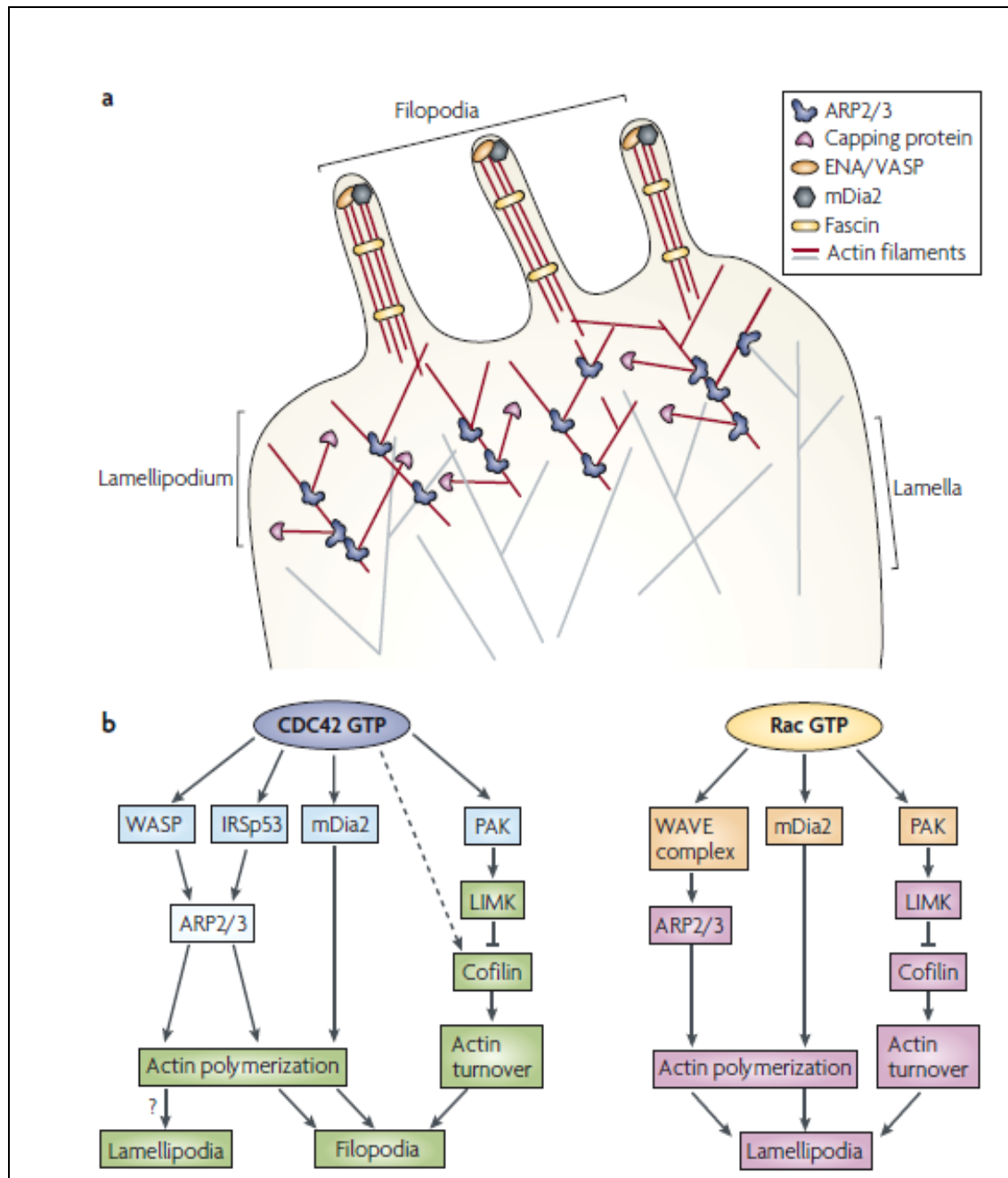


Figure 2.9: Schematic representation of the formation of lamellipodia and filopodia (adapted from Heasman and Ridley, 2008).

In Figure 2.9A, a network of branched actin filaments formation with new actin filaments extended from the sides of existing filaments at the leading edge of the cell. During lamellipodium formation, Rac signal transduction activates downstream WAVE-Arp2/3 [(Wiskott–Aldrich syndrome protein (WASP)-family verprolin-homologous protein)-(actin-related protein-2/3)] complex machinery that lead to actin polymerization. The possibly involvement of mDia2 (formin mammalian diaphanous-2), which nucleates unbranched actin filaments in actin polymerization process. Extension of actin filaments were terminated when capping proteins bind to the barbed ends. The lamella is located behind the lamellipodium which has longer and less branched actin filaments. Filopodia are thin fingerlike protrusions with non-branched parallel of actin filaments that are bundled together beyond the leading edge of lamellipodia of migratory cells. Filopodia were proposed to have possible function as sensory antenna toward environment or cell-cell contacts establishment (Heasman and Ridley, 2008).

In Figure 2.9B, Cdc42 bind to WASP, the related Neural (N)-WASP, or through the insulin-receptor substrate p53 (IRSp53) tyrosine kinase with Arp2/3 complex to induce branched actin filaments polymerization. Rac activates Arp2/3 complex through the WAVE complex. The contribution of these to filopodium protrusion is unknown. MDia2 activation by Cdc42 and Rac also trigger actin polymerization. In addition, the activation of Paks (p21-activated kinases), Pak1-3, the family of Ser/Thr protein kinases are one of the important downstream effectors of Rac and Cdc42. Paks then transphosphorylates and activates downstream LIM kinase (LIMK), which phosphorylates and inhibits cofilin, thus regulating actin-filament turnover (Heasman and Ridley, 2008).

Integrin signalling transduction cascade has been implicated in cancers and metastasis progression. A study done by Mizejewski (1999) showed a signature expression of integrins in malignant tumours compared with pre-neoplastic tumours. Strong expression of integrin $\alpha\beta3$ were reported in high metastatic human melanoma cells and ectopic expression of integrin $\beta3$ subunit increases metastatic potential of melanoma cell line, this suggested that integrin play a role in invasive and metastatic cancer properties (Gehlsen *et al.*, 1992; Filardo *et al.*, 1995). Also, increase evidences of Rho GTPases family influence a variety of processes in cancer, including cell transformation, survival, invasion, metastasis, and angiogenesis (Espina *et al.*, 2008). Furthermore, Fak, the downstream signalling molecule of integrin signalling is associated with cancer metastasis where high Fak expression was observed in metastatic cancer (Cance *et al.*, 2000).

2.5 MicroRNA (miRNA)

Cancer is a complex genetic disease involving structural and expression abnormalities of genes with the accumulation of genomic alterations that activate oncogenes and inactivate tumour suppressors. A large number of cancer susceptibility genes have been identified in a variety of cancers in the past four decades. The discovery of genes that produce non-protein coding RNA transcript, known as microRNAs (miRNAs). Involvement of miRNAs in cancer pathogenesis have increased the genomic complexity of cancer cells in the past few years which might give a better understanding of tumorigenesis (Calin and Carlo, 2006; Yu *et al.*, 2007).

2.5.1 MicroRNA Biogenesis

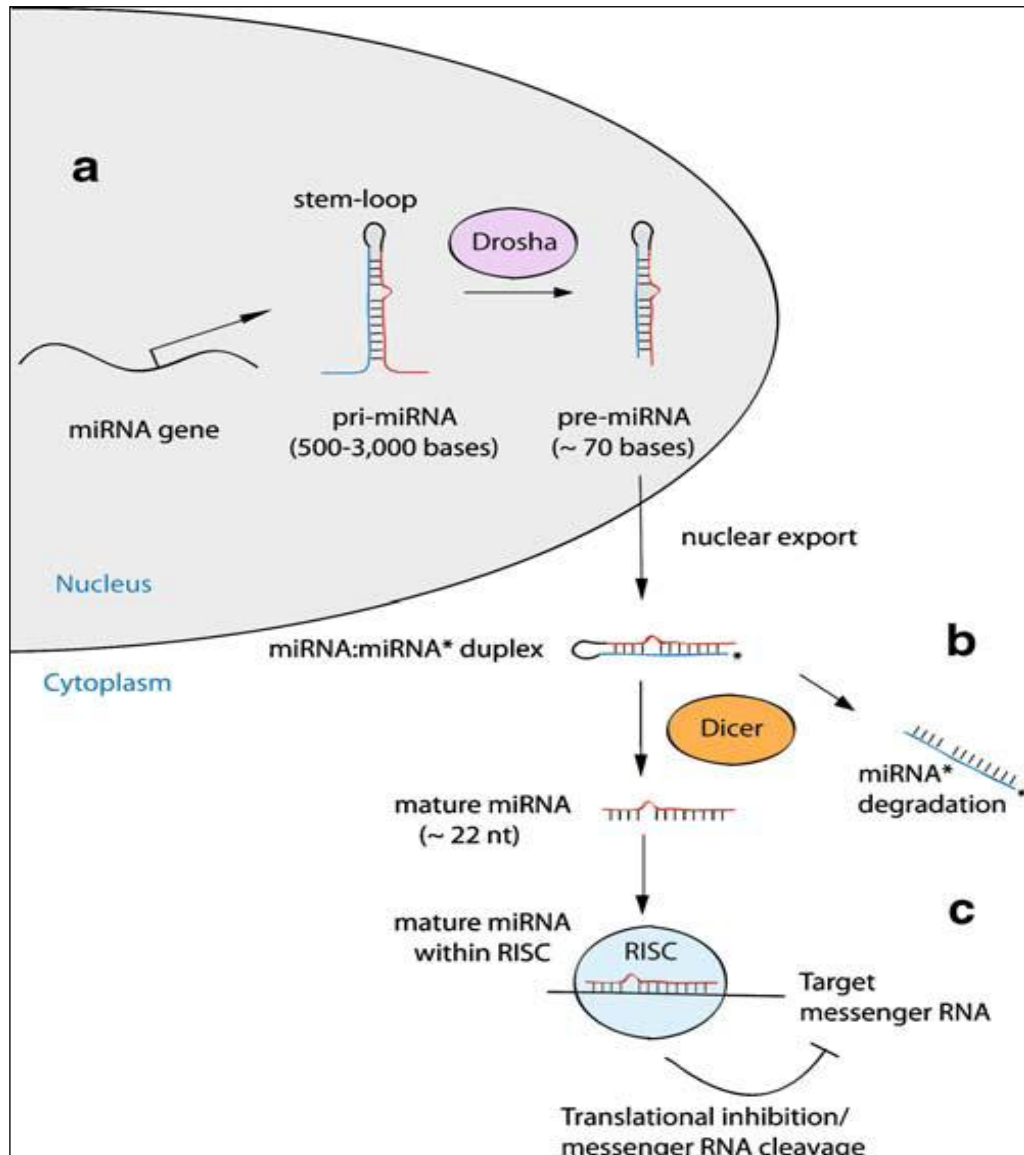


Figure 2.10: Biogenesis and function of miRNAs (adapted from Sassen *et al.*, 2008).

MiRNAs are short non-protein-coding RNAs of 20-22 nucleotides that post-transcriptionally regulate gene expression. Primary miRNAs (pri-miRNA) are long transcripts with hundred to thousand of nucleotides transcribed by RNA polymerase II before capping and polyadenylation. In Figure 2.10, pri-miRNA, which contains one or more stem-loop structures of about 60 to 100 nucleotides, are then excised by type III ribonuclease (Drosha) into precursor miRNA (pre-miRNA) in the nucleus. Pre-miRNA is exported into the cytoplasm and subsequently cleaved by the ribonuclease Dicer to generate a short RNA duplex (miRNA: miRNA*). The single stranded mature miRNA

(also known as guided strand) regulate gene expression in a sequence-specific fashion by incorporating it into an RNA-inducing silencing complex (RISC), while the miRNA* (also known as passenger strand or complementary strand) is generally degraded immediately. This mature miRNA binds to the 3' untranslated region (3' UTR) of target messenger RNAs (mRNAs) through imperfect complementarity with the seed sequence. Seed sequence is the bases 2 to 8 at the 5' end of the mature miRNA, which defines miRNA families and is important for proper target recognition. The binding of miRNA to the 3' UTR of mRNA causes inhibition of mRNA translation and impairs the stability of the mRNA, leading to a reduction in protein expression levels (Calin and Croce, 2006; Sassen *et al.*, 2008; Nicoloso *et al.*, 2009).

Computational target prediction algorithms have been developed to identify putative mRNA targets based on the seed sequence of miRNA to search for complementary sequences in the 3'-UTRs of known genes that exhibit conservation across species. Due to the imperfect base pairing by miRNA, each miRNA is estimated to potentially target up to 200 mRNA targets and estimated to regulate up to one third of the human protein coding gene expression and potential regulators of many signalling pathways (Lewis *et al.*, 2005; Yu *et al.*, 2007; Heneghan *et al.*, 2009).

2.6 MiRNAs and Cancer

MiRNAs have been shown to be involved in diverse biological processes, including development, cell proliferation, differentiation and apoptosis by simultaneously controlling the expression levels of hundreds of genes (Wu *et al.*, 2007). Emerging data indicate that dysregulation of miRNAs were associated with certain types of cancer and also alteration in miRNA expression is likely to contribute to the initiation and progression of human cancer (Gregory and Shiekhattar, 2005; Sassen *et al.*, 2008).

MiRNAs can affect tumourigenesis due to their ability to suppress target gene expression through base-pairing interactions with their target mRNAs. Some miRNAs can function as oncogenes. When a gene encoding a miRNA that targets one or more tumour suppressor genes is over-expressed, genomic amplification, or loses epigenetic silencing, tumourigenesis will be enhanced. By contrast, a miRNA act as a tumour suppressor when the situation above is the same except that the target of miRNA is an oncogene. The deletion in gene copy number or epigenetic silencing of a miRNA that functions to suppress the expression of oncogene(s) might allow the target mRNA and protein expression to increase and gain oncogenic potency. Mutations at the seed sequence of the mature miRNA could reduce or eliminate binding to key targets or even severely change its specificity for binding to the right targets, thereby altering the balance of genes and proteins expression for normal biological processes and thus lead to tumourigenesis (Venture and Jacks, 2009).

The abnormal expression levels of miRNAs in tumours have important pathogenetic consequences. MiRNAs that are over-expressed in tumours generally function as oncogenes by exerting pro-oncogenesis effects by inhibiting key tumour suppressors. For example, the miR-17-92 cluster, located at the genomic regions amplified in lymphomas, promotes tumourigenesis by inhibiting tumour suppressor E2F1 transcription factor. Also, miR-21 represses the tumour suppressor phosphatase and tensin homolog (PTEN) in hepatocellular carcinoma (HCC). MiRNAs deleted or down-regulated in tumours generally participate in oncogene over-expression. For example, the down-regulation of tumour suppressor miRNA, let-7 in lung cancer allow the over-expression of its target oncogenes such as KRAS, NRAS, high mobility group A2 (HMGA2) and MYC. Besides that, down-regulation of tumour suppressor genes of miR-15a–miR-16-1 cluster allow for the expression of B-cell CLL/lymphoma 2

(BCL2), an anti-apoptotic gene in B-cell chronic lymphocytic leukaemia (B-CLL) (Bracken *et al.*, 2009; Nicoloso *et al.*, 2009).

MiRNA-expression profiling of human tumours provide a remarkable ability to distinguish tumour from normal tissue. This revealed a list of specific miRNA signatures associated with cancer diagnosis, staging, progression, metastasis, prognosis, survival rates and response to treatment. This may be of particular benefit for the diagnosis of cancers of histologically uncertain origin, where miRNA profiling may be of greater significance than mRNA profiling in the ability to diagnose the origin (Calin and Croce, 2006; Bracken *et al.*, 2009).

2.7 MiRNAs and Cancer Metastasis

MiRNA was first recognized to play a role in human cancer in 2006. Following that, many studies have indicated that miRNA target multiple proteins that are essential for various signalling pathways (Nicoloso *et al.*, 2009). The ability of miRNAs post-transcriptionally regulate various target genes enabling them interference at multiple steps of the invasion metastasis cascade. Therefore, miRNAs are particularly attractive candidates as upstream regulators of tumourigenesis and metastasis (Bracken *et al.* 2009).

Multiple miRNAs that are associated with metastasis and poor prognosis have been identified through miRNA profiling or functional studies. MiRNA regulates metastasis-associated genes that are vital in tumour invasion and metastasis through inhibitory process. Metastasis-associated miRNAs is grouped into pro-metastatic miRNA and anti-metastatic miRNA. A pro-metastatic miRNA targets and inhibits metastasis-suppressor genes, thus promoting cancer metastasis, whilst an anti-metastatic miRNA suppresses metastasis-promoting genes, hence demoteing cancer metastasis (Zhang *et al.*, 2010).

2.7.1 Pro-Metastatic MiRNAs

miR-10b. miR-10b was first discovered by Ma and colleagues (2007) as a pro-metastatic miRNA. miR-10b was highly expressed in metastatic cells and potentially regulates cell migration and invasion of breast tumour. miR-10b was ectopically over-expressed in non-invasive breast cells to explore the ability to drive metastasis. The result showed that extopic expression of miR-10b allowed non-invasive cells to gain invasion and metastatic properties *in vitro* and *in vivo* without affecting the viability or proliferation properties.

Homeobox 10 (HOXD10), a transcription factor that is associated with cell migration and ECM remodeling was validated as a target of miR-10b. Down-regulation of HOXD10, by over-expression of miR-10b, led to de-repression of the downstream HOXD10 target RhoC, a pro-metastatic Rho-family GTPase. Thereby, through repression of HOXD10, miR-10b promotes RhoC expression and, hence, promotes metastasis. This is shown clinically in metastatic free patient with reduced expression of miR-10b, whilst increased expression is noted in 50% of patient with metastasis. These findings represent the first functional evidence that over-expression of a miRNA can contribute to tumour invasion and metastasis (Ma *et al.*, 2007).

Later in 2010, Ma and colleagues published another paper that demonstrated tumour-bearing mice treated systemically with miR-10b antagomirs able to suppress breast cancer metastasis. Silencing of miR-10b with antagomirs significantly reduced miR-10b levels and increased the levels of HOXD10 in both *in vitro* and *in vivo*. Administration of miR-10b antagomirs to mice bearing highly metastatic cells do not have effect on the growth of the primary tumour but significantly suppresses lung metastasis. As a result, miR-10b antagomir appears to be a potential candidate for the development of new anti-metastasis agents as it is well tolerated by normal animals.

miR-373 and miR-520c. Huang and colleagues (2008) revealed both miR-373 and miR-520c did not affect cell proliferation, but promoted MCF7 cells migration *in vitro*. By introducing MCF7 cells with miR-373 or over-expressing miR-520c in nude mice, these miRNAs were found to increase *in vivo* metastasis with formation of secondary tumours in bone, brain and lung, whilst the parental MCF7 cells failed to form metastases. CD44 adhesion molecule was found to be the common target of miR-373 and miR-520c (Huang *et al.*, 2008; Yang *et al.*, 2009). Moreover, miR-373 as a metastasis-associated miRNA was further supported by clinical breast cancer data where miR-373 is over-expressed and inversely correlated with CD44 expression in breast carcinomas, especially in those with lymph node metastasis (Huang *et al.*, 2008). In another lab, miR-373 was identified as an oncogene in testicular germ-cell tumours that promoted cellular proliferation and tumourigenesis but not metastasis (Voorhoeve *et al.*, 2006; Zhang *et al.*, 2010).

miR-21. Multiple independent studies have indicated a direct link to the over-expression of miR-21 with an increase in cancer metastasis by down-regulating several metastasis suppressor gene expression that encoded programmed cell death 4 (PDCD4), maspin, phosphate and tensin homolog (PTEN), tropomyosin 1 and tissue inhibitor of metalloprotease-3 (TIMP3). These genes act as suppressors in neoplastic transformation, cell motility and invasiveness (Meng *et al.*, 2007; Asangani *et al.*, 2008; Frankel *et al.*, 2008; Gabriely *et al.*, 2008; Lu *et al.*, 2008; Zhu *et al.*, 2008). In addition, Huang and colleagues (2009) reported that miR-21 is associated with up-regulation of human epidermal growth factor receptor 2 (HER2)/neu and is functionally involved in HER2/neu-induced breast cancer cell invasion. In addition, a significant correlation between the expression of miR-21 with advanced clinical stage, metastasis and poor prognosis in tumours were observed (Krichevsky and Gabriely, 2009).

miR-182. Comparison between normal melanocytes and melanoma cell lines expression profiles revealed over-expressed miR-182 as a pro-metastatic miRNA in melanoma cell lines. Over-expression of miR-182 induces migration and metastasis of melanoma cells *in vitro* and *in vivo* by directly repressing microphthalmia-associated transcription factor-M (MITF) and forkhead box O3 (FOXO3). In contrast, down-regulation of miR-182 suppress invasion and induce apoptosis, thus silencing miR-182 could be a therapeutic strategy for melanoma (Segura *et al.*, 2009; Baranwal and Alahari, 2010, Zhang *et al.*, 2010).

miR-9. miR-9 is a pro-metastatic miRNA that targets mRNA encoding E-cadherin, a key metastasis-suppressing protein that plays a vital role in tumour migration and invasion. Animal model study showed that over-expression of miR-9 in non-metastatic breast tumour cells allowed the cells to gain ability to metastasize, whilst suppression of miR-9 expression causes the highly malignant cells to lost its metastatic ability (Ma *et al.*, 2010). Later, Zhu and colleagues (2011) demonstrated participation of miR-9 in regulating metastatic process of colorectal cancer (CRC) though promoting cell migration. Recently, miR-9 was identified to inhibit melanoma proliferation and metastasis through inhibition of NF- κ B-Snail1 pathway by up-regulation of E-cadherin (Liu *et al.*, 2012).

2.7.2 Anti-Metastatic MiRNAs

miR-335, miR-126 and miR-206. Tavazoie *et al.* (2008) identified three lower expression miRNAs, miR-335, miR-126 and miR-206 in both metastatic breast cell lines and metastases. Restoration of these miRNAs expression in metastatic MDA-MB-231 cells not only decreased cell migration and invasion *in vitro* but also significantly decreased the number of metastases in mouse model. SRY-box containing transcription factor (SOX4), tenascin C (TNC), receptor-type tyrosine protein phosphatase (PTPRN2) and c-Mer tyrosine kinase (MERTK) are the set of genes regulated by miR-335 and is associated with distal metastasis risk. Furthermore, patients with primary breast cancer expressing low levels of miR-335, miR-206 and miR-126 were associated with metastatic relapse (Bracken *et al.*, 2009). Recently, the expression of miR-206 was inversely associated with invasion and metastatic capacities of lung cancer (Wang *et al.*, 2011).

miR-146a/b. A reduction in MDA-MB-231 breast cancer cell line metastatic capacity was seen when expression of miR-146a and miR-146b suppressed NF- κ B through repression of interleukin 1 receptor-associated kinase 1 (IRAK1) and tumor necrosis factor receptor-associated factor 6 (TRAF6) (Bhaumik *et al.*, 2008). Hurst and coworkers (2009) showed that miR-146 expression regulated by breast cancer metastasis suppressor 1 (BRMS1) inhibit breast cancer metastasis through NF- κ B pathway. Ectopic expression of miR-146a or miR-146b in MDA-MB-231 inhibiting invasion and migration *in vitro* as well as lung metastasis *in vivo* through suppression of epidermal growth factor receptor (EGFR) expression.

miR-183. Wang and coworkers (2008) identified miR-183 as a negative regulator of lung cancer metastasis through screening on low and high metastatic lung cancer cell lines using miRNA array. Ectopic expression of miR-183 in highly metastatic cells could inhibit cell migration and invasion of lung cancer cells. Ezrin, a

well established gene that mediating cell migration and metastasis through controlling the actin cytoskeleton, cell adhesion and motility was confirmed as a target gene of miR-183 by luciferase reporter gene assay.

miR-205. Invasion of breast cancer and esophageal squamous cell carcinoma (ESCC) was modulated by miR-205. A significant lower expression of miR-205 in breast tumour compared to normal breast tissue were observed. In addition, miR-205 has lower expression in breast cancer cell lines (MCF-7 and MDA-MB-231) compared with the non-malignant breast cell line, MCF-10A. This is supported by ectopic expression of miR-205 in breast cancer cell lines significantly suppresses cell proliferation, encourage independent growth, cell invasion and metastasis. They also demonstrated that miR-205 was able to block breast cancer *in vivo* metastasis to lung. Finally, western blotting combined with the luciferase reporter assays show that vascular endothelial growth factor A (VEGF-A) and ErbB3 are direct targets for miR-205. Together, these results suggest that miR-205 act as an anti-metastatic miRNA in breast cancer (Wu *et al.*, 2009; Wu and Mo, 2009).

2.7.3 MiRNA and Epithelial-Mesenchymal Transition

EMT is characterized by the conversion of non-motile epithelial cells via lossing cell adhesion, repression of E-cadherin expression, then acquisition of mesenchymal markers (such as vimentin, fibronectin, and N-cadherin) into mesenchymal cells with increased cell motility and invasiveness (Ma and Weinberg, 2008; Ouyang *et al.*, 2010). During tumour progression and differentiation, cancer cells undergo EMT to enhance tumour invasion and metastasis and resulting in poor clinical outcome. Multiple miRNAs that regulates EMT were indentified in recent years (Nicoloso *et al.*, 2009).

miR-200 family and miR-205. The miR-200 family (miR-200a, miR-200b, miR-200c, miR-141 and miR-429) and miR-205 are key regulators of E-cadherin and were down-regulated in the cancer cells that undergo EMT. In year 2008, scientist from different labs have shown that miR-200 family suppress EMT and cancer cell migration and invasion by direct repressing mRNA encoding E-cadherin transcriptional repressors of ZEB1 and ZEB2. MET occurred in cells that had previously undergone EMT when ectopic expression of the miR-200 family or miR-205, followed by down-regulation of ZEB1 and ZEB2 and up-regulation of E-cadherin (Gregory *et al.*, 2008; Korpala *et al.*, 2008; Park *et al.*, 2008). Gregory and coworkers (2008) showed that miR-200 family and miR-205 may be the downstream molecules of the TGF- β as the miR-200 family and miR-205 are markedly down-regulated in cells that undergo EMT in response to TGF- β . TGF- β is a very important mediator of EMT in late-stage carcinomas to promote invasion and metastasis. ZEBs is able to form a reciprocal-negative feedback loop between the miR-200 family and ZEB1/ZEB2 by repressing the transcription of miR-200. Such a feedback loop enables maintenance of a stable bi-phasic state whilst retaining the ability to switch between states after an appropriate stimulus such as TGF- β (Bracken *et al.*, 2009). These miRNAs were proposed to as a control switch between EMT and MET in normal tissue homeostasis (Zhang *et al.*, 2010; Baranwal and Alahari, 2009).

miR-101. miR-101 is another important regulator in EMT by directly targeting mRNA encoding enhancer of zeste homolog 2 (Ezh2). Ezh2, a histone methyl transferase, is an epigenetic regulator contributing to the epigenetic silencing of E-cadherin and other target genes to control tumour cell proliferation, invasiveness and metastatic ability. Ectopic expression of miR-101 suppresses invasion capacity, while Ezh2 expression restoration rescues the invasiveness of PC-3 prostate cells. Also, miR-101 differentially modulates prostate cancer cell proliferation (Cao *et al.*, 2010).

2.7.4 MiRNAs Modulate Cancer Angiogenesis

Angiogenesis is essential for tumour cells to intravasate and disseminate through the systemic circulation to distant site (Zhang *et al.*, 2010). Recent studies suggested miRNAs play a key role in angiogenesis during tumour progression. Several miRNAs have been showed to have pro-angiogenesis and anti-angiogenesis properties.

mir-17-92 cluster. Mir-17-92 cluster (including miR-17, miR-18a, miR-19a, miR-20a, miR-19b and miR-92a) was found to play a role in tumour angiogenesis-promoting activity. In RAS-expressing cells, these miRNAs that activated by MYC can enhance growth in tumour blood supply. Connective tissue growth factor (CTGF) and adhesive glycoprotein thrombospondin 1 (Tsp1) are both anti-angiogenic genes that are targeted by the miR-17-92 cluster where down-regulation of both CTGF and Tsp1 were reported to promote neovascularization. Restoration of Tsp1 and CTGF expression were observed after knockdown of miR-17-92 (Dews *et al.*, 2006). Otsuka *et al.* (2008) demonstrated miR-17-5p inhibits proliferation and motility of endothelial cell by targeting and down-regulating the expression of anti-angiogenic factor of TIMP-1 in mouse model.

miR-126. miR-126 is an endothelial-specific miRNA which is highly expressed in human endothelial cells. miR-126 reported to play an essential role in the regulation of various aspects of endothelial cell biology *in vitro*, including cell migration, organization of the cytoskeleton, and capillary network stability (Wu *et al.*, 2009). Knockout of miR-126 in zebrafish and mice showed loss of vascular integrity and neoangiogenesis. The pro-angiogenic activity of miR-126 enhance VEGF levels and endothelial cell proliferation by directly suppressing negative regulators of the VEGF pathway such as sprouty-related protein 1 (SPRED1) and phosphoinositol-3 kinase regulatory subunits 2 (PIK3R2) (Fish *et al.*, 2008; Wang *et al.*, 2009).

miR-296. Würdinger *et al.* (2008) reported up-regulation of miR-296 in primary tumour endothelial cells as compared to normal brain endothelial cells. Inhibition of miR-296 suppresses angiogenesis in animal model. The hepatocyte growth factor-regulated tyrosine kinase substrate (HGS) is a direct target of miR-296 that inhibits angiogenesis by mediating degradation of pro-angiogenesis receptors of VEGF receptor 2 (VEGFR2) and platelet-derived growth factor (PDGF) receptor β (PDGFR- β). Thus, elevated expression of miR-296 leading to decrease of HGS followed by indirectly up-regulation of the expression of receptor for pro-angiogenic ligands VEGF and PDGF in tumour associated endothelial cells to promote angiogenesis.

miR-211 and miR-222. Both miR-211 and miR-222 are highly expressed in endothelial cells that exerts anti-angiogenic effects. Transfection of endothelial cells with miR-221 and miR-222 can reduce endothelial cell migration, proliferation, and angiogenesis *in vitro* by post-transcriptionally inhibiting the expression of protein c-Kit, the receptor for stem cell factor (SCF) (Poliseno *et al.*, 2006). Also, another research showed miR-221/222 might be involved in vasculogenesis where over-expression of both miRNAs indirectly regulate the expression of the endothelial nitric oxide synthase (eNOS) in Dicer-knockdown endothelial cells (Suárez *et al.*, 2007).

CHAPTER 3: METHODOLOGY

3.1 Cancer Cell Cultures

3.1.1 Cultivation of Cell Lines

A549 (human lung adenocarcinoma epithelial cell line) and MCF7 (human breast adenocarcinoma cell line) were obtained from Cancer Research Initiatives Foundation (CARIF), while MDA-MB-231 (human breast adenocarcinoma cells) and PC-3 (human prostate cancer cell line) were purchased from American Type Culture Collection (ATCC).

A549, PC-3 and MCF7 were maintained in Roswell Park Memorial Institute 1640 (RPMI 1640) (Thermo Scientific Hyclone, USA) culture media whilst MDA-MB-231 was cultivated in Dulbecco's Modified Eagle Medium (DMEM) (Thermo Scientific Hyclone, USA) culture media. Culture media was supplemented with 10.0 % (v/v) fetal bovine serum (FBS) (JR Scientific Inc, USA) to provide complete nutrient for cell growth. All cell lines were adherent cells that were cultured on a 25.0 cm² T-25 culture flask (Nunc, Denmark) and incubated at 37°C in a carbon dioxide (CO₂) incubator (Mettler, Germany) with 95.0 % humidified atmosphere. Culture media have buffer system that contained appropriate amount of bicarbonate where 5.0 % atmosphere CO₂ levels help maintain culture media in a balanced controlled pH (7.0 to 7.6).

Subculturing of cells was performed when monolayer cell culture attained 70-90% confluency to maintain healthy cell growth. First, the spent media was discarded and washed with 5.0 ml 1X Phosphate Buffered Saline (PBS). Then, 1.0 ml of 0.1 % (v/v) Trypsin-0.53 mM EDTA was added and incubated in 37°C for 10 min to detach the cells. 2.0 ml of culture media with 10.0 % (v/v) FBS was added to inactivate trypsin activity. 0.5 ml of the cell suspension was mixed with 4.5 ml of fresh culture media and transferred all into a new T-25 culture flask.

3.1.2 Preparation of Frozen Stocks

Cancer cells were plated on a T-25 culture flask and grown to 70% confluency. Once desired confluency was obtained, the spent culture medium on the plate was discarded, cells were washed with 1X PBS and 1.0 ml of 0.1% (v/v) Trypsin-0.53 mM EDTA was added to detach cells from the culture flask for 10 min. 2.0 ml of culture media supplemented with 10.0 % (v/v) FBS were added to inactivate trypsin activity. Cell suspension was pipetted into 15.0 ml tubes and centrifuged at 125 x *g* for 10 min using Centrifuge 5702 (Eppendorf, USA). Supernatant was discarded and cell pellet was re-suspended with cyroprotectant medium supplemented with 20.0 % (v/v) FBS, 10.0 % (v/v) Dimethyl sulfoxide (DMSO) (Merck, Germany). Several stocks of 1.0 ml aliquots of cells were prepared in 2.0 ml cryovials, frozen gradually at -4°C, -20°C for 3 h each and finally long term stored in liquid nitrogen at -196°C.

3.1.3 Thawing of Cryopreserved Cells

Cyropreserved cells were removed from liquid nitrogen and the vials were thawed by gently agitation in 37°C water bath for 2 min. Each 1.0 ml of thawed cell suspension was then diluted with 9 ml of culture medium supplemented with 10.0 % (v/v) FBS and centrifuged at 125 x *g* for 7 min. Cell pellet was re-suspended with culture medium supplemented with 10.0 % (v/v) FBS.

3.1.4 Trypan Blue Dye Exclusion Assay

Trypan blue dye exclusion assay was used to determine the number of viable cell in a cell suspension. Cells were detached, centrifuged and re-suspended in culture media. 1:1 dilution was prepared where 20.0 μ l of cell suspension was suspended with 20.0 μ l of 0.04 % (w/v) trypan blue dye (Merck, Germany) and mixed thoroughly. Cell mixture was loaded into the counting chamber of a haemocytometer and only viable cells that excluded stain lying within the grid line of 1 mm² area were counted under Nikon ECLIPSE TS-100 inverted microscope (Nikon, Japan).

$$\text{Cell concentration (cells/ml)} = \frac{n \times 10^4 \times (\text{dilution factor} = 2)}{\text{Number of squares counted}} \quad (\text{Equation 3.1})$$

where, n = total viable cells counted

3.2 Serial Selection of High and Low Invasiveness Sub-Cell Lines

Selection of highly invasive subpopulations from parental cell lines A549, MCF7, MDA-MB-231 and PC-3 was performed using 24-well transparent PET membrane 8.0 μ m pore size inserts (BD Biosciences, USA). Transwell inserts were coated with 100.0 μ l of 1.5 mg/ml Matrigel (BD Biosciences, USA). Cells were re-suspended in culture media supplemented with 10.0 % (v/v) FBS and seeded into the upper chamber, while the bottom chamber was filled with media supplemented with 20.0 % (v/v) FBS as chemo-attractant to create a chemotactic gradient for cell invasion to the bottom well. Following incubation for 48 h at 37°C, invasive cells invaded through the Matrigel and attached on the bottom of the membrane, while remaining non-invasive cells on the top membrane were harvested aseptically and cultured for enough cells to subjected sequential selection. Selection for low invasiveness cells and high invasiveness cells was continued up to the seventh generation. Those low

invasiveness cancer cells which failed to invade all 7 rounds of selection were designated as A549-NI7, MCF7-NI7, MDA-MB-231-NI7 and PC-3-NI7 sub-cell lines, whilst those high invasiveness cancer cells successfully invaded through all 7 rounds were designated as A549-I7, MCF7-I7, MDA-MB-231-I7 and PC-3-I7 sub-cell lines (Figure 3.1).

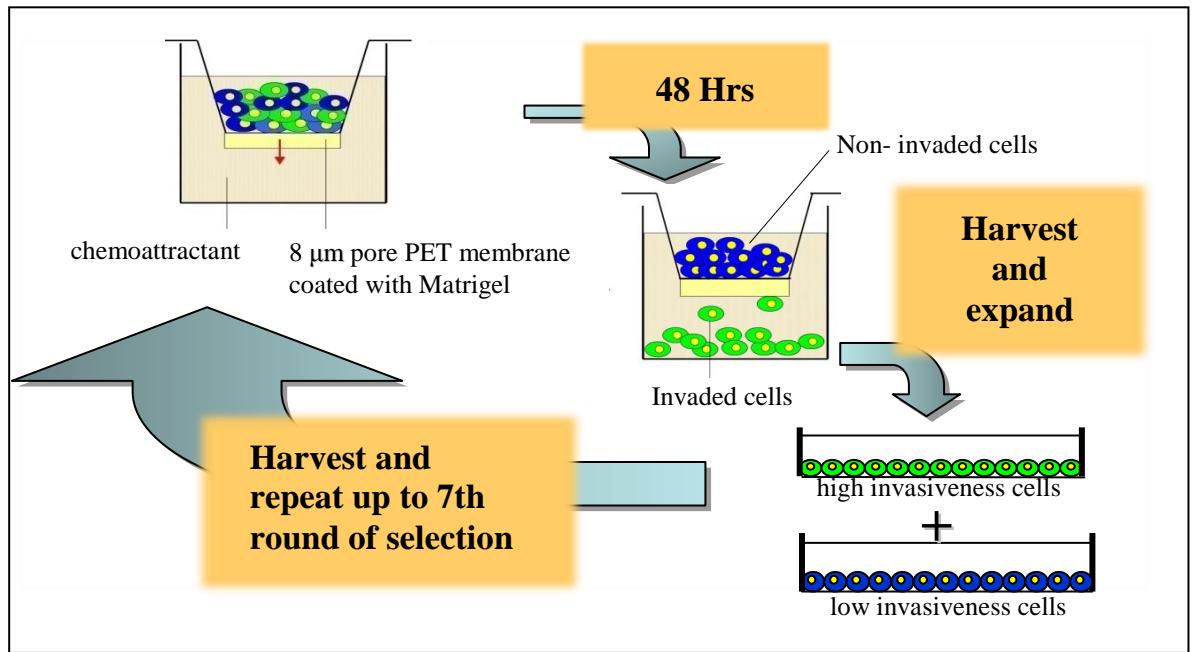


Figure 3.1: An illustration of high and low invasiveness sub-cell line selection using serial transwell invasion assay.

3.3 Transwell Invasion Assay

Cell invasiveness capacity of selected cancer sub-cell lines was examined using Transwell Invasion assay by measuring the number of cells transmigrating through a layer of extracellular matrix, Matrigel. 24-well transparent PET membrane 8.0 µm pore size inserts were coated with 70.0 µl of 1.5 mg/ml Matrigel (BD Biosciences, USA). 70% confluent cells were starved with serum free media and harvested at 24 h. A density of 1.0×10^5 cells were resuspended with 500.0 µl of serum free media (Thermo Scientific Hyclone, USA) were added to the upper insert, whilst media with 20.0 % (v/v) FBS were added at a lower insert as a chemoattractant. The cells were incubated

for 22 h at 37 °C. Cells in the upper insert were removed by swiping with cotton swabs and those invading cells on the underside of the membrane were fixed in 100.0 % ethanol for 2 min, followed by staining with 1.0 % (w/v) methylene blue (Sigma, USA) for 20 min. Number of invaded cells in eight random fields of each transwell invasion membrane insert areas were counted under Nikon ECLIPSE TS-100 inverted microscope (Nikon, Japan) at 200X magnification.

3.4 Wound Healing Assay

Wound healing assay was performed to examine the cell migration capacity. The selected low and high invasiveness sub-cell lines were grown to 100.0 % confluence in 6-well plates and treated with Mitomycin C (Merck, Germany) at 1.0 µg/ml for 2 h to halt cell proliferation. A wound was created by dragging a 200.0 µl pipette tip through the cell monolayer. Cells were washed with 1x PBS to remove cell debris. The cells were then cultured in serum free media and allowed cells to migrate for 23 to 28 h. The wound healing activity of the same area was captured under an inverted microscope (Nikon, Japan) at 100X magnification at 0 h and 23 to 28 h. The open wound area of each image was assessed by TScratch software version 7.8 (Gebäck *et al.*, 2009). The cell migrated or wound healing rate was calculated using the formulas shown in equations 3.2 and 3.3.

$$\text{Wound healing (\%)} = \frac{(\text{open image area at start} - \text{open image area at end})}{\text{open image area at start}} \times 100$$

(Equation 3.2)

$$\text{Fold change} = \frac{\% \text{ of wound healing of high invasive sub-cell line}}{\% \text{ of wound healing of low invasive sub-cell line}}$$

(Equation 3.3)

3.5 Cell Proliferation Assay

Cell proliferation rate of parental, high and low sub-cell lines were determined by plating 2×10^4 viable cells in 6-well plates with complete media. Spent media were discarded and replenished with fresh complete culture media every 2 days to ensure optimum growing condition for cells. Total viable cell number was counted every 24 h for 7 days using trypan blue dye exclusion assay. Cells were harvested, stained with trypan blue (Sigma Aldrich, USA) and total viable cells number were counted using a haemocytometer. A line graph was plotted with total viable cell number against harvested day.

$$\text{Doubling time} = \frac{\ln 2}{\ln (\text{ratio})} \times \text{number of days} \quad (\text{Equation 3.4})$$

$$\text{where, Ratio} = \frac{\text{Total viable cell number on harvest day}}{\text{Total viable cell number seeded on day-0}}$$

3.6 Total RNA Extraction

Total RNA including small RNA population was extracted from 70.0 % confluency cultured low and high invasiveness sub-cell lines of A549, MCF7 and PC-3 using Qiagen miRNeasy mini kit (Qiagen, Germany) according to manufacturer's instruction. First, cells ($\leq 1 \times 10^7$ cells) were harvested by centrifuging for 10 min using Centrifuge 5702 (Eppendorf, USA). The tube was flicked thoroughly to loosen the cell pellet. A total of 700.0 μl of QIAzol lysis (Qiagen, Germany) was added and vortexed to mix. Cell lysates were homogenized by QIAshredder homogenizers (Qiagen, Germany) at maximum centrifuge speed for 2 min. The homogenate lysates were placed on the benchtop at room temperature for 5 min to promote dissociation of nucleoprotein complexes. 140.0 μl of chloroform was added to each of the tube containing the homogenate lysate and securely capped to shake vigorously for 15 s. The homogenate

lysates were placed on the benchtop at room temperature for 2-3 min for phase separation, then the lysates were centrifuge for 15 min at 12,000 x *g* at 4 °C to separate the sample into 3 phases: an upper, colorless, aqueous phase containing RNA; a white interphase containing DNA; and a lower, red, organic phase containing protein. The solution at upper aqueous phase containing RNA was transferred to a new RNase free collection tube. 1.5 volumes of 100.0 % ethanol was added and mixed thoroughly by pipetting. 700.0 µl of the sample was pipetted into an RNeasy Mini spin column (Qiagen, Germany) in a 2.0 ml collection tube and centrifuge at 8,000 x *g* for 15 s at room temperature. The flow-through was discarded. 500.0 µl Buffer RPE (Qiagen, Germany) was pipetted onto the RNeasy Mini spin column and centrifuged for 15 s at 8,000 x *g* to wash the column. The flow-through was discarded. Another 500.0 µl of Buffer RPE was added to the RNeasy Mini spin column and was centrifuged for 2 min at 8,000 x *g* to final dry the RNeasy Mini spin column membrane. The RNeasy Mini spin column was transferred to a new RNase free 1.5 ml collection tube and 40.0 µl of RNase-free water was added directly onto the RNeasy Mini spin column membrane and centrifuged for 1 min at 8,000 x *g* for RNA elution. RNA samples were then stored at -30 °C until further experiments.

3.7 RNA Quality Control

3.7.1 Nanodrop Spectrophotometry

The purity and quantity of isolated RNA samples were assessed using Nanodrop 2000 spectrophotometer (Thermo Scientific, USA). First, Nucleic Acid application module was selected and the “RNA” option was chosen in the operating software to performing measurement of RNA concentration and purity. 1.0 µl of RNase-free water was used to clean the measurement pedestal. 1.0 µl of RNase-free water was initially measured and stored as blank in the operating software prior making a sample

measurement. Later, 1.0 μl of RNA sample was pipetted to the lower measurement pedestal and sampling arm was closed and clicked “measure”. A spectral measurement was initiated using the operating software on the computer. The sampling arm was opened when the measurement was completed and the sample from both upper and lower pedestal were wipe using delicate task wipers (Kimberly-Clark, Canada). Same procedures were performed for all the RNA samples.

3.7.2 Agilent Bioanalyzer

RNA sample integrity (RIN), purity and concentration of extracted total RNA for each sub-cell lines of A549, PC-3 and MCF7 were evaluated to increase accuracy of miRNA microarray expression profile, using the Agilent RNA 6000 Nano kit (Agilent Technologies, USA) on Agilent Bioanalyzer 2100 (Agilent Technologies, USA) following manufacturer’s protocol. First, chip priming station (Agilent Technologies, USA) was set up with syringe, the base plate adjusted to position C and the syringe clip was adjusted to the top position. 550.0 μl of RNA 6000 Nano gel matrix (Agilent Technologies, USA) were pipetted into spin filter and centrifuge at 1,500 x g for 10 min at room temperature. 65.0 μl of filtered gel was aliquoted into 0.5 ml RNase-free microfuge tubes. The aliquots were stored at 4°C for 4 weeks. RNA 6000 Nano dye (Agilent Technologies, USA) was equilibrated to room temperature for 30 min and later was vortex for 10 s and spun down. 1.0 μl of dye was then added into a 65.0 μl aliquot of filtered gel, vortexed and spun down at 13,000 x g for 10 min at room temperature. A new RNA 6000 Nano Chip (Agilent Technologies, USA) was placed on the chip priming station. 9.0 μl of gel-dye mix was pipetted into the well marked with G and the lid of the chip priming station was closed. Plunger on the chip priming station was pressed until it is held by the clip and slowly pull back plunger to 1.0 ml position after 5s. Chip priming station was opened and 9.0 μl of gel-dye mix was pipetted into the

well marked with G. 5.0 μ l of RNA 6000 Nano marker was pipette in all 12 sample wells and in the well marked with ladder symbol. RNA ladder aliquot was preheated at 70°C for 2 min, then 1.0 μ l of RNA ladder was pipetted into well marked with ladder symbol. 1.0 μ l of RNA sample was loaded in each of the 12 sample wells. The chip was placed horizontally in the adapter of the IKA vortexer (Agilent Technologies, USA) and vortexed for 1 min at 2,400 rpm. The chip was inserted in the Agilent Bioanalyzer 2100 within 5 min. RNA quality control analysis was performed using Eukaryote total RNA Nano assay class of Agilent 2100 expert software. The quality of RNA samples were assessed based on both RIN and 28S/18S rRNA ratios.

3.8 MiRNA Microarrays

The differences in global miRNAs expression pattern between low and high invasiveness cancer sub-cell lines (A549, PC-3, MCF7) were assayed using GeneChip[®] miRNA Arrays (Affymetrix, USA) platform together with FlashTag[™] Biotin RNA labeling kit (Genesphere, USA) according to manufacturer's protocol.

3.8.1 RNA Poly (A) Tailing and Labelling

All reagents of FlashTag[™] Biotin RNA labeling kit were thawed according to protocol. 1.5 μ g of total RNA was used as a starting material for poly (A) tailing. The volume of 1.5 μ g of each total RNA sample was adjusted to 8.0 μ l with nuclease-free water (Qiagen, Germany) and incubated on ice. Preparation of poly (A) tailing step was carried out by adding 2.0 μ l of RNA Spike Control Oligos (Genesphere, USA), 1.5 μ l of 10X Reaction Buffer (Genesphere, USA), 1.5 μ l of 25 mM MnCl₂ (Genesphere, USA), 1.0 μ l of diluted ATP Mix (diluted in 1:500 with 1.0 mM Tris) (Genesphere, USA) and 1.0 μ l of PAP Enzyme (Genesphere, USA) to the 8.0 μ l of 1.5 ng of total RNA. This 15.0 μ l cocktail was mixed gently without vortex and briefly spun down in a

microcentrifuge. The reaction cocktail was then incubated in a 37°C heat block for 15 min for poly (A) tailing step. 15.0 µl of tailed RNA was briefly spun and placed on ice before proceeding to FlashTag ligation.

4.0 µl 5X FlashTag Ligation Mix Biotin (Genesphere, USA) and 2.0 µl of T4 DNA Ligase (Genesphere, USA) were added into the poly (A) tailed RNA tube, mixed gently and was microfuged. The mixture was incubated at room temperature for 30 min for complete FlashTag ligation. 2.5 µl Stop Solution (Genesphere, USA) was added to the reaction cocktail to stop ligation reaction. 2.0 µl of the biotin-labeled sample was aliquoted into 1.5 ml microcentrifuge tubes for the Enzyme Linked Oligosorbent Assay (ELOSA) QC assay. The remaining 21.5µl biotin-labeled sample was kept in -20°C immediately.

3.8.2 ELOSA QC Assay

Before proceed to array hybridization, ELOSA QC assay was performed to verify the biotin labelling process by the FlashTag Biotin Labeling Kit. First, the ELOSA Spotting Oligos (Genesphere, USA) was diluted in 1:50 ratio with 1X PBS. 75.0 µl of diluted ELOSA Spotting Oligos was added to each well of the plate or strip (total 8 wells: 6 well for samples, 1 well for positive control and 1 well for negative control). All the wells was covered with adhesive plate sealer and incubated overnight at 2-8°C.

After overnight incubation, the ELOSA Spotting Oligos solution was discarded into a sink. The wells were washed two times with 1X PBS, 0.02 % (v/v) Tween-20 solution followed by blotted dry on papers. Each well was then blocked with 150.0 µl of 5.0 % (w/v) BSA in 1X PBS solution and incubated for 1 h at room temperature. Later, BSA blocking solution was discarded and the wells plate was blotted dry.

2.5 μl of 25.0 % dextran sulfate (Genisphere, USA) and 48.0 μl of solution of 5X SSC, 0.05% SDS, 0.005% BSA added, gently vortexed and was briefly spun. 2.0 μl of ELOSA positive control (Genisphere, USA) was added to positive control labeled microcentrifuge tube, while 2.0 μl of 5X SCC, 0.05% (v/v) SDS, 0.005% (w/v) BSA was added to negative control labeled 1.5 ml microcentrifuge tube. 50.5 μl of master mix was added into each six 2.0 μl of the biotin-labeled samples, a positive control and a negative control labeled 1.5 ml microcentrifuge tube. The mixtures were vortexed gently and spun briefly. Each 52.5 μl of hybridization solution was loaded into each designated well and incubated for 1 h at room temperature. Hybridization solution was removed by expelling and washed vigorously for four times with 1X PBS, 0.02% (v/v) Tween 20 solution, then blotted dry.

0.5 μl of Streptavidin (SA)-HRP (Thermo Scientific, USA) was diluted in 2.0 ml of 5 % (w/v) BSA in 1X PBS with a dilution factor of 1:4000 for SA-HRP binding step. 75.0 μl of the diluted SA-HRP was added into each well and incubated for 30 min at room temperature. SA-HRP was discarded into a sink after 30 min and vigorously washed 4 times with 1X PBS, 0.02% (v/v) Tween-20, then blotted dry. 100.0 μl of TMB substrate (Thermo Scientific, USA) was added to each well. The wells were covered and incubated at room temperature in the dark for 30 min. The intensity of blue color substrate in each well was observed after 30 min of incubation.

3.8.3 Hybridization of GeneChip[®] miRNA Arrays

Hybridization of biotin-labeled RNA samples onto GeneChip[®] miRNA Arrays were performed once FlashTag labeling process was verified by ELOSA QC assay. 20X Eukaryotic Hybridization Control (Genisphere, USA) was thawed and heated for 5 min at 65°C. 21.5 µl of biotin-labeled sample was mixed with 50.0 µl 2X Hybridization Mix (Genisphere, USA), 10.0 µl of nuclease-free water, 5.0 µl of Deionized formamide (molecular biology grade) (Genisphere, USA), 10 µl of DMSO (Genisphere, USA), 5.0 µl of 20X Eukaryotic Hybridization Control (Genisphere, USA) and 1.7 µl of Control Oligonucleotide B2, 3nM (Genisphere, USA). The sample mixture was gently mixed by flicking the tube and kept on ice. GeneChip[®] miRNA arrays were unwrapped and warmed to room temperature for 10 min. Mark each array with a meaningful designation. The sample mixtures were incubated at 99°C on heat block for 5 min, then 45°C in Affymetrix Hybridization Oven 640 (Affymetrix, USA) for 5 min. A 20.0 µl unfiltered type pipette tip was inserted into the upper right septum of GeneChip[®] miRNA arrays to allow for proper venting when hybridization cocktail is injected. 100.0 µl sample was aspirated and injected into an array. The pipette tip was removed from the upper right septum of the array and covered both septa with 1/2" Tough-Spots (Biversified Biotech, USA) to minimize evaporation and prevent leaks. The arrays were loaded into hybridization oven trays and were incubated in Affymetrix Hybridization Oven 640 at 48°C and 60 rpm for 16 h.

3.8.4 Array Washing, Staining and Scanning

All arrays were taken out from oven after 16 h of hybridization and Tough-Spots were removed. The hybridization cocktail was extracted from each array and transferred to a new tube and stored at -80°C for long-term storage and later can be use for Array Rehybridization Procedure if necessary. Each array was filled with 100.0 µl of Array Holding Buffer and was equilibrated to room temperature before washing and staining steps. GeneChip Fluidics Station 450 was placed with a vial (amber) of 600.0 µl Stain Cocktail 1 in sample holder 1, a vial (amber) of 600.0 µl Stain Cocktail 2 in sample holder 2 and a vial (clear) of 800.0 µl Array Holding Buffer in sample holder 3. Arrays were washed and stained by Fluidics Station 450 using fluidics script FS450_0003 program. After washing and staining, arrays were checked to make sure there are no air bubbles by manually filling the array with Array Holding Buffer. Both septa of arrays were covered with 3/8" Tough-Spots. The array glass surface was wiped with clean lab wipe, then hybridization signal of each array was detected by GeneChip® scanner 3000 7G (Affymetrix, USA).

3.8.5 MiRNAs Expression Analysis

MiRNA microarray raw CEL file format data were imported into Partek Genomic Suite v 6.4 (Partek Inc., St. Louis, MO) using default parameters including robust-multichip average (RMA) for data normalization between triplicate samples, which includes background adjustments, normalization and summarization. A list of miRNAs with significantly differential expression between paired sub-cell lines were developed based on the criteria of gene expression ≥ 2.00 fold change and significant unadjusted p -values ≤ 0.05 using analysis of variance (ANOVA).

3.9 Quantitative Real-Time PCR

Quantitative Real-Time PCR was performed on the selected miRNAs of hsa-miR-92b, hsa-miR-378, hsa-miR-671-5p and hsa-miR-1827 for miRNA microarray data validation. Total RNA from A549-I7 and A549-NI7 cells were extracted using Qiagen miRNeasy mini kit (Qiagen, Germany). Single-stranded cDNA was synthesized from total RNA (5.0 to 20.0 ng) using specific miRNA primers supplied together with TaqMan[®] microRNA assay and TaqMan[®] MicroRNA Reverse Transcription Kit (Applied Biosystems, USA). The specific miRNA primers of TaqMan[®] miRNA assay (Applied Biosystems, USA) together with TaqMan[®] Fast Advanced Master Mix (Applied Biosystems, CA, USA) were used to quantitate mature miRNAs of hsa-miR-92b, hsa-miR-378, hsa-miR-671-5p and hsa-miR-1827 using CFX96 Real-Time PCR system (Bio-Rad, USA) according to standard manufacturer's protocol.

3.9.1 Reverse Transcription

Single-stranded cDNA was synthesized from total RNA using specific miRNA primers supplied together with TaqMan[®] microRNA assay and TaqMan[®] MicroRNA Reverse Transcription Kit (Applied Biosystems, USA) following the manufacturer's optimized protocol and cycling condition. The components of TaqMan[®] MicroRNA Reverse Transcription Kit and reverse transcription (RT) primer of TaqMan[®] microRNA assay were thawed on ice. 5.0 to 30.0 ng total RNA (5.0 ng for hsa-miR-92b, hsa-miR-378 and RNU6B, 10.0 ng for hsa-miR-671-5p, 30.0 ng for hsa-miR-1827) were diluted with nuclease-free water to final volume of 5.0 μ l. Reverse transcription cocktail was prepared by mixing 0.15 μ l dNTP mix, 1.00 μ l of multiscribe RT enzyme, 1.50 μ l 10X RT buffer, 0.19 μ l RNase Inhibitor, 4.16 μ l nuclease free water, 5.0 μ l of total RNA and 3 μ l of specific miRNA RT primer into each labeled PCR tubes (Bio-Rad, USA). These cocktail was mixed gently without vortex, centrifuged briefly and

incubated on ice until ready to load into thermal cycler. Reverse transcription was performed with the program in Table 3.1 CFX96 Real-Time PCR system (Bio-Rad, USA). The reaction volume was set at 15.0 μ l and the PCR tubes were placed into the thermal cycler for reverse transcription.

Table 3.1: Temperature and time for program for reverse transcription run.

Step type	Time (min)	Temperature (°C)
Hold	30	16
Hold	30	42
Hold	5	85
Hold	∞	4

3.9.2 Real-Time PCR Amplification

Real-Time PCR amplification of mature miRNA from cDNA sample was performed using TaqMan microRNA assay (containing miRNA-specific forward and reverse PCR primer together with TaqMan MGB probe) together with the TaqMan[®] Fast Advanced Master Mix (Applied Biosystems, USA) following the manufacturer's optimized protocol and cycling condition. A cocktail of 1.0 μ l of cDNA, 5.0 μ l TaqMan Fast advanced Master mix (Applied Biosystems, USA), 3.5 μ l of nuclease free water and 0.5 μ l of TaqMan miRNA assay (Applied Biosystems, USA) were mixed gently into each specific PCR reaction tubes then centrifuged briefly. Thermal-cycling of Real-Time PCR amplification was ran according to the condition in Table 3.2.

Table 3.2: Thermal cycling condition for Real-Time PCR amplification step.

Step	Enzyme activation	PCR	
	Hold	Cycles (40 cycles)	
		Denature	Anneal/Extend
Time (s)	20	3	20
Temperature (°C)	95	95	60

Data were normalized against an RNU6B internal control, and fold changes of each miRNA was generated using $2^{-\Delta\Delta Ct}$. Pearson correlation plot was performed to assess the correlation between microarray and quantitative Real-Time PCR data.

3.10 Pathway Enrichment Analysis

DIANA-mirPath (employed DIANA-microT-4.0 prediction data) was performed for Kyoto Encyclopedia of Genes and Genomes (KEGG) pathways enrichment analysis on the differential expressed miRNAs in A549 (Papadopoulos *et al.*, 2009). 10 miRNAs (miR-378, miR-671-5p, miR-25, miR-92b, miR-106b, miR-550, miR-629, miR-576-3p, miR-886-5p, miR-487b) were input for KEGG pathways enrichment except of miR-1827 which was not in the DIANA-mirPath gene input list. Top eight metastasis related KEGG pathways were filtered out from the KEGG pathways list with a $-\ln(p\text{-value})$ score of ≥ 3.00 . Due to the scarce number of miRNA* included in the DIANA-mirPath algorithm (miR-25*, miR-106b*, miR-550* and miR-629* were not included), the guided strands (miR-25, miR-106b, miR-550 and miR-629) were selected from the DIANA-mirPath gene input list for KEGG pathways enrichment to obtain a more comprehensive analysis. Later, the top eight metastasis-related KEGG pathways were combined with the target prediction data from TargetScan 5.2 of total context score of ≤ -0.10 with regardless of the conservation site (http://www.targetscan.org/vert_50/) and DIANA-microT 4.0 (Maragkakis *et al.*, 2011) of miTG score of ≥ 0.20 to investigate the possible molecular components of signalling network in A549 cancer metastasis. MiRNAs* were included into the signalling pathway analysis based on the DIANA-microT 4.0 prediction data where this algorithm has miRNAs* (miR-25*, miR-106b*, miR-550* and miR-629*) in the gene input list. A hypothetical signalling network was proposed based on the KEGG pathways from DIANA-mirPath that combined with the target prediction data of DIANA-microT 4.0 and TargetScan 5.2

with a $-\ln(p\text{-value})$ score of ≥ 3.00 , miTG score of ≥ 0.20 and total context score of ≤ -0.10 .

3.11 Statistical Analysis

All data were collected in triplicates with the exception of wound healing assays which were carried out in four replicates. Statistical analyses were performed using a one-tailed Student's *t* test. Differences with *p*-values of ≤ 0.05 were considered significant.

CHAPTER 4: RESULTS

4.1 Establishment of High and Low Invasiveness Cancer Sub-Cell Lines with Similar Proliferation Properties and Distinctly Different Invasion and Migration Attributes

4.1.1 Serial Selection of High and Low Invasiveness Sub-Cell Lines

In order to study cancer metastasis, high and low invasiveness cancer sub-cell lines were established from parental human lung cancer cell lines A549, prostate cancer cell line PC-3, two breast cancer cell lines MDA-MB-231 and MCF7 using sequential transwell invasion assay. The high invasiveness cells successfully invaded through Matrigel for all 7 rounds were designated as A549-I7, PC-3-I7, MCF7-I7 and MDA-MB-231-I7 sub-cell lines, whilst the low invasiveness cancer cells failed to invade through Matrigel for all 7 rounds of selection were designated as A549-NI7, PC-3-NI7, MCF7-NI7 and MDA-MB-231-NI7 sub-cell lines (Figure 4.1).

All high invasiveness sub-cell lines were also observed with weakened adhesion properties to culture plates during sub-culturing. High invasiveness sub-cell lines took shorter time to detached from the culture plate upon exposure of trypsin compared to low invasiveness sub-cell lines and parental A549 cells (result not shown).

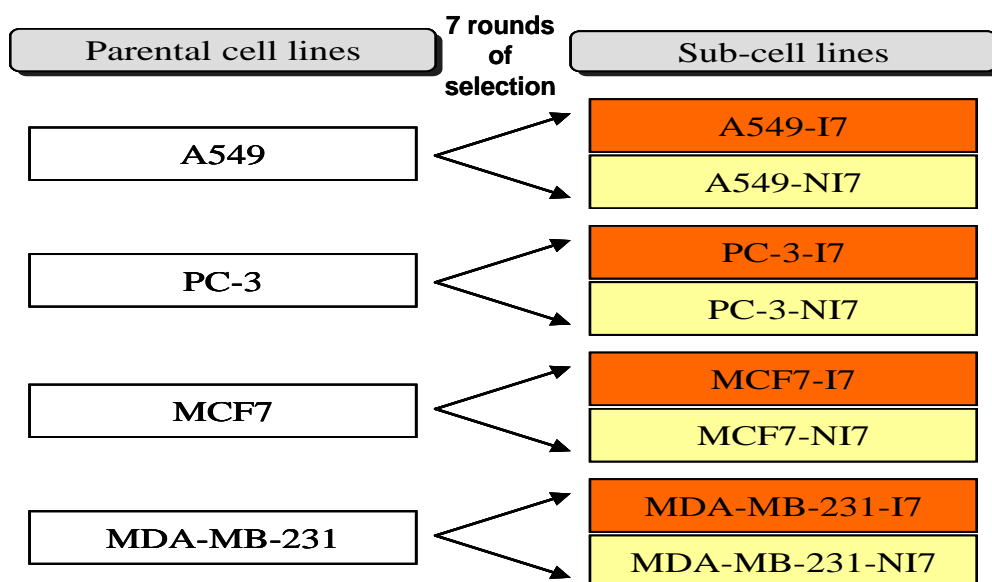


Figure 4.1: Diagram showing high (A549-I7, PC-3-I7, MCF7-I7 and MDA-MB-231-I7) and low (A549-NI7, PC-3-NI7, MCF7-NI7 and MDA-MB-231-NI7) invasiveness sub-cell lines were established from each parental cell lines of A549, PC-3, MCF7 and MDA-MB-231 using serial transwell invasion approach.

4.1.2 Transwell Invasion Assay

After serial selection of high and low invasiveness sub-cell lines from parental cell lines, invasion properties of each selected sub-cell lines were validated with transwell invasion assay. Number of methylene blue stained invaded cells per field was calculated based on the average of eight random transwell invasion insert membrane at 200X magnification fields for each sub-cell lines. Each selected high invasiveness sub-cell lines were validated with greater invasive capacities compared to the low invasiveness sub-cell lines (Figure 4.2 to 4.9).

4.1.2.1 Transwell Invasion Assay of A549

An increased number of invaded A549-I7 cells compared to A549-NI7 cells were observed in Figure 4.2 using transwell invasion assay. A549-I7 was significantly 3 fold greater in the capacity to invade through Matrigel coated transwell membrane insert compared to A549-NI7 with p -value of 0.023 (Figure 4.3).

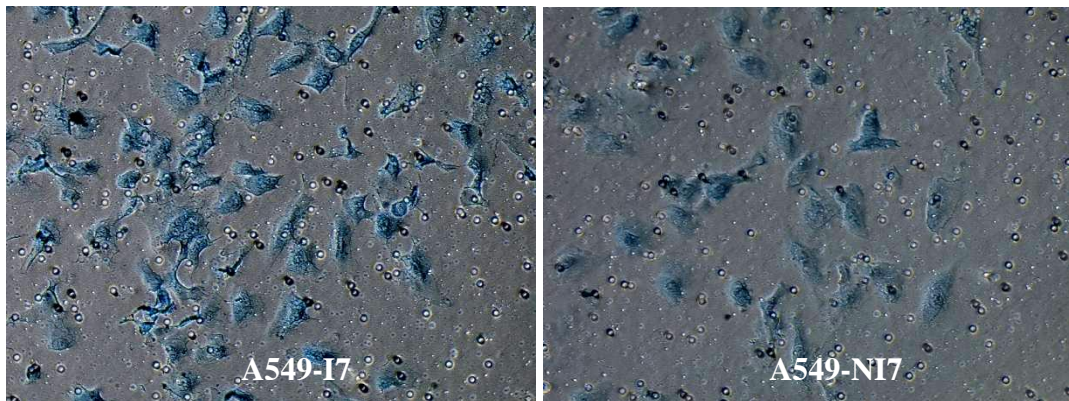


Figure 4.2: Representative cell fields of methylene blue stained invaded cells on the bottom membranes of Matrigel transwell invasion insert for A549-I7 and A549-NI7 at 200X magnification.

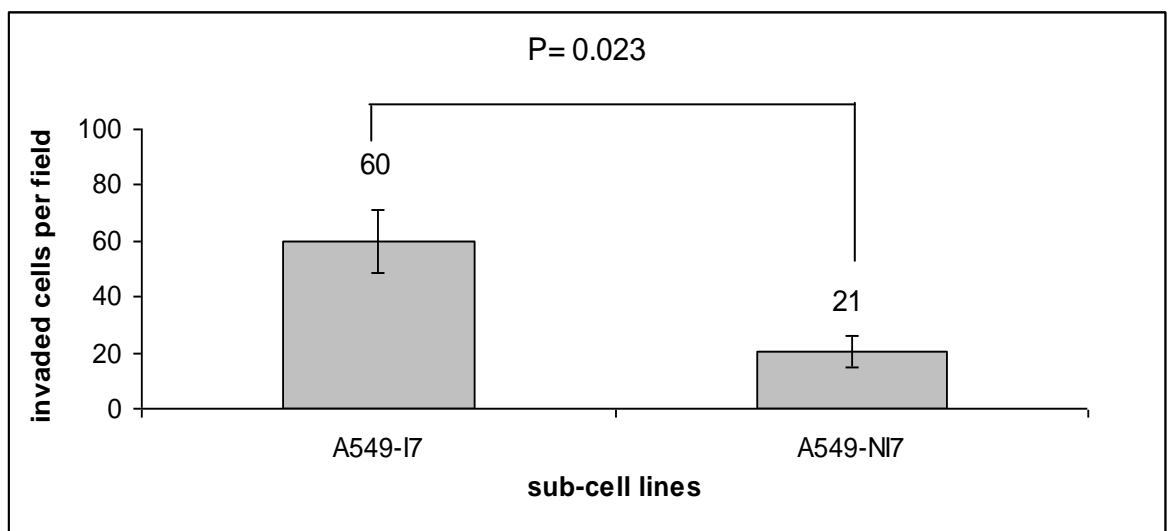


Figure 4.3: A bar graph represents the average invaded cells per field of A549-I7 and A549-NI7 with data presented as mean \pm SEM of three independent experiments with p -value <0.05 .

4.1.2.2 Transwell Invasion Assay of PC-3

An increased number of invaded PC-3-I7 cells compared to PC-3-NI7 cells were observed in Figure 4.4 using transwell invasion assay. PC-3-I7 was significantly 3.5 fold greater in the capacity to invade through Matrigel coated transwell membrane insert compared to PC-3-NI7 with p -value of 0.014 (Figure 4.5).

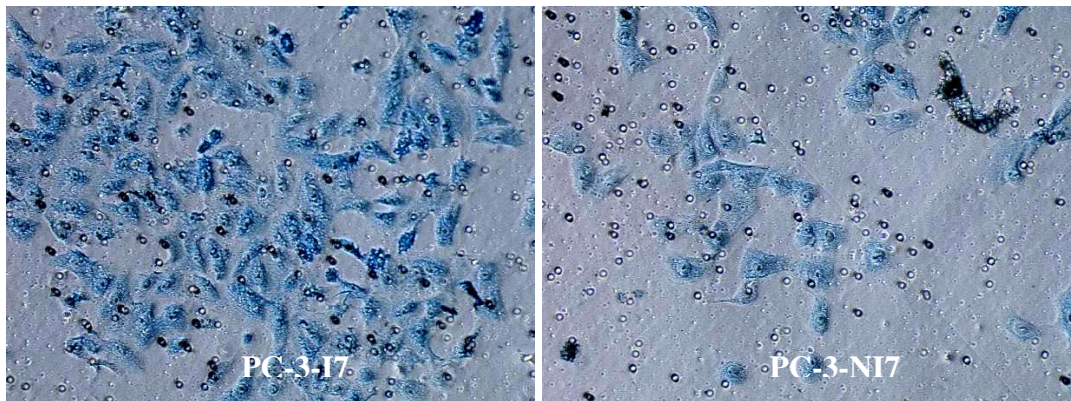


Figure 4.4: Representative cell fields of methylene blue stained invaded cells on the bottom membranes of Matrigel transwell invasion insert for PC-3-I7 and PC-3-NI7 at 200X magnification.

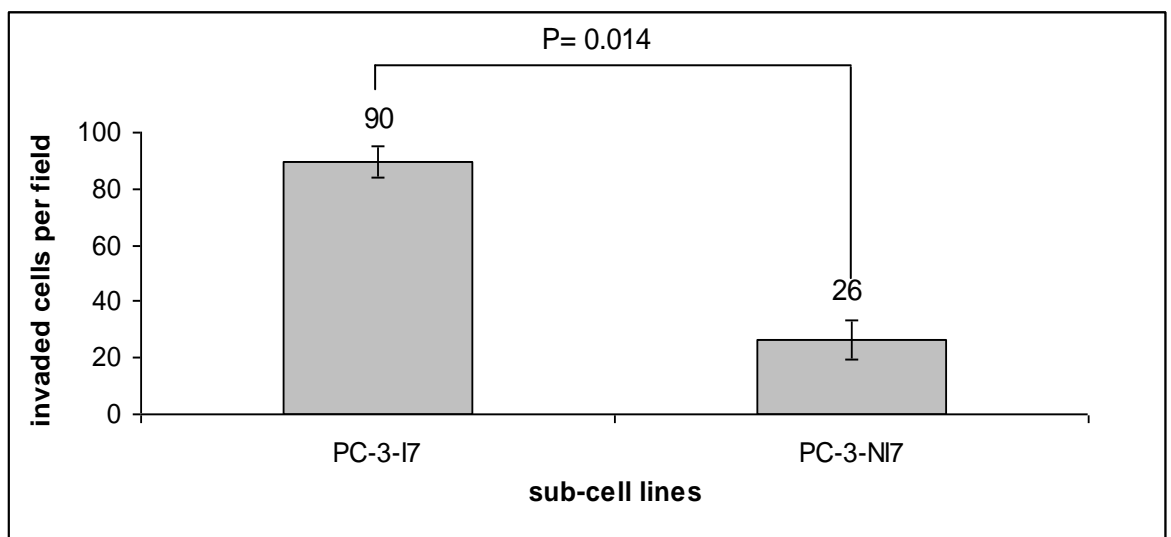


Figure 4.5: A bar graph represents the average invaded cells per field of PC-3-I7 and PC-3-NI7 with data presented as mean \pm SEM from three independent experiments with p -value <0.05 .

4.1.2.3 Transwell Invasion Assay of MCF7

An increased number of invaded MCF7-I7 cells compared to MCF7-NI7 cells were observed in Figure 4.6 using transwell invasion assay. MCF7-I7 was significantly 3 fold greater in the capacity to invade through Matrigel coated transwell membrane insert compared to MCF7-NI7 with p -value of 0.027 (Figure 4.7).

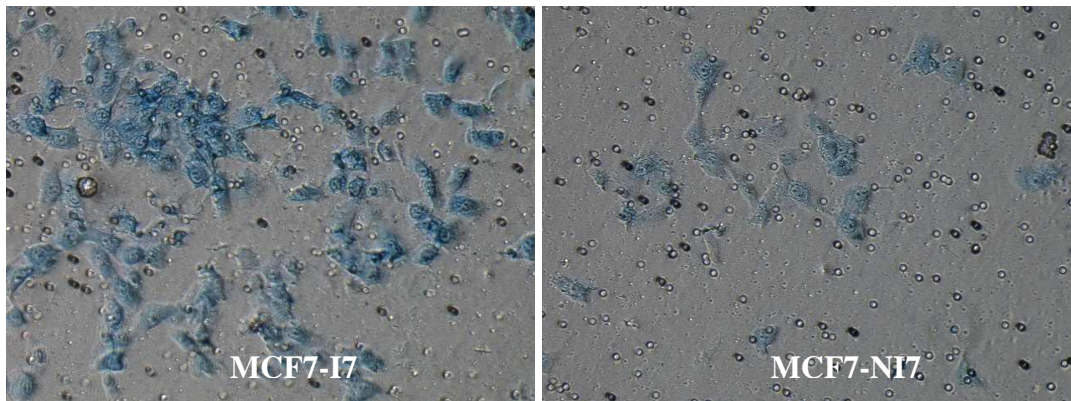


Figure 4.6: Representative cell fields of methylene blue stained invaded cells on the bottom membranes of Matrigel transwell invasion insert for MCF7-I7 and MCF7-NI7 at 200X magnification.

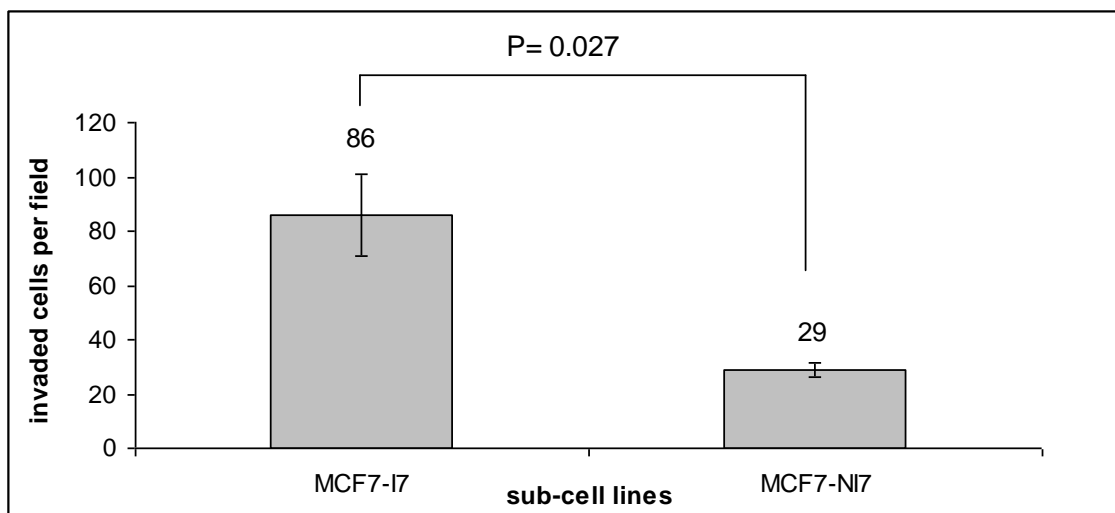


Figure 4.7: A bar graph represents the average invaded cells per field of MCF7-I7 and MCF7-NI7 with data presented as mean \pm SEM from three independent experiments with p -value <0.05 .

4.1.2.4 Transwell Invasion Assay of MDA-MB-231

An increased number of invaded MDA-MB-231-I7 cells compared to MDA-MB-231-NI7 cells were observed in Figure 4.8 using transwell invasion assay. MDA-MB-231-I7 was significantly 3.4 fold greater in the capacity to invade through Matrigel coated transwell membrane insert compared to MDA-MB-231-NI7 with p -value of 0.044 (Figure 4.9).

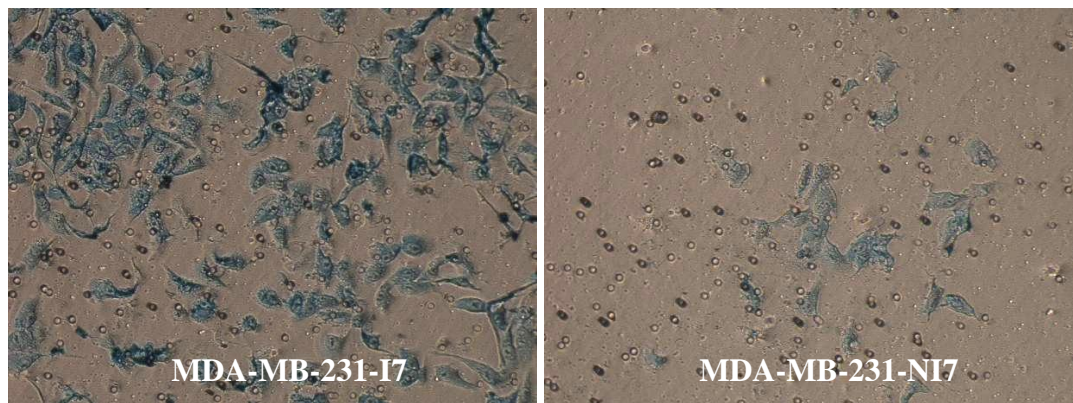


Figure 4.8: Representative cell fields of methylene blue stained invaded cells on the bottom membranes of Matrigel transwell invasion insert for MDA-MB-231-I7 and MDA-MB-231-NI7 at 200X magnification.

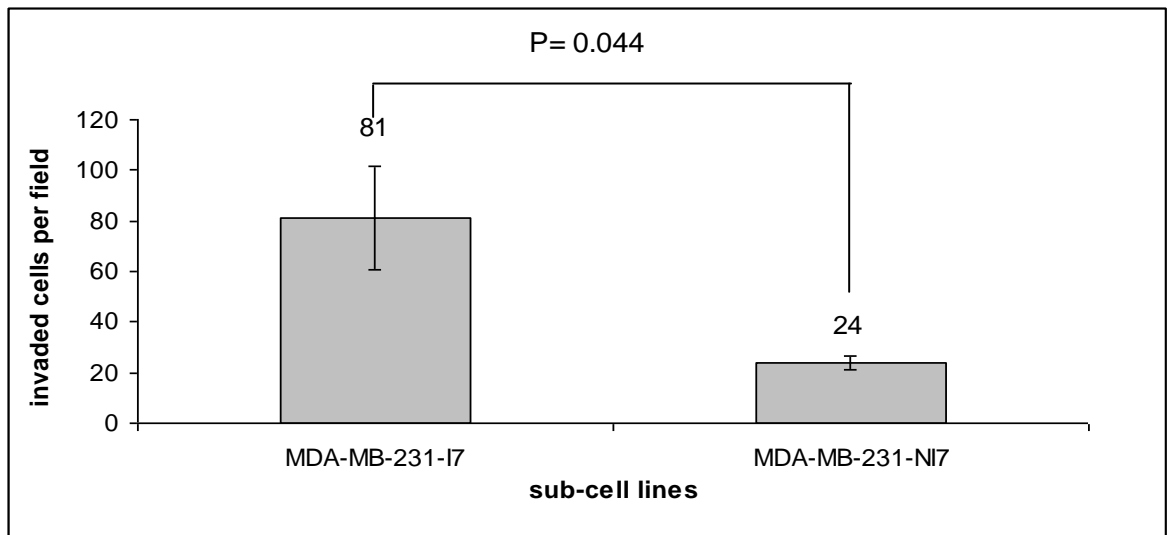


Figure 4.9: A bar graph represents the average invaded cells per field of MDA-MB-231-I7 and MDA-MB-231-NI7 with data presented as mean \pm SEM from three independent experiments with p -value <0.05 .

4.1.3 Wound Healing Assay

Wound healing assay was used to validate migratory potential of each selected sub-cell lines. The percentage of wound healing for A549-I7 and A549-NI7 with data presented as mean \pm SEM from four independent experiments using T-Scratch software. Each selected high invasiveness sub-cell lines were validated with higher migration abilities compared to the low invasiveness sub-cell lines (Figure 4.10 to 4.17).

4.1.3.1 Wound Healing Assay of A549

A549-I7 was observed to close the scratch wound faster than A549-NI7 at 28 h time point (Figure 4.10). A549-I7 has 2.8 fold greater migration capacity as compared to A549-NI7 with *p*-value of 0.003 (Figure 4.11).

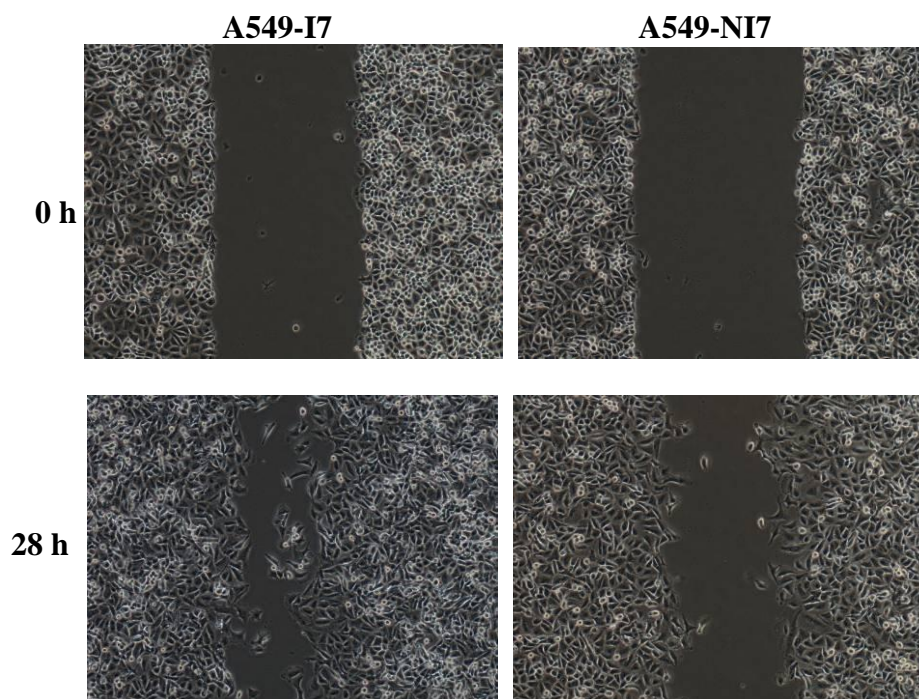


Figure 4.10: Migrations of A549-I7 and A549-NI7 cells into the wound were captured at 0 h and 28 h time at 100X magnification.

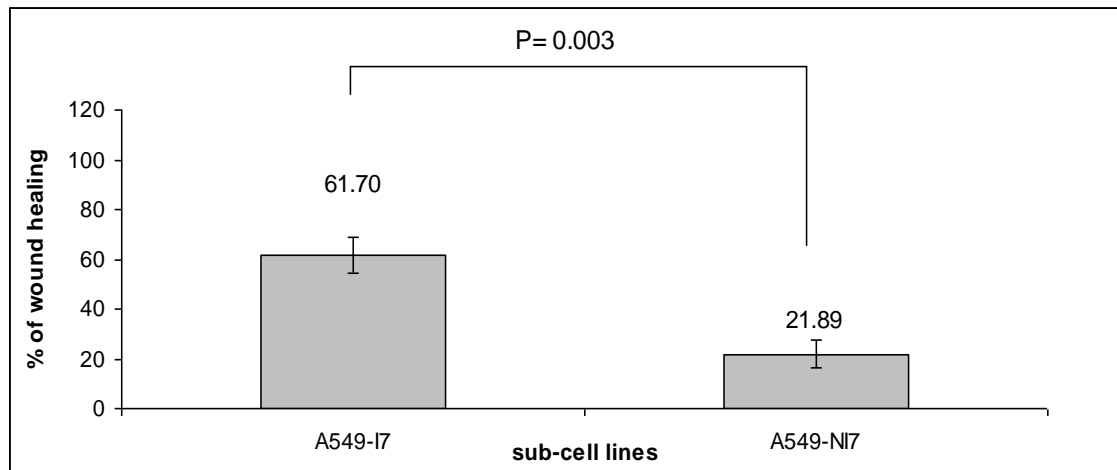


Figure 4.11: A bar chart represents the percentage of wound healing for A549-I7 and A549-NI7 with data presented as mean \pm SEM from four independent experiments.

4.1.3.2 Wound Healing Assay of PC-3

PC-3-I7 was observed to close the scratch wound faster than PC-3-NI7 at 28 h time point (Figure 4.12). PC-3-I7 has 1.8 fold greater migration capacity as compared to PC-3-NI7 with p -value of 0.002 (Figure 4.13).

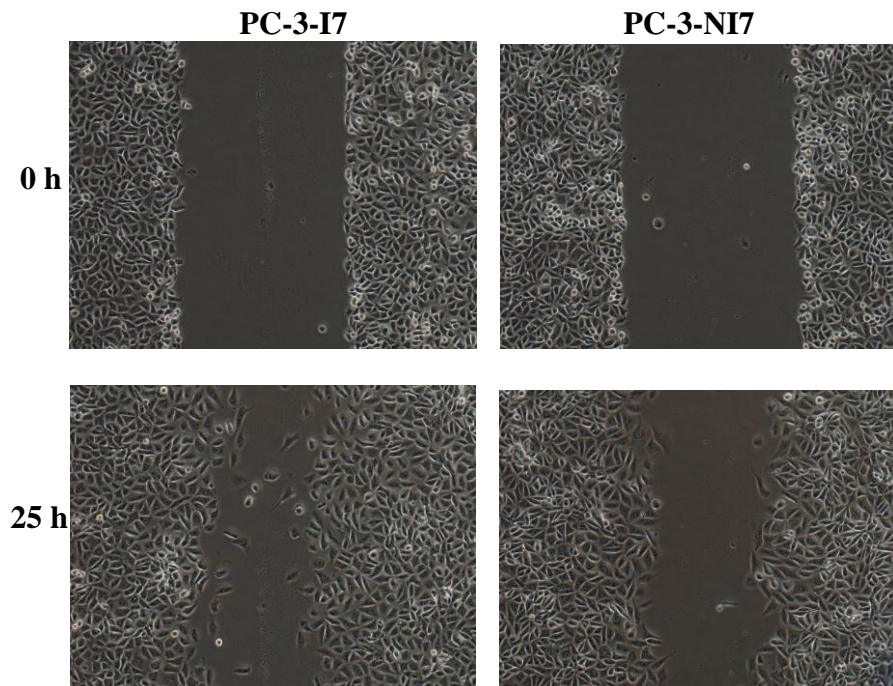


Figure 4.12: Migrations of PC-3-I7 and PC-3-NI7 cells into the wound were captured at 0 h and 28 h time at 100X magnification.

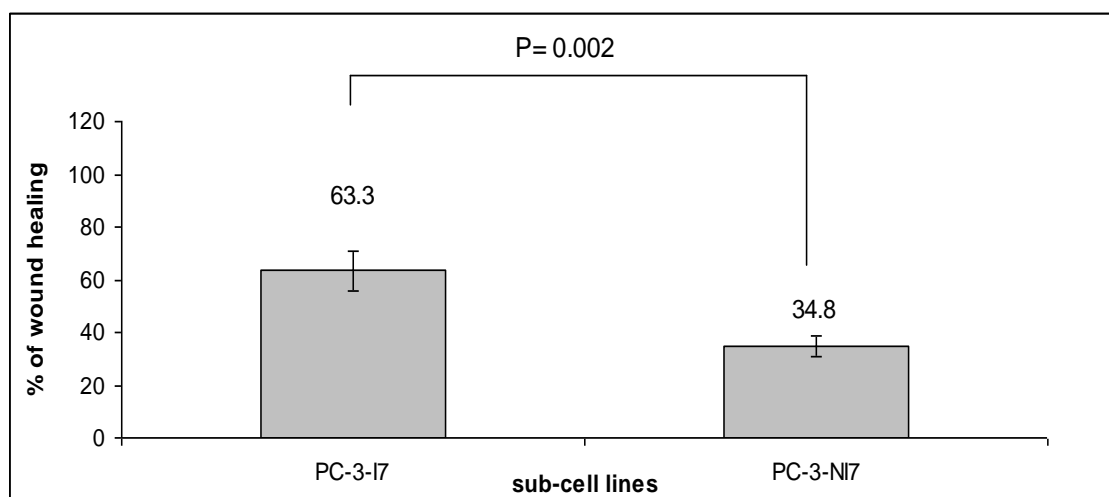


Figure 4.13: A bar chart represents the percentage of wound healing for PC-3-I7 and PC-3-NI7 with data presented as mean \pm SEM from four independent experiments.

4.1.3.3 Wound Healing Assay of MCF7

MCF7-I7 was observed to close the scratch wound faster than MCF7-NI7 at 23 h time point (Figure 4.14). MCF7-I7 has 2.0 fold greater migration capacity as compared to MCF7-NI7 with *p*-value of 0.004 (Figure 4.15).

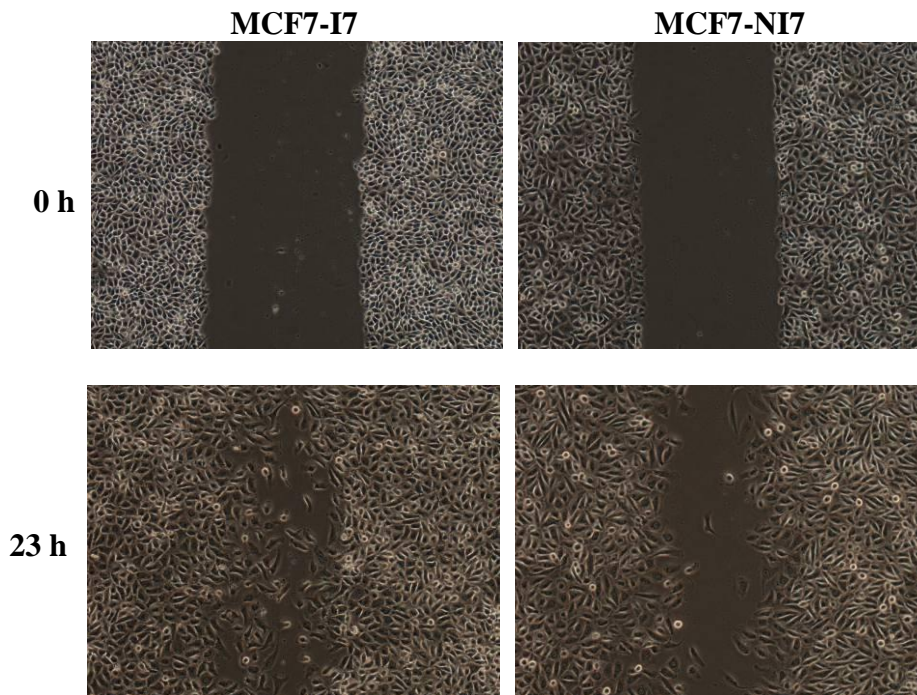


Figure 4.14: Migrations of MCF7-I7 and MCF7-NI7 cells into the wound were captured at 0 h and 23 h time at 100X magnification.

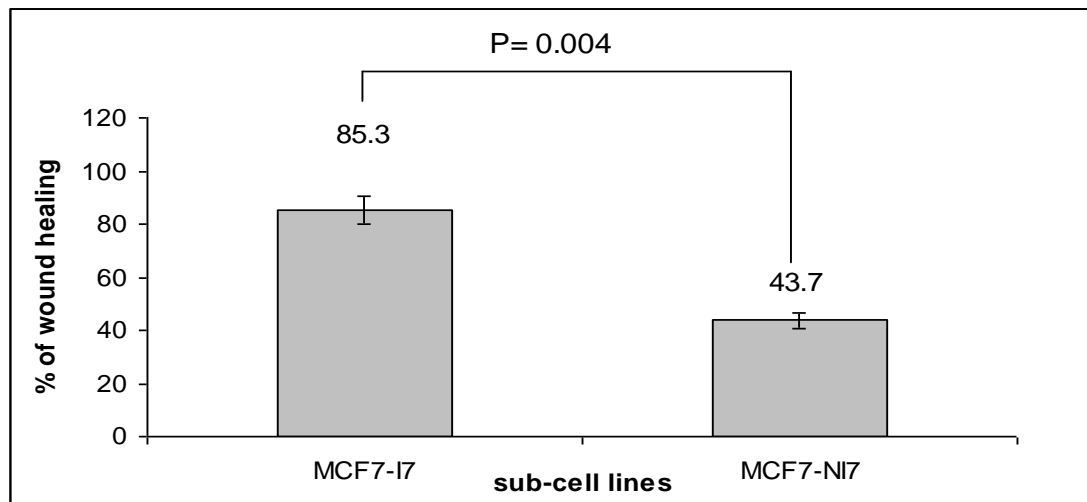


Figure 4.15: A bar chart represents the percentage of wound healing for MCF7-I7 and MCF7-NI7 with data presented as mean \pm SEM from four independent experiments.

4.1.3.4 Wound Healing Assay of MDA-MB-231

MDA-MB-231-I7 was observed to close the scratch wound faster than MDA-MB-231-NI7 at 28 h time point (Figure 4.16). MDA-MB-231-I7 has 1.8 fold greater migration capacity as compared to MDA-MB-231-NI7 with p -value of 0.018 (Figure 4.17).

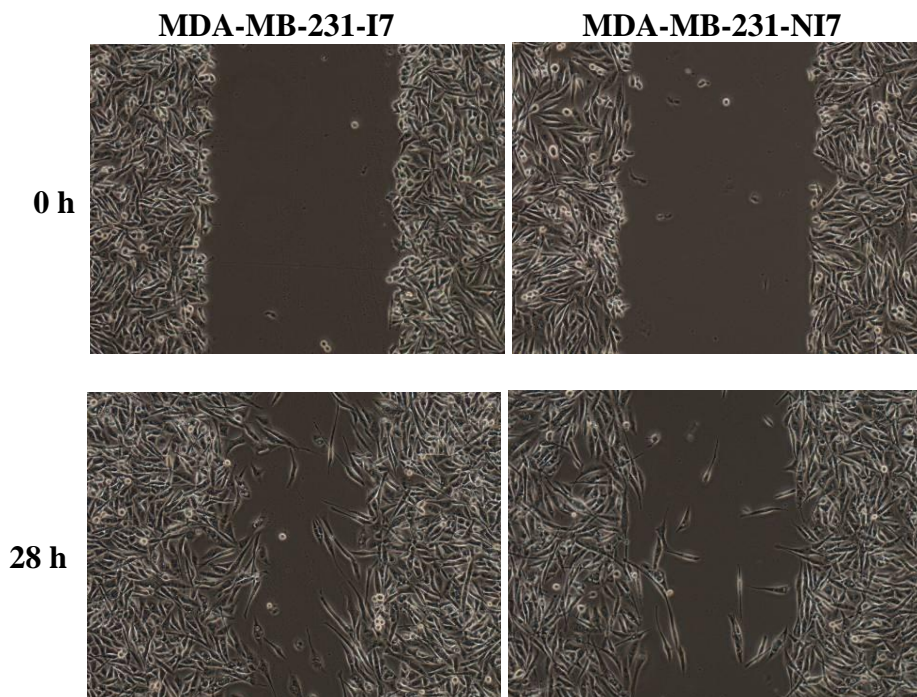


Figure 4.16: Migrations of MDA-MB-231-I7 and MDA-MB-231-NI7 cells into the wound were captured at 0 h and 23 h time at 100X magnification.

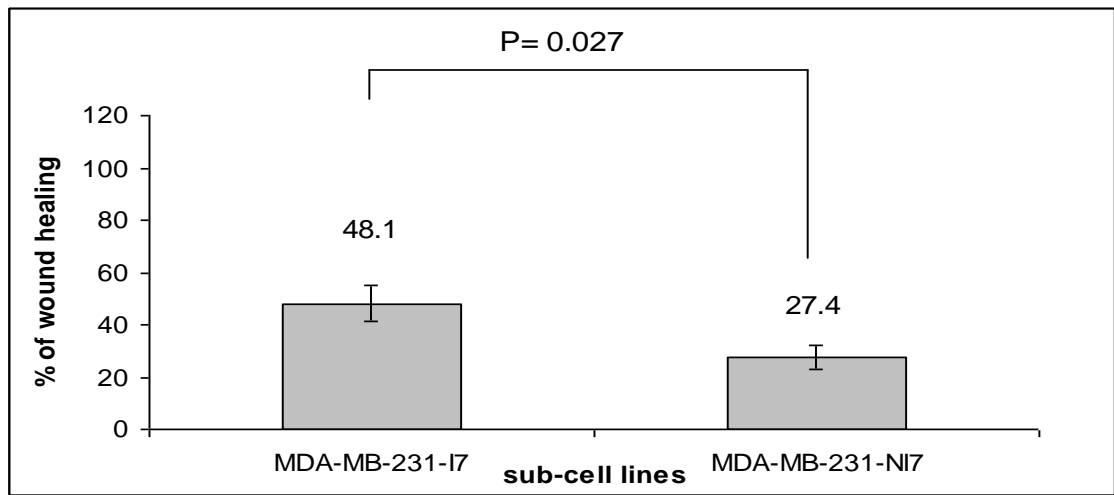


Figure 4.17: A bar chart represents the percentage of wound healing for MDA-MB-231-I7 and MDA-MB-231-NI7 with data presented as mean \pm SEM from four independent experiments.

4.1.4 Cell Proliferation Assay

Cell proliferation assay was used to validate proliferation rate of the selected sub-cell lines. Consistent cell proliferation rate between each parental, high invasiveness and low invasiveness sub-cell lines were observed (Figure 4.18 to 4.25) (Appendix 5.2).

4.1.4.1 Cell Proliferation Assay of A549

In Figure 4.18, number of viable cells on the log phase of the growth curve (day 4) was used to calculate the doubling time of A549-I7, A549-NI7 and A549 using equation 3.4. Consistent cell proliferation rate between A549-I7, A549-NI7 and A549 with doubling time of approximately 19 h were observed (Figure 4.19).

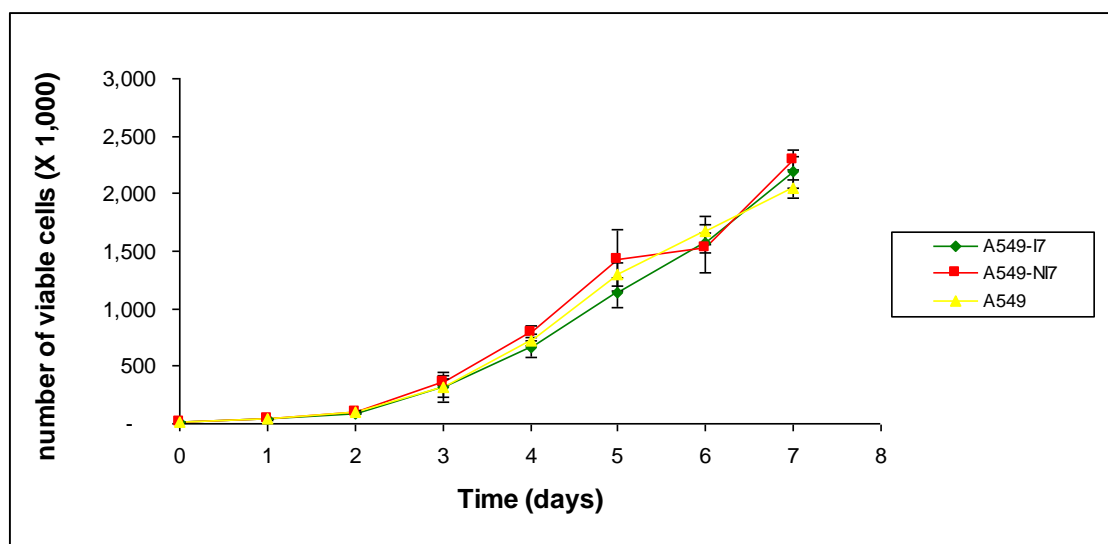


Figure 4.18: Cell proliferation curve for A549-I7, A549-NI7 and A549 over 7 days with number of viable cells on each day presented as mean \pm SEM from the three individual experiments.

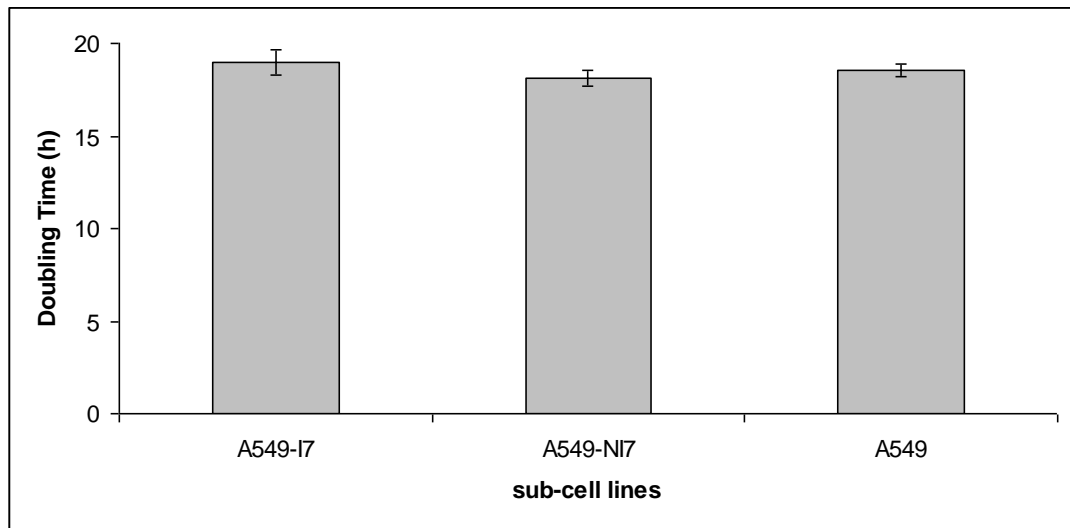


Figure 4.19: A bar chart representing the doubling time (h) for A549-I7, A549-NI7 and A549 are presented as mean \pm SEM from the three individual experiments.

4.1.4.2 Cell Proliferation Assay of PC-3

In Figure 4.20, number of viable cells on the log phase of the growth curve (day 4) was used to calculate the doubling time of PC-3-I7, PC-3-NI7 and PC-3 using equation 3.4. Consistent cell proliferation rate between PC-3-I7, PC-3-NI7 and PC-3 with doubling time of approximately 18 h were observed (Figure 4.21).

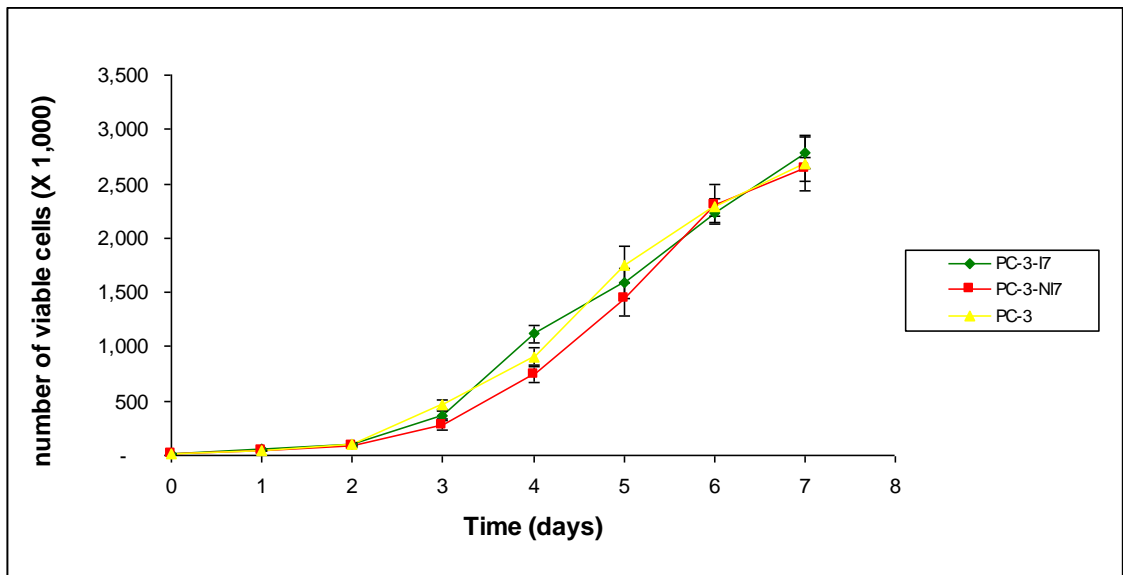


Figure 4.20: Cell proliferation curve for PC-3-I7, PC-3-NI7 and PC-3 over 7 days with number of viable cells on each day presented as mean \pm SEM from the three individual experiments.

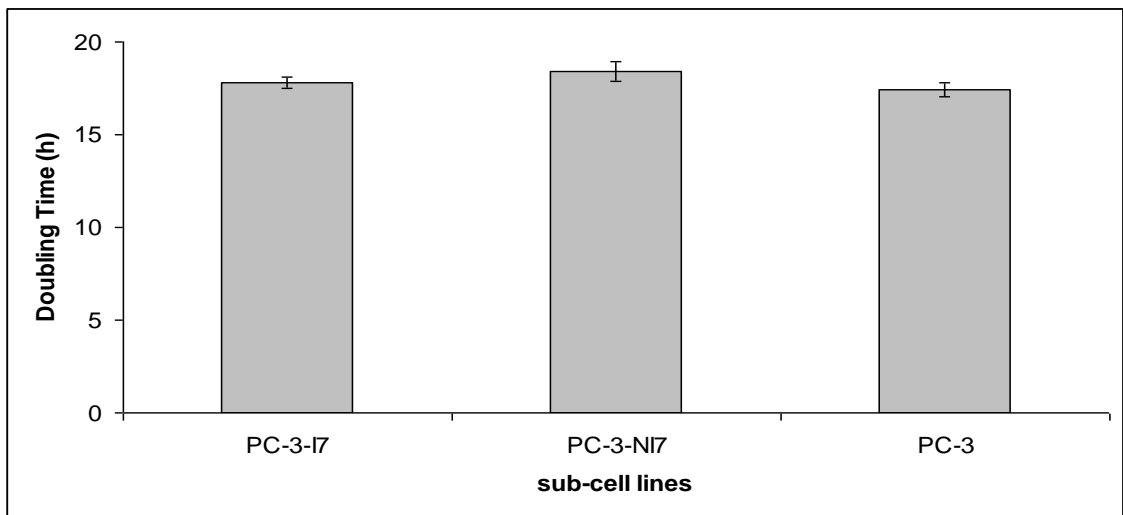


Figure 4.21: A bar chart representing the doubling time (h) for PC-3-I7, PC-3-NI7 and PC-3 are presented as mean \pm SEM from the three individual experiments.

4.1.4.3 Cell Proliferation Assay of MCF7

In Figure 4.22, number of viable cells on the log phase of the growth curve (day 4) was used to calculate the doubling time of MCF7-I7, MCF7-NI7 and MCF7 using equation 3.4. Consistent cell proliferation rate between MCF7-I7, MCF7-NI7 and MCF7 with doubling time of approximately 17 h were observed (Figure 4.23).

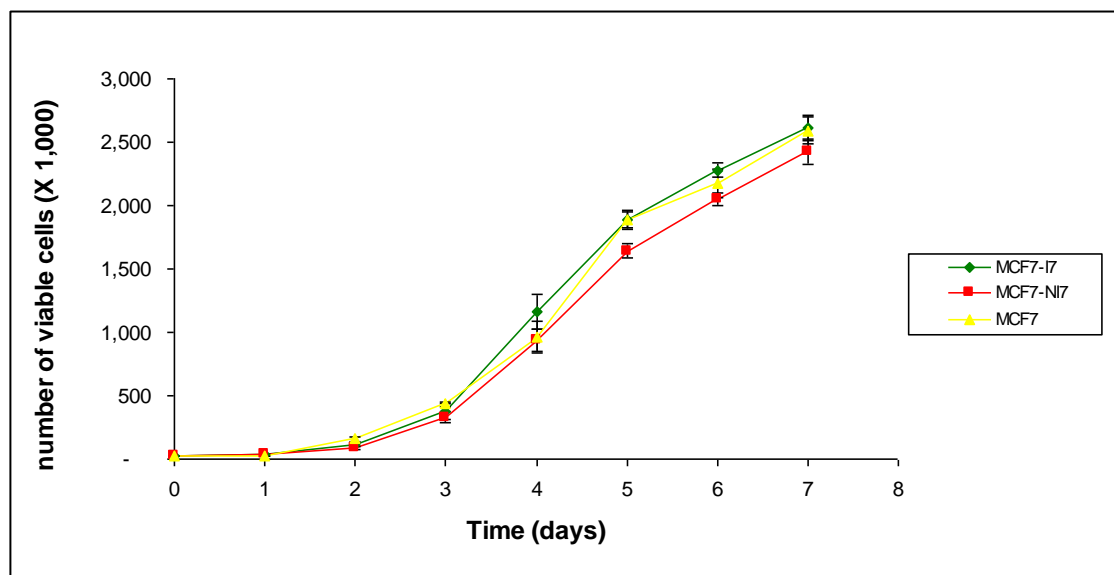


Figure 4.22: Cell proliferation curve for MCF7-I7, MCF7-NI7 and MCF7 over 7 days with number of viable cells on each day presented as mean \pm SEM from the three individual experiments.

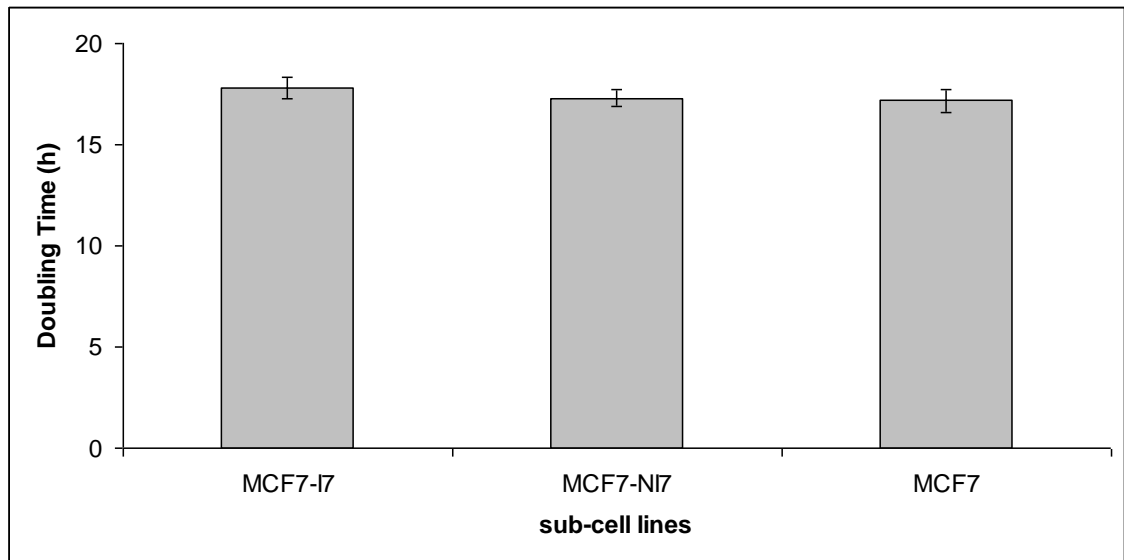


Figure 4.23: A bar chart representing the doubling time (h) for MCF7-I7, MCF7-NI7 and MCF7 presented as mean \pm SEM from the three individual experiments.

4.1.4.4 Cell Proliferation Assay of MDA-MB-231

In Figure 4.24, number of viable cells on the log phase of the growth curve (day 4) was used to calculate the doubling time of MDA-MB-231-I7, MDA-MB-231-NI7 and MDA-MB-231 using equation 3.4. Consistent cell proliferation rate between MDA-MB-231-I7, MDA-MB-231-NI7 and MDA-MB-231 with doubling time of approximately 17 h were observed (Figure 4.25).

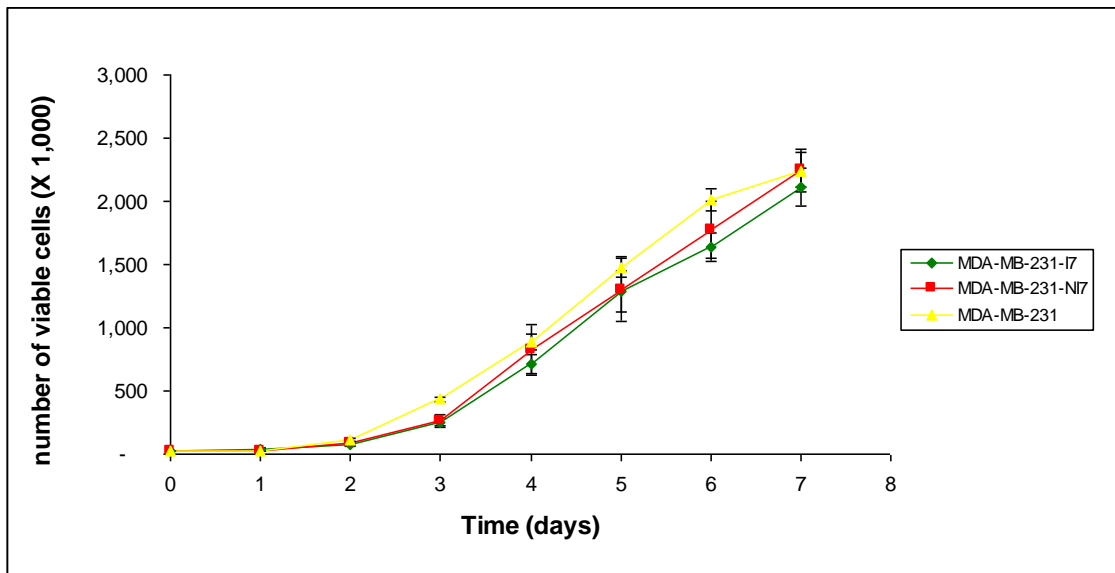


Figure 4.24: Cell proliferation curve for MDA-MB-231-I7, MDA-MB-231-NI7 and MDA-MB-231 over 7 days with number of viable cells on each day presented as mean \pm SEM from the three individual experiments.

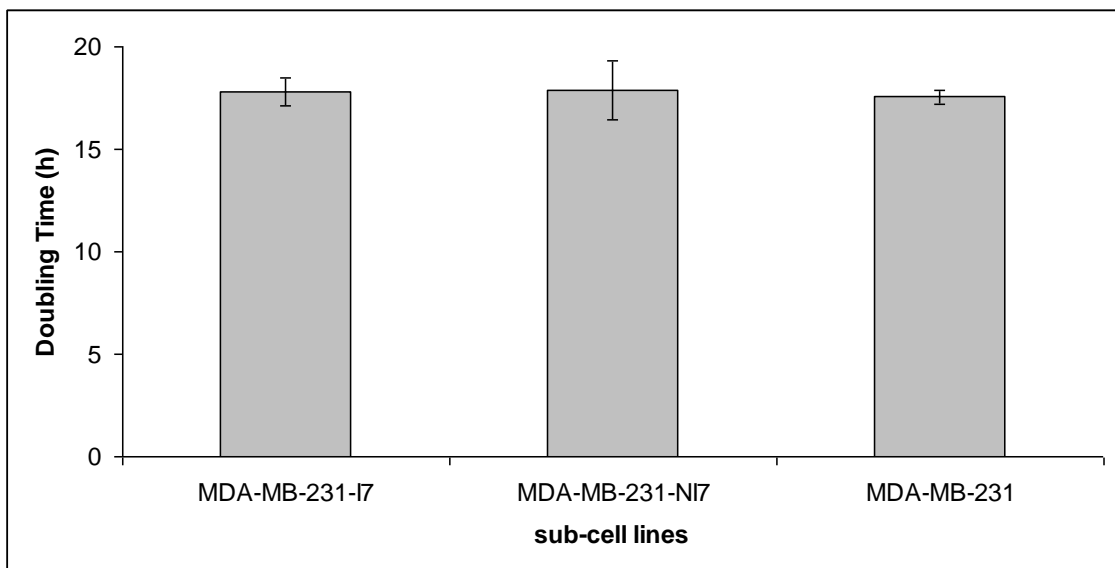


Figure 4.25: A bar chart representing the doubling time (h) for MDA-MB-231-I7, MDA-MB-231-NI7 and MDA-MB-231 are presented as mean \pm SEM from the three individual experiments.

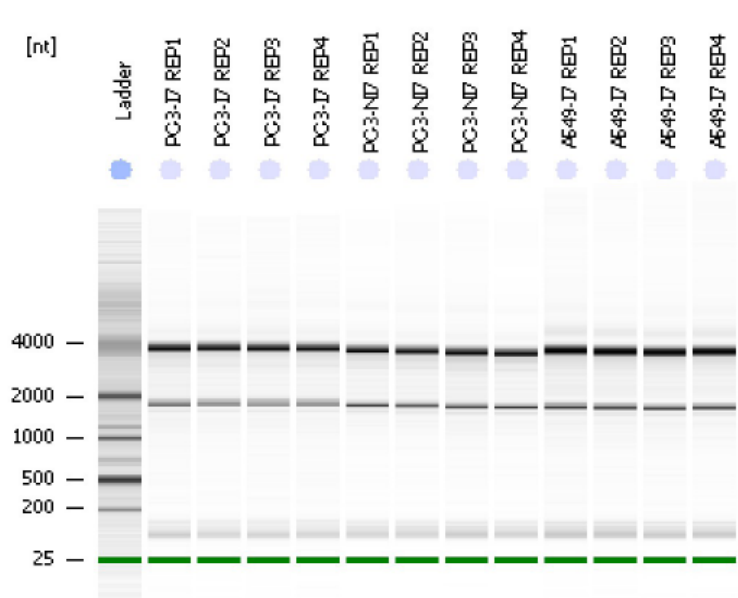
4.2 Identification and Validation of Differentially Expressed Metastasis-Related MiRNAs

4.2.1 Total RNA Quality Control Using Agilent Bioanalyzer

Only A549, PC-3 and MCF7 were selected to proceed to total RNA extraction for miRNA microarray analysis. Both MCF7 and MDA-MB-231 are breast cancer cell lines, MDA-MB-231 was filtered out due to the reasons of less migration and invasion capacities as compared to MCF7.

Gel matrix electrophoresis images of RNA samples by bioanalyzer analysis are shown in Figure 4.26. In Table 4.1, RNA integrity number (RIN) are listed for each four replicates of PC-3-I7, PC-3-NI7, A549-I7, A549-NI7, MCF7-I7 and MCF7-NI7 RNA samples. The RIN values of all samples were obtained between 8.9 to 9.7, which are above the minimum recommended RIN value of 7. Only three RNA samples for each sub-cell lines with better RNA quality were picked for miRNA microarray analysis based on RIN value and 28S/18S rRNA ratio.

(A)



(B)

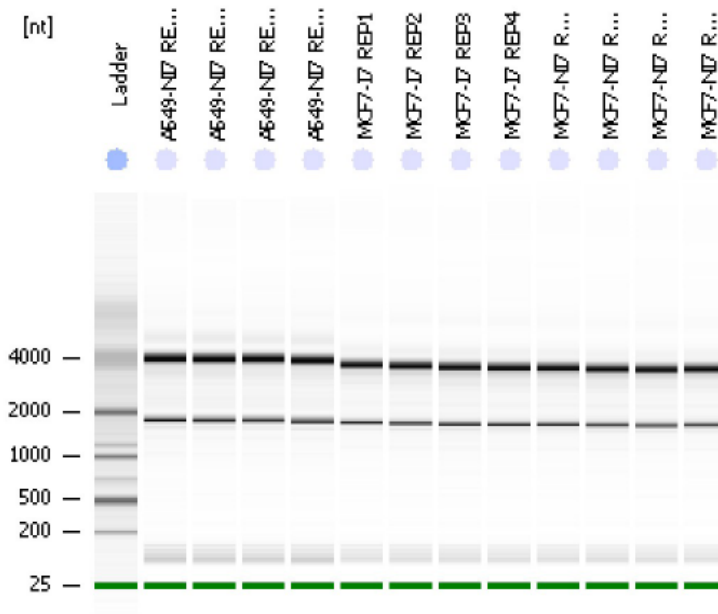


Figure 4.26: Bioanalyzer analysis of four replicates of total RNA extracted from high and low invasiveness sub-cell lines of PC-3, A549 and MCF7. (A) PC-3-I7, PC-3-NI7 and A549-I7; (B) A549-NI7, MCF7-I7 and MCF7-NI7.

Table 4.1: RIN range (0.0 min. to 10.0 max.) of total RNAs extracted from high and low invasiveness sub-cell lines of PC-3, A549 and MCF7 using Agilent Bioanalyzer 2100 RNA 6000 Nano kit.

Sub-cell line	Replicate	RNA Integrity Number (RIN)	Used for miRNA microarray
PC-3-I7	1	9.30	Yes
	2	9.50	Yes
	3	9.20	Yes
	4	9.30	No
PC-3-NI7	1	9.30	Yes
	2	9.20	Yes
	3	9.00	Yes
	4	8.90	No
A549-I7	1	9.40	Yes
	2	9.40	Yes
	3	9.30	No
	4	9.60	Yes
A549-NI7	1	9.30	No
	2	9.60	Yes
	3	9.70	Yes
	4	9.50	Yes
MCF7-I7	1	9.70	Yes
	2	9.40	No
	3	9.40	Yes
	4	9.60	Yes
MCF7-NI7	1	9.50	Yes
	2	9.50	No
	3	9.60	Yes
	4	9.60	Yes

4.2.2 MiRNA Microarray Analysis

In order to investigate the miRNAs potentially involved in lung, prostate and breast cancer invasion and migration, we examined global miRNA expression in both paired cell lines of A549, PC-3 and MCF7 using the miRNA microarray platform, GeneChip[®] miRNA Array. RNA samples were confirmed to be successfully biotinylated as seen by the blue substrate color intensity observed after 30 min of incubation using ELOSA assay before sample hybridization on GeneChip[®] miRNA Array (result not shown). These arrays revealed the expression of nearly thousand of human miRNAs in each sub-cell lines. CEL files were imported into Partek Genomic Suite v 6.4 (Partek Inc., St. Louis, MO) for analyses. Identifying differentially expressed miRNAs between paired sub-cell lines involved three major steps of normalization, preliminary analysis and statistical analysis. Normalization of miRNA array data was performed as robust-multichip average (RMA) for data normalization between triplicate samples which includes background adjustments, normalization and summarization. Principle component analysis (PCA) was carried out before statistical analysis. Later, a list of miRNAs with significantly differential expression between paired sub-cell lines were developed based on the criteria of gene expression ≥ 2.00 fold change and significant unadjusted p -values ≤ 0.05 using analysis of variance (ANOVA).

4.2.2.1 MiRNA Microarray Analysis of A549

The A549 microarray data distribution pattern was relatively close as shown in PCA plots of Figure 4.27. A total of 11 out of 846 human miRNAs were found to be differentially expressed with a fold change of ≥ 2.0 between A549-I7 and A549-NI7 with p -value < 0.05 . 6 miRNAs (miR-378, miR-671-5p, miR-25*, miR-92b, miR-106b* and miR-550*) were up-regulated with miR-378 displaying the highest fold change in A549-I7, while 5 miRNAs (miR-629*, miR-576-3p, miR-886-5p, miR-487b and miR-1827) were down-regulated in A549-I7 with miR-629* displaying the highest fold change (Table 4.2). MiRNA* known as passenger strand or complementary strand of the double-stranded RNA duplexes. Among 11 differentially expressed A549 metastasis-related miRNAs, 4 of them are miRNA*.

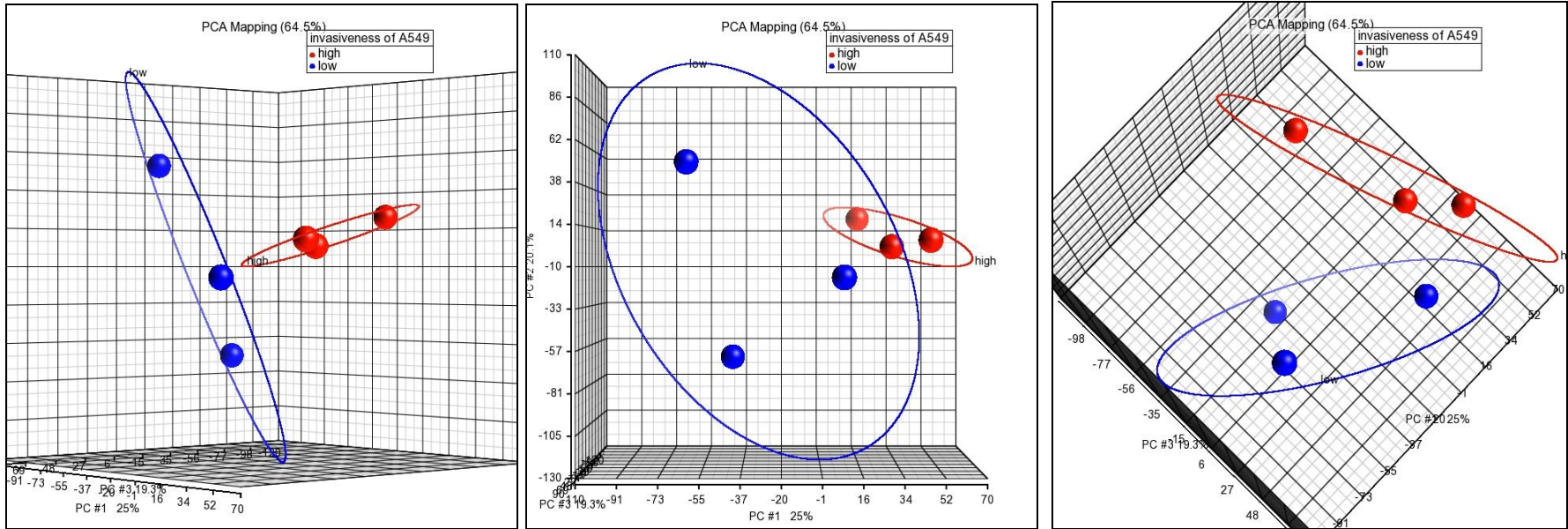


Figure 4.27: Three different plane views of PCA of A549-I7 (red) and A549-NI7 (blue) displayed the distribution of microarray data replicates.

Table 4.2: Differentially expressed metastasis-related miRNAs between A549-I7 and A549-NI7 with p -value ≤ 0.05 and fold change ≥ 2.0 filtering using Partek[®] Genomics Suite[™] software.

miRNA Expression in A549-I7	microRNAs	Fold change [†] (A549-I7/A549-NI7)	p -value
Up-regulated	miR-378	3.389	0.033
	miR-671-5p	2.852	0.001
	miR-25*	2.840	0.050
	miR-92b	2.600	0.004
	miR-106b*	2.500	0.011
	miR-550*	2.280	0.046
Down-regulated	miR-629*	-2.915	0.007
	miR-576-3p	-2.780	0.038
	miR-886-5p	-2.538	0.013
	miR-487b	-2.231	0.001
	miR-1827	-2.142	0.004

[†] Positive values denote up-regulation; negative values denote down-regulation.

4.2.2.2 MiRNA Microarray Analysis of PC-3

The PC-3 microarray data distribution pattern was relatively close as shown in PCA plots of Figure 4.28. A total of 20 out of 846 human miRNAs were found to be differentially expressed with a fold change of ≥ 2.0 between PC-3-I7 and PC-3-NI7 with p -value < 0.05 . 4 miRNAs (mir-129-1*, mir-606, mir-34b* and mir-19b-1) were up-regulated with miR-129-1* displaying the highest fold change in PC-3-I7, while 15 miRNAs (miR-320a, miR-132*, miR-744, miR-654, miR-409, miR-1180, miR-503, miR-423, miR-382, miR-487b, miR-409, miR-210, miR-342, miR-134, miR-379 and miR-708) were down-regulated in PC-3-I7 with miR-708 displaying the highest fold change (Table 4.3). Among 20 differentially expressed A549 metastasis-related miRNAs, 3 of them are miRNA* which also known passenger strand or complementary strand of the double-stranded RNA duplexes.

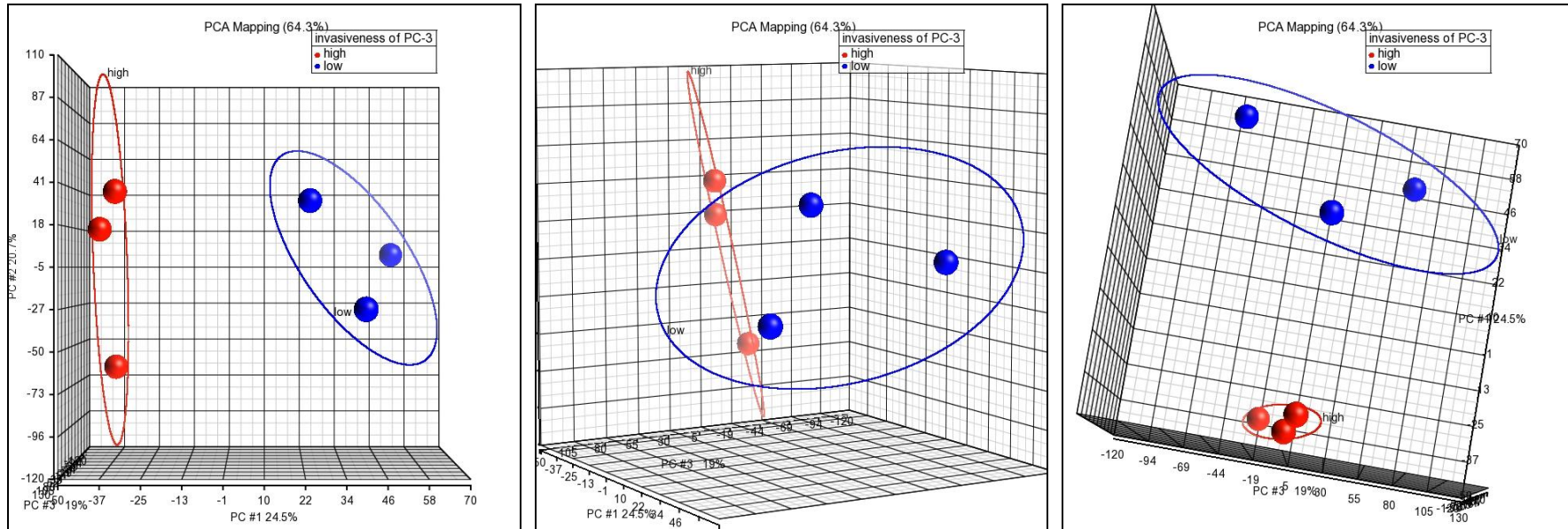


Figure 4.28: Three different plane views of PCA of PC-3-I7 (red) and PC-3-NI7 (blue) displayed the distribution of microarray data replicates.

Table 4.3: Differentially expressed metastasis-related miRNAs between PC-3-I7 and PC-3-NI7 with p -value ≤ 0.05 and fold change ≥ 2.0 filtering using Partek[®] Genomics Suite[™] software.

miRNA Expression in PC-3-I7	miRNAs	Fold change [†] (PC-3-I7/PC-3-NI7)	p -value
Up-regulated	miR-129-1*	3.227	0.026
	miR-606	2.784	0.005
	miR-34b*	2.263	0.001
	miR-19b-1	2.123	0.013
Down-regulated	miR-320a	-2.014	0.004
	miR-132*	-2.029	0.026
	miR-744	-2.206	0.019
	miR-654	-2.208	0.041
	miR-409	-2.287	0.011
	miR-1180	-2.330	0.045
	miR-503	-3.051	0.044
	miR-423	-3.528	0.016
	miR-382	-3.584	0.005
	miR-487b	-3.636	0.003
	miR-409	-4.358	0.000
	miR-210	-4.862	0.003
	miR-342	-6.492	0.034
	miR-134	-7.168	0.002
	miR-379	-7.530	0.000
	miR-708	-9.256	0.001

[†] Positive values denote up-regulation; negative values denote down-regulation.

4.2.2.3 MiRNA Microarray Analysis of MCF7

The MCF7 microarray data distribution pattern was relatively close as shown in PCA plots of Figure 4.29. A total of 32 out of 846 human miRNAs were found to be differentially expressed with a fold change of ≥ 2.0 between MCF7-I7 and MCF7-NI7 with p -value < 0.05 . 22 miRNAs (miR-302c*, miR-496, miR-135b, miR-324, miR-181d, miR-1252, miR-93, miR-376c, miR-30b*, miR-616, miR-664, miR-891b, miR-448, miR-543, miR-624, miR-624*, miR-1234, miR-199a-1, miR-578, miR-513a-1, miR-603 and miR-1231) were up-regulated with miR-302*c displaying the highest fold change in MCF7-I7, while 10 miRNAs (miR-183, miR-1827, miR-129-2, miR-1246, miR-519e*, miR-1247, miR-365a, miR-503, miR-152 and miR-10a) were down-regulated in MCF7-I7 with miR-10a displaying the highest fold change (Table 4.4). Among 32 differentially expressed A549 metastasis-related miRNAs, 3 of them are miRNA* which also known as passenger strand or complementary strand of the double-stranded RNA duplexes.

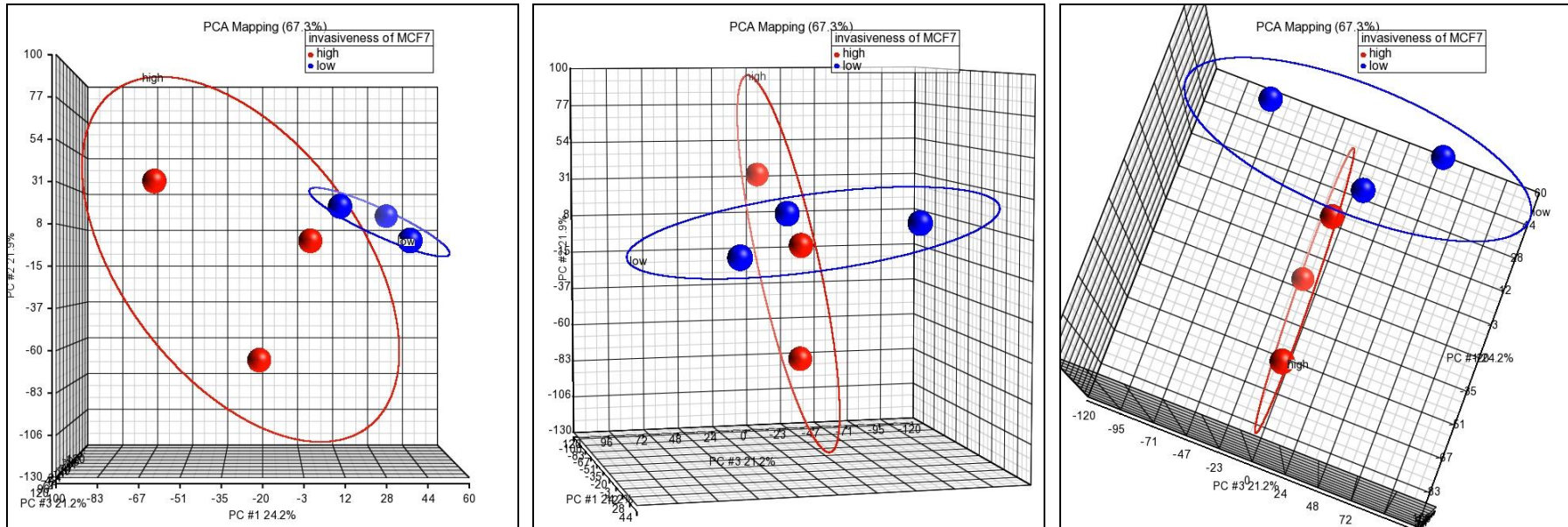


Figure 4.29: Three different plane views of PCA of MCF7-I7 (red) and MCF7-NI7 (blue) displayed the distribution of microarray data replicates.

Table 4.4: Differentially expressed metastasis-related miRNAs between MCF7-I7 and MCF7-NI7 with p -value ≤ 0.05 and fold change ≥ 2.0 filtering using Partek[®] Genomics Suite[™] software.

miRNA Expression in MCF7-I7	miRNAs	Fold change [†] (MCF7-I7/MCF7-NI7)	p-value
Up-regulated	miR-302c*	11.280	0.034
	miR-496	9.880	0.027
	miR-135b	9.478	0.001
	miR-324	8.572	0.015
	miR-181d	5.592	0.028
	miR-1252	5.272	0.027
	miR-93	5.098	0.044
	miR-376c	4.961	0.026
	miR-30b*	4.547	0.028
	miR-616	4.249	0.003
	miR-664	3.989	0.038
	miR-891b	3.931	0.017
	miR-448	3.618	0.004
	miR-543	3.307	0.023
	miR-624	3.032	0.012
	miR-624*	2.913	0.003
	miR-1234	2.732	0.020
	miR-199a-1	2.658	0.001
	miR-578	2.619	0.005
	miR-513a-1	2.233	0.007
miR-603	2.219	0.000	
miR-1231	2.139	0.018	
Down-regulated	miR-183	-2.575	0.008
	miR-1827	-2.777	0.017
	miR-129-2	-4.466	0.036
	miR-1246	-4.798	0.046
	miR-519e*	-6.161	0.017
	miR-1247	-7.007	0.021
	miR-365a	-9.723	0.001
	miR-503	-14.291	0.041
	miR-152	-15.518	0.000
	miR-10a	-137.587	0.001

[†] Positive values denote up-regulation; negative values denote down-regulation.

4.2.3 Quantitative Real-Time PCR

Out of three cell lines conducted, A549 were chosen for further analysis because less research work were carried out on miRNAs in lung cancer metastasis. Also, miRNAs such as miR-378 were found to be involved in regulating cancer metastasis in a recent research (Chen *et al.*, 2011). RNA concentration and the quality of RNA extracted from A548 were assessed by Nanodrop Spectrophotometer in Table 4.5. Microarray data of A549 were validated via Real-Time PCR on 4 representative miRNAs (miR-92b, miR-378, miR-671-5p and miR-1827) using RNU6B as an endogenous control (Figure 4.30).

4.2.3.1 Nanodrop Spectrophotometer

RNA samples were extracted from A549-I7 and A549-NI7. All RNA samples were diluted in 1:10 ratio with nuclease-free water before RNA quantification using Nanodrop Spectrophotometer 2000 (Thermo Scientific, USA). RNA purity can be assessed based on the absorbance ratio of 260/280 in Table 4.5.

Table 4.5: RNA concentration, absorbance and absorbance ratio of both A549-I7 and A549-NI7 using Nanodrop Spectrophotometer 2000 in three replicates.

RNA sample	Replicate	Concentration (ng/ μ l)	A ₂₆₀	A ₂₈₀	A ₂₆₀ /A ₂₈₀	A ₂₆₀ /A ₂₃₀
A549-I7	1	24.7	0.616	0.301	2.05	2.13
A549-I7	2	32.1	0.802	0.393	2.04	2.28
A549-I7	3	48.8	1.320	0.591	2.07	2.08
A549-NI7	1	57.4	1.436	0.702	2.04	2.21
A549-NI7	2	40.7	1.017	0.479	2.12	2.15
A549-NI7	3	55.6	1.466	0.711	2.06	2.20

4.2.3.2 Pearson Correlation Plot

Real-Time PCR data were in accordance with expression pattern of A549-I7 in relative to A549-NI7 with miRNA microarray data. Pearson correlation showed a high and positive correlation ($R=0.809$) between data generated by miRNA microarray and qRT-PCR, which confirmed the validity of all miRNA expression patterns obtained (Figure 4.31).

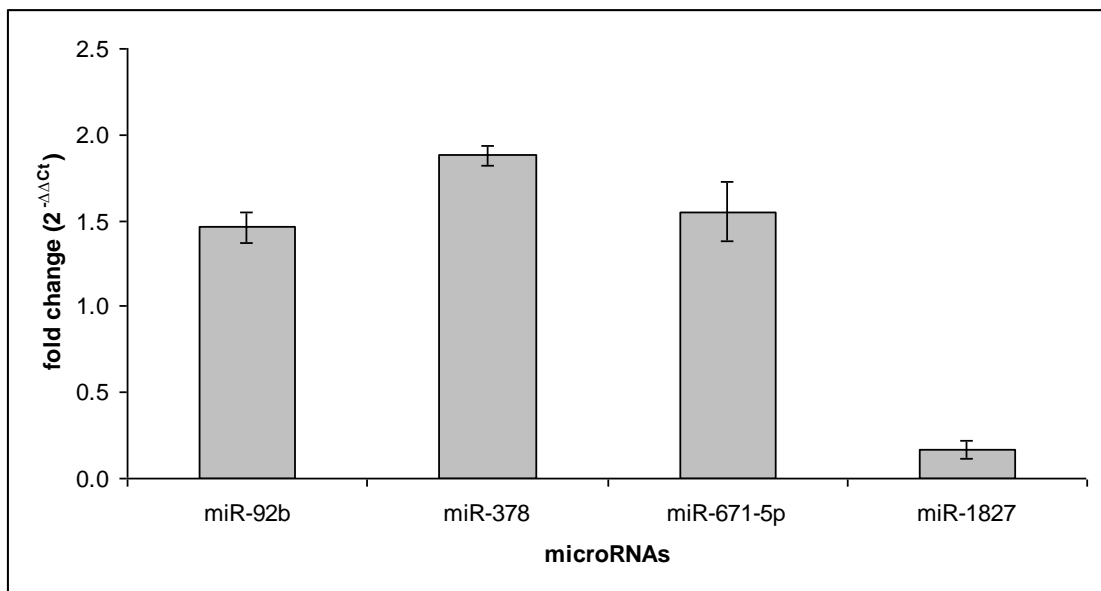


Figure 4.30: Four differentially expressed miRNAs (miR-92b, miR-378, miR-671-5p and miR-1827) between A549-I7 and A549-NI7 validated using Real-Time PCR.

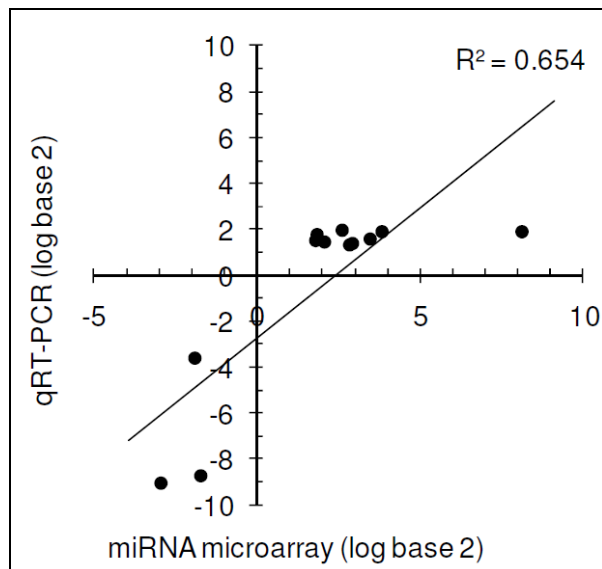


Figure 4.31: A pearson's correlation plot between miRNA microarray and Real-Time PCR data.

4.3 Predicted Targets of A549 Metastasis-Related MiRNAs Enriched in Metastasis-Related Signalling Pathways

4.3.1 Pathways Enrichment Analyses

A miRNA potentially act on several mRNA targets, that is, a single mRNA can be targeted by multiple miRNAs (Esquela-Kerscher and Slack, 2006). Based on growing evidences of co-operative miRNA activity, it is essential to perform pathway enrichment analysis to investigate combinatorial effects of all dysregulated miRNAs in cancer metastasis progression (Dombkowski *et al.*, 2011). Since combinatorial effects of different pathways govern the physiological and pathological outcomes of cancer progression, it is essential to have all miRNAs included for analysis using DIANA-mirPath (employed DIANA-microT-4.0 algorithm). DIANA-mirPath enriches the KEGG pathways downstream of differentially expressed miRNAs between A549-I7 and A549-NI7 cells, hence revealing the relationship between individual miRNAs and their influence on targeted genes. A descending list of the top eight cancer metastasis-related KEGG pathways based on a $-\ln(p\text{-values})$ score threshold of ≥ 3.00 of DIANA-mirPath (DIANA-microT-4.0), which corresponded to A549-I7 lung cancer invasion properties are summarized in Table 4.6. Enrichment of genes involved in cancer

metastasis-related pathways indicated possible involvement of Wnt/planar cell polarity (PCP), TGF- β , mitogen-activated protein kinase (MAPK), focal adhesion, adherens junction, mammalian target of rapamycin (mTOR), ECM receptor interaction and actin cytoskeleton regulation signalling pathways in cancer invasion and migration by dysregulated miRNAs.

Table 4.6: Top eight descending list of metastasis-related KEGG pathways that were predicted to be contribute in A549 cancer metastasis using the DIANA-mirPath algorithm employing DIANA-microT-4.0 as a prediction software with a $-\ln(p\text{-value})$ threshold of ≥ 3.00 .

KEGG pathway	$-\ln(p\text{-value})$ [†]
Wnt signalling pathway	23.63
TGF- β signalling pathway	15.94
MAPK signalling pathway	14.70
Focal adhesion	9.60
Adherens junctions	8.08
mTOR signalling pathway	7.01
ECM receptor interaction	4.12
Regulation of actin cytoskeleton	3.53

[†]*Input gene list of 10 miRNAs (miR-378, miR-671-5p, miR-25, miR-92b, miR-106b, miR-550, miR-629, miR-576-3p, miR-886-5p, miR-487b) except of miR-1827 which was not in the DIANA-mirPath algorithm gene input list.*

In Figure 4.32, a hypothetical signalling network showing the interaction of miRNAs and their putative targets in regulating A549 lung cancer metastasis using DIANA-mirPath (DIANA-microT-4.0) together with DIANA microT 4.0 and TargetScan 5.2 database with a $-\ln(p\text{-value})$ score of ≥ 3.00 , miTG score of ≥ 0.20 and total context score of ≤ -0.10 . All these miRNAs were proposed to act in concert to modulating pathways of non-canonical Wnt/PCP, TGF- β , integrin-FAK-Src, MAPK and mTOR signaling cascades to promote lung cancer migration and invasion. As negative regulators, targets of up-regulated miRNAs were largely found to be inhibitors of cancer progression and metastasis such as mRNAs encoding Smad7, Smad ubiquitin regulatory factors (Smurf), prickle and secreted frizzled-related protein (sFRP), while targets of down-regulated miRNAs were mainly of a pro-metastatic nature such as mRNAs encoding TGF- β , Wnt, frizzled (Fzd), KAI1 COOH-terminal interacting tetraspanin (KITENIN) and integrins.

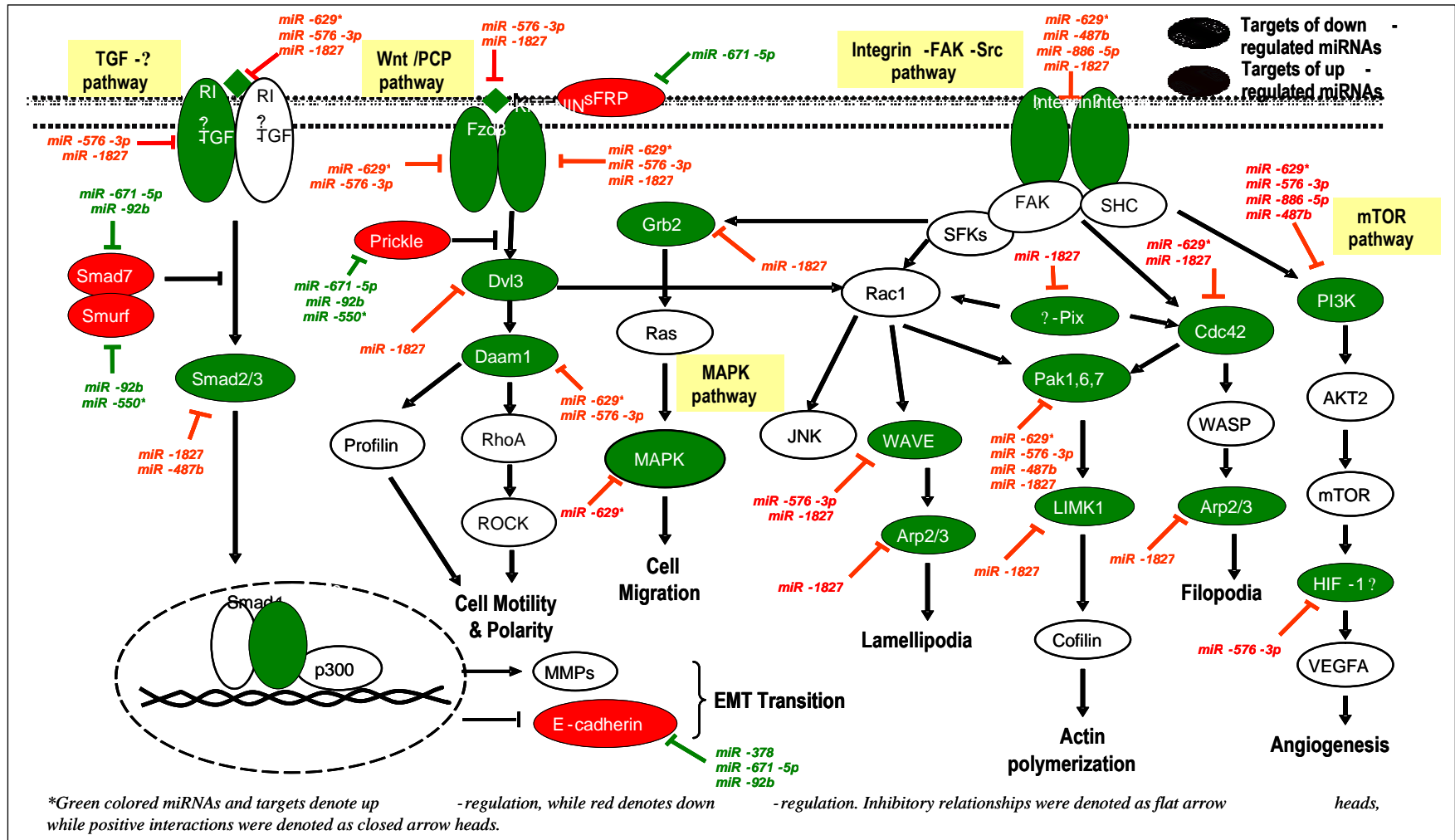


Figure 4.32: A hypothetical signalling network showing the interaction of miRNAs and their putative targets in regulating A549 lung cancer metastasis.

CHAPTER 5: DISCUSSION

Cancer metastasis involved complex process where primary cancerous cells successfully passed through all the sequential steps of detachment, migration, adhesion, invasion of ECM, extravasation to a distant organ parenchyma, angiogenesis and growth at secondary site (Ma & Weinberg, 2008). Even though past studies have focused on issues of metastasis, there are still no major breakthroughs in terms of preventing cancer metastasis. Thus, there is a great need to understand the molecular alterations in cancer invasion and metastasis that confer a poor prognosis.

In order to have a suitable cell line model to study the cancer metastatic process, we had established four set of high and low invasiveness cancer sub-cell lines from A549, PC-3, MCF7 and MDA-MB-231 cell lines with different potential in invasion and migration properties using serial transwell invasion approach (Figure 4.1 to 4.17). As the proliferation capacity of the parental and sub-cell lines were found to be the same, it might not contribute to the variation of invasion and migration properties of the sub-cell lines (Figure 4.18 to 4.25). Also, invasiveness of sub-cell lines were observed to possess weakened adhesion properties to cultures plates upon exposure to trypsin compared to low invasiveness cancer sub-cell lines and parental cell lines (result not shown). This may indicate that the cells from the highly invasive sub-cell lines has less adherence ability to cells or the ECM, which may facilitate them to break away easily and migrate or invade through the ECM.

Since the identification of miRNAs as master regulators of gene expression networks and recent implications of miRNAs in metastatic progression, therefore identification and characterization of miRNAs involved in cancer invasion and metastasis have been of great importance (Bracken *et al.*, 2009; Wentz-Hunter and Potashkin, 2011). MiRNA microarray analyses were performed to identify the involvement of miRNAs in cancer invasion and migration of lung, breast and prostate cancer cell lines. We obtained a list of differential expressed metastasis-related miRNAs for A549, PC-3 and MCF7. Given that each paired sub-cell lines with different metastatic potential were derived from a single parental cell line with similar genetic background, therefore the differentially expressed miRNAs population between the paired sub-cell lines might play a role in cancer invasion and migration.

5.1 Hypothetical A549 Lung Cancer Metastasis Signalling Network Model

Given that 75% to 85% of diagnosed lung cancers to-date are non-small cell lung cancer (NSCLC) with an increasing histopathological portion of it being adenocarcinoma subtypes (Koparal and Zeytinoglu, 2003; Berghmans *et al.*, 2011), thus a NSCLC adenocarcinoma cell line A549 was chosen in this study.

A549 miRNA microarray data revealed 4 out of 6 up-regulated miRNAs (miR-671-5p, miR-25*, miR-106b* and miR-550*) were found located at chromosome 7. This might indicate that the cell population of A549-I7 had more than 2 copies of chromosomes 7 since cytogenetics analysis revealed that A549 is an aneuploid human cell line that consist of multiple cells clones averaging a total of 62 to 72 of chromosomes in cells (Isaka *et al.*, 2003). MiRNA microarray data also revealed 4 miRNAs* strands (miR-25*, miR-106b*, miR-550* and miR-629*) out of 11 differentially expressed miRNAs (Table 4.2). During miRNA biogenesis, one strand of short RNA duplex is preferentially selected for entry into the silencing complex,

whereas the other strand known as miRNA* strand or passenger RNA is typically degraded and commonly viewed as non-functional. However, certain miRNA* strands have been reported as highly expressed mature functional miRNAs, which alters the overall miRNA/miRNA* ratio during the development of vertebrates (Guo and Lu, 2010; Yang *et al.*, 2011). Therefore, we are also reporting these four significantly expressed miRNA* in the pathway analysis to determine whether they might have an important functional role in regulating cancer metastasis.

Some of the differentially expressed miRNAs have been reported to play a role in regulating cancer metastasis progression. For example, in a recent research work done by Chen and co-workers (2011) have indicated that overexpression of miR-378 is associated with NSCLC brain metastasis by promoting cell migration, invasion and tumour angiogenesis, together with its potential use as a biomarker for characterizing NSCLC brain metastasis (Chen *et al.*, 2011). The over-expression of miR-378 in A549-I7 in this study was found to be in accordance with Chen *et al.*, 2011, where lower protein expression of suppressor of fused homolog (SuFu) was detected in miR-378 expressing A549 cells. TargetScan 5.2 algorithm suggested that SuFu encoding gene was a putative target of miR-378 with a context score of -0.14 [Appendix 9 (A)].

Among other miRNAs found to be down-regulated in A549-I7 including miR-1827, miR-487b and miR-886-5p, all of which have been reported to play a role in cancer progression and metastasis (Liang *et al.*, 2010; Gattolliat *et al.*, 2011; Xiong *et al.*, 2011). Attenuated interaction of miR-1827 with its 3' UTR target gene L-MYC oncogene was reported to be more vulnerable to develop small cell lung cancer (SCLC) (Xiong *et al.*, 2011). MiR-487b was significantly down-regulated in the high-risk neuroblastoma group and under-expression of miR-487b was proposed to be a biomarker of relapse among those classified as low-risk neuroblastoma patients (Gattolliat *et al.*, 2011). Besides that, under-expression of miR-886-5p was reported in

aggressive ovarian cancer cells with high invasive and metastatic capacity (Liang *et al.*, 2010).

In this study, A549 was chosen to study the possible signalling pathways regulated by these 11 differentially expressed miRNA for lung cancer metastasis using pathway enrichment analyses to predict miRNA:target gene interactions. Taking into account that miRNAs suppress expression of targeted genes, as a result it should have an inverse correlation between the expression level of a given miRNA and the expression level of its putative targets (Ritchie *et al.*, 2009). Based on past research works that reported gene expression during cancer metastasis, we included only expression of putative target genes that were inversely correlated with our miRNA expression to filtered out huge number of computationally predicted target genes from further analysis. Bioinformatics tools analysis together with literature surveys revealed the possible involvement of non-canonical Wnt/PCP, TGF- β , integrin-FAK-Src, MAPK and mTOR signalling as the key signalling pathways of these miRNAs in modulating A549 lung cancer metastasis.

5.1.1 Metastasis-Related MiRNAs in Relation To Wnt/PCP Signalling Pathway

Canonical Wnt pathway disruption leading to cancer progression was well documented in past research (Lee *et al.*, 2008). Recently, an accumulating amount of research evidence have revealed the importance of the previously unacknowledged role of aberrant non-canonical Wnt/PCP signalling activation in human cancer progression such as abnormal tissue polarity, invasion, metastasis, and angiogenesis independent of the involvement of β -catenin (Lee *et al.*, 2008; Wang *et al.*, 2009).

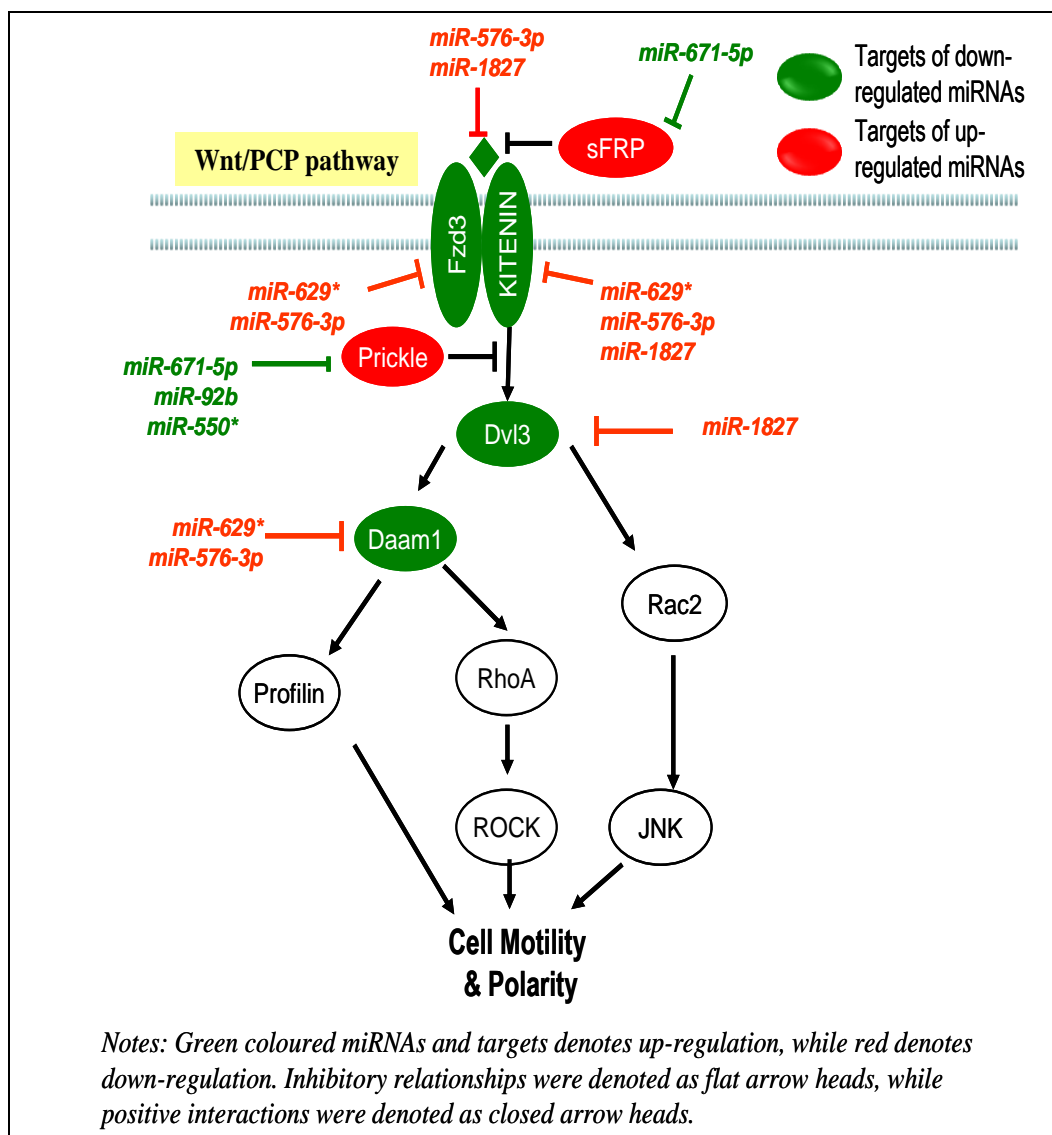


Figure 5.1: Illustration of hypothetical Wnt/PCP signalling pathway as regulated by a list of significantly expressed miRNAs.

According to DIANA-mirPath (MicroT-4.0) together with DIANA-microT 4.0 and TargetScan 5.2 prediction algorithm, we postulated these miRNAs are targeting the components of non-canonical Wnt/PCP pathway in order to modulate invasion and migration of A549-I7. This study has provided some initial evidence of Wnt-related miRNAs that has yet to be reported (miR-576-3p, miR-629* and miR-1827) and were found to be down-regulated in invasive A549-I7 cells. Among the putative targets of these miRNAs are mRNAs encoding Wnt-5A, Fzd3 receptors, KITENIN, Dvl3 and Daam1, all of which are predicted to be up-regulated since they are putatively targeted by the down-regulated miRNAs. Targets of up-regulated Wnt-related miRNAs (miR-671-5p, miR-92b and miR-550*) on the other hand, included mRNAs encoding for the two Wnt inhibitor of secreted frizzled-related proteins (sFRP) and prickles, which are both predicted to be down-regulated in A549-I7 cells (Figure 5.1).

Wnt-5A, Wnt-5B, and Wnt-11 are the non-canonical Wnt ligands transduce signals through it binding to Fzd3 or Fzd6 receptors to activate PCP pathway (Kotah, 2005). Studies have reported the role of Wnt-5A promoting metastasis through Rac and JNK activation in melanoma, gastric cancer, and breast cancer (Weeraratna *et al.*, 2002; Kurayoshi *et al.*, 2006; Pukrop *et al.*, 2006). In our study, we found that both miR-576-3p and miR-1827 which targets Wnt-5A were down-regulated in A549-I7 when compared to A549-NI7. Down-regulation of both miRNAs and a predicted up-regulation of Wnt-5A suggest that metastatic promotion might occur through non-canonical Wnt/PCP pathway activation in NSCLC.

sFRP is a negative regulator of Wnt signalling that prevents Wnt ligands from binding to Fzd receptor (Bhat *et al.*, 2007). Lower expression of sFRP4 was observed in the more aggressive form of endometrial stromal sarcoma (Hrzenjak *et al.*, 2004). Down-regulation of sFRP1 due to hypermethylation silencing of the associated promoter has been reported in NSCLC and mesothelioma (Lee *et al.*, 2004; Fukui *et al.*, 2005). In this study, the mRNA encoding sFRP4 was predicted to be targeted by up-regulated miR-671-5p, thus lower expression of sFRP4 was expected in A549-I7.

Past studies showed the three different Fzd (Fzd3, 6, and 7) are commonly up-regulated in HCC cells. Suppression of Fzd7 by small-interfering RNA (siRNA) in colon cancer cells reduced invasion and motility activities through both canonical and non-canonical Wnt signalling pathway (Bengochea *et al.*, 2008; Ueno *et al.*, 2009). A series of research found higher expression of Vangl1 (Van Gogh, *Drosophila*)-like 1 (VANGL1), renamed as KAI1 C-terminal interacting tetraspanin (KITENIN) in various metastatic lymph nodes and tissues. KITENIN play a potential role in promoting tumour invasion and metastasis by forming a functional complex with Dvl and PKC δ to modulate cell motility (Kho *et al.*, 2008; Lee *et al.*, 2009). Moreover, the metastasis-promoting function of KITENIN was validated by Lee and coworkers (2005) where siRNA silenced the expression of KITENIN can inhibit colon cancer metastasis in mice model experiment. Fzd3 and KITENIN protein expression were predicted to be up-regulated since their inhibitor regulators of miR-629*, miR-576-3p and miR-1827 were down-regulated in A549-I7, thus contribute to the invasion and metastatic capabilities of A549-I7.

Dvl homolog of Dvl-1, Dvl-2 and Dvl-3 are downstream effectors of Fzd receptors of PCP signalling. Significantly higher expression of Dvl-1 and Dvl-3 were reported in NSCLC clinical tumour specimens with nodal metastases and suppression of Dvl-1, -2 and -3 inhibits cell proliferation in human NSCLC cell lines (Uematsu *et al.*, 2003; Wang, 2009). Daam1, Profilin, RhoA/ROCK and Rac/JNK are also downstream effectors of PCP signalling that regulate cell movement via regulating stress fibers and actin cytoskeleton changes (Strutt *et al.*, 1997; Habas *et al.*, 2001; Habas *et al.*, 2003; Katoh, 2005; Sato *et al.*, 2006; Li *et al.*, 2011). Dvl-dependent Wnt/PCP signals are transduced to RhoA signalling cascade through Daam1 and Daam2 (Katoh, 2005). The mRNA of Dvl-3 and Daam1 were not inhibited by its endogenous inhibitors of down-regulated miR-629*, miR-576-3p and miR-1827 in A549-I7, allowing the expression of Dvl-3 and Daam1. Hence, activation of Wnt/PCP signalling pathway in A549-I7 was expected to transduce signals from Wnt ligands to the downstream effectors to activate profilin, RhoA/ROCK and Rac/JNK signalling cascade, that results in induction of actin cytoskeleton reorganization and cell movement of A549-I7 (Figure 5.1).

5.1.2 Metastasis-Related MiRNAs in Relation To TGF- β Signalling Pathway

TGF- β signalling pathway plays a biphasic role in tumour progression. TGF- β exerts anti-proliferative effects on normal epithelial cells and in early tumour development, but as tumours develop, they start to produce TGF- β , and TGF- β signalling promotes EMT, tumour invasiveness and metastases (Leivonen and Kähäri, 2007; Jeon and Jen, 2010).

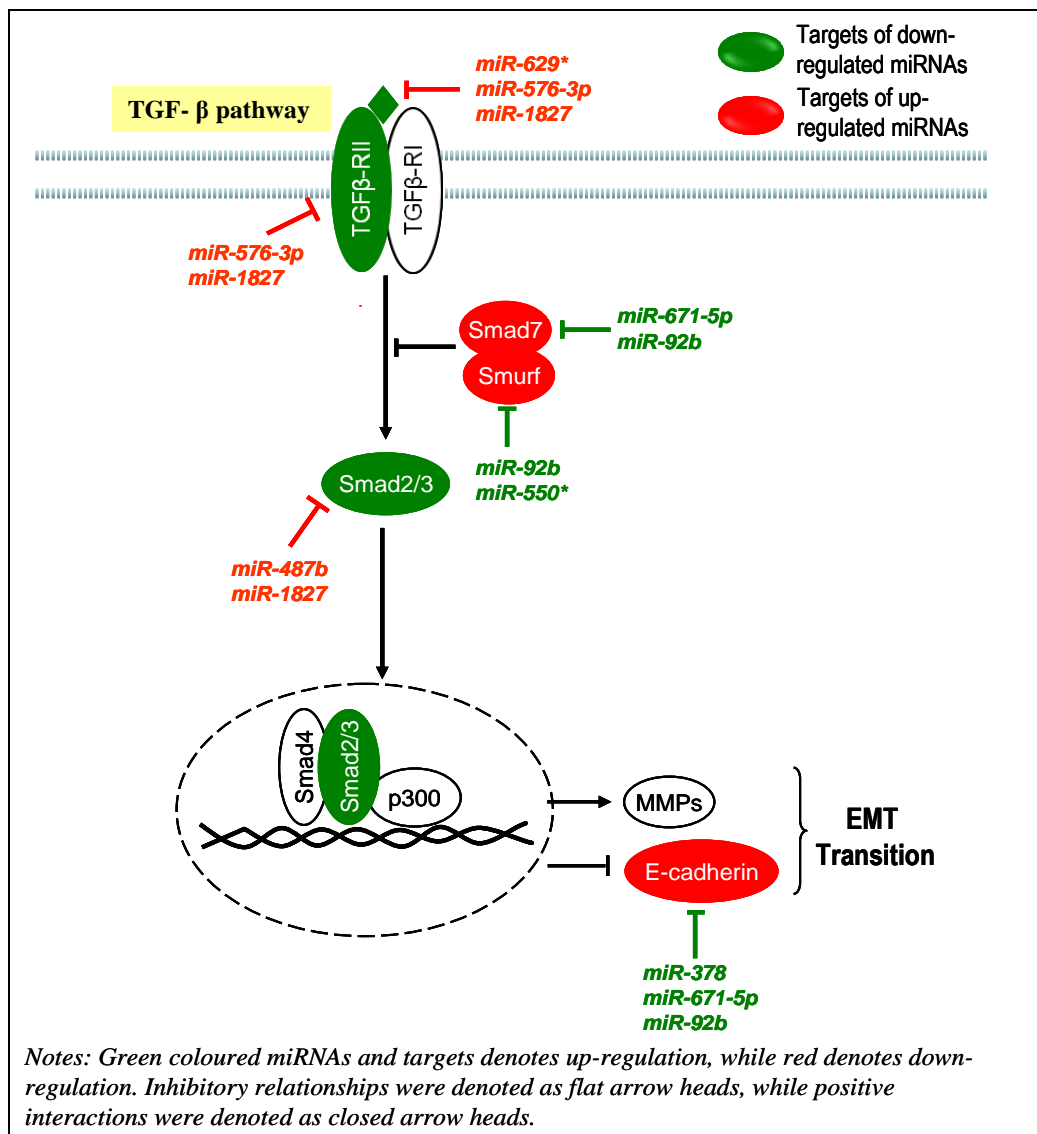


Figure 5.2: Illustration of hypothetical TGF- β signalling pathway as regulated by a list of significantly expressed miRNAs.

TGF- β ligands expression activates TGF- β signalling pathway to promote tumour invasion and metastasis, while inhibition of TGF- β and TGF- β -RII has been shown to suppress cancer metastasis (Biswas *et al.*, 2007; Leivonen and Kähäri, 2007; Xu *et al.*, 2011). In Figure 5.2, we reported that the down-regulated miR-629*, miR-576-3p and miR-1827 were predicted as endogenous inhibitors for both pro-metastatic proteins of TGF- β and TGF- β -RII. Therefore, activation of TGF- β signalling pathway was forecasted as the expression of pro-metastatic TGF- β and TGF- β -RII in A549-I7.

Past reports have also indicated that the inhibition of Smad3 or Smad2/3 in lung and breast cancer cell lines can lead to suppression of EMT and metastasis (Tian *et al.*, 2003; Reka *et al.*, 2010). Smad2 and Smad3 of A549-I7 were predicted to be targets of the down-regulated miR-487b and miR-1827, which promote invasive and metastatic properties.

Inhibition of metastasis and tumourigenesis in breast and melanoma cancers were observed with overexpression of Smad7. This associated with up-regulation of E-cadherin and down-regulation of MMP-2, MMP-9 and N-cadherin expression (Azuma *et al.*, 2005; Javelaud *et al.*, 2005). Smurf, an E3 ubiquitin ligase is another negative regulator of TGF- β signalling has been reported to work together with Smad7 to induce ubiquitination and degradation of Smad1, Smad2 and TGF- β family receptors (Ebisawa *et al.*, 2001; Shi *et al.*, 2004; Zhang *et al.*, 2007). Xu and colleagues reviewed that activated Smads mediate transcriptional regulation through transcription factors of Snail, ZEB and bHLH family, resulting in repression of expression epithelial marker gene (e.g. E-cadherin) and activation of mesenchymal gene expression (e.g. N-cadherin, fibronectin, MMPs) during loss of cell-cell adherence (Xu *et al.*, 2009). In this study, both negative regulators of TGF- β signalling, Smad7 and Smurf were predicted as the targets of three up-regulated miRNAs (miR-671-5p, miR-92b and miR-550*) in A549-I7 cells. This prevented TGF- β receptor degradation and allows nuclear translocation of

Smad2/3, hence, regulating the expression of EMT-related targets such as MMPs and E-cadherin proteins. E-cadherin is predicted as a target of three up-regulated miRNAs (miR-378, miR-671-5p and miR-92b) in A549-I7, thus further suppressing E-cadherin translation, resulting in the loss of cell-cell adhesion properties which might explain the observed weakened adhesion properties of A549-I7 during sub-culturing.

5.1.3 Metastasis-Related MiRNAs in Relation To Integrin Signalling Pathway

Tumour cell migration through tissue requires a combination of multiple cellular events where actin cytoskeleton is dynamically remodelled to produce the force necessary for cell migration (Pollard and Borisy, 2003).

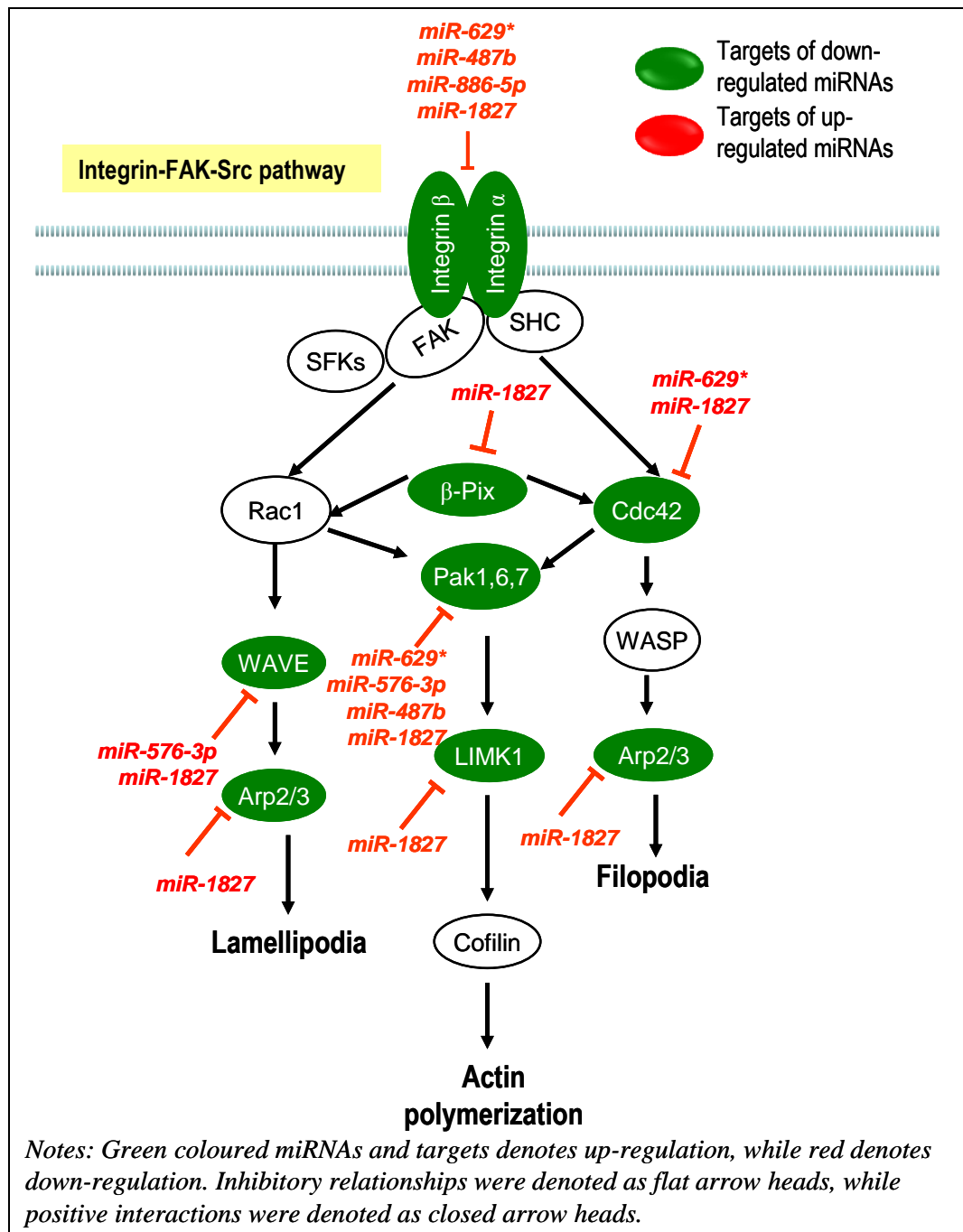


Figure 5.3: Illustration of hypothetical integrin signalling pathway as regulated by a list of significantly expressed miRNAs.

The heterodimers transmembrane receptors of integrin (α and β) are fundamental for cell invasion and migration and has been implicated in the progression of cancer invasion and metastasis. For example, over-expression of integrin $\alpha v \beta 3$ heterodimers were reported in the more metastatic human melanoma cells and ectopic expression of αv or $\beta 3$ integrin subunit able to increase metastatic potential of melanoma cell line (Gehlsen *et al.*, 1992; Filardo *et al.*, 1995; Neto *et al.*, 2007). Also, past research found integrin $\beta 8$ subunit plays a critical role in brain angiogenesis as ablation of this protein can interrupt brain blood vessel formation (Zhu *et al.*, 2002). Target prediction analyses have predicted four down-regulated miRNAs (miR-629*, miR-487b, miR-886-5p and miR-1827) targeting mRNAs encoding heterodimeric transmembrane receptor integrin subunits (Figure 5.3). Up-regulation of integrin expression and clustering triggers downstream activation of integrin-FAK-Src intracellular signalling cascade in A549-I7 cells, encouraging cells to loosen their adhesion to the ECM and acquire a migratory and invasive phenotype (Hood and Cheresch, 2002).

The best characterized mammalian Rho GTPases are RhoA, Rac, and Cdc42 which could regulate reorganization of the actin cytoskeleton to form stress fibers, lamellipodia, and filopodia, respectively (Nobes and Hall, 1995; Ridley, 2006). Rac1 and Cdc42 activation depend on the ligation of integrins, whereas Rho is activated by integrins, syndecan-4 or other cell-surface receptors (Hood and Cheresch, 2002). Overexpression of RhoA, Rac1, and Cdc42 were associated with carcinogenesis and tumour progression (Fritz *et al.*, 1999). Price and colleagues (1998) shown that activation of Rac and Cdc42 by intergin promoted cell spreading. β -p21-activated kinase-interacting exchange factor (β -Pix) is a guanine nucleotide exchange factor (GEF) for both GTPases of Rac1 and Cdc42 -targeting and -activating proteins. The binding of β -Pix with Rac1 to regulates membrane ruffles and focal adhesions for cell spreading (ten Klooster *et al.*, 2006). Wiskott-Aldrich syndrome protein family

verprolin-homologous protein (WAVE) and Arp2/3 complex, are primary effectors of Rac1 for cell migration and invasion through actin polymerization to form lamellipodia protrusions at the leading edge that push the cell membrane forward (Takenawa and Miki, 2001; Suetsugu *et al.*, 2002). Researchers reported WAVEs function as a metastasis-promoting protein downstream of Rac where knockdown of either WAVE2 or WAVE3 resulted in significant decrease cell motility, migration and invasive properties (Kurusu *et al.*, 2005; Sossey-Alaoui *et al.*, 2007). Recently, Sossey-Alaoui and coworkers demonstrated an inverse correlation between WAVE3 and miRNAs of miR-200 and miR-31 expression levels in invasive *versus* non-invasive cancer cells where miRNAs play a crucial role in cancer cell invasion by regulating WAVE3 expression leading to cytoskeleton remodeling (Sossey-Alaoui *et al.*, 2009; Sossey-Alaoui *et al.*, 2011). In our study, β -pix was predicted to be a putative target of the down-regulated miR-1827 and therefore β -pix was expected to have an increased expression and binding with Rac to mediate cell spreading in A549-I7. The down-regulated miR-1827 and miR-576-3p were predicted to target the downstream targets of Rac1 (WAVE2, WAVE3 and Arp2/3), thus up-regulating the expression of WAVEs and Arp2/3. As a result, β -Pix together with WAVE complex and Arp2/3 promote the formation of lamellipodia in A549-I7 during cell migration.

The activation of p21-activated kinase (Pak) is one of the important downstream effector of Rac and Cdc42 to regulate cytoskeletal reorganization at the leading edge of migratory cells (Sells *et al.*, 1997; Bokoch, 2003). Pak1 and pPak levels are increased in aggressive papillary thyroid cancers invasive fronts and the activity of PAK has been linked to regulate tumour invasiveness and motility of various human cancer cell lines (Kumar *et al.*, 2006; McCarty *et al.*, 2010). Pak as well as Rho, Rac, Cdc42, and ROCK can then trans-phosphorylate and activate LIM kinase (LIMK) (Bernard, 2007). Several reports indicate LIMK promotes cell invasion *in vitro* where higher LIMK expression

level in invasive prostate and breast cancer cell lines in comparison with less invasive cells were observed (Davila *et al.*, 2003; Yoshioka *et al.*, 2003). *In vivo* studies showed increased in LIMK induces tumour metastases (Bagheri-Yarmand *et al.*, 2006). MiR-629*, miR-487b, miR-576-3p, and miR-1827 were predicted to target Pak1, Pak6, Pak7 and LIMK1 and their expression are expected to be up-regulated in A549-I7 to promote signal transduction cascade for actin polymerization.

On the other hand, studies showed that Cdc42 activates Neural Wiskott-Aldrich syndrome protein (N-WASP), a WASP members of nucleation proteins, forms a complex with Arp2/3 in promoting actin polymerization, filopodia formation, cell motility, and invasion (Lorenz *et al.*, 2004; Yamaguchi *et al.*, 2005). Both miR-629* and miR-1827 were predicted to target mRNA encoding Cdc42, β -pix and Arp2/3 complex. Therefore, β -pix, Cdc42 and Arp2/3 complex were supposed to over-express in A549-I7 and lead to the formation of filopodia that facilitate cancer migration.

5.1.4 Metastasis-Related MiRNAs in Relation To MAPK and mTOR Signalling Pathways

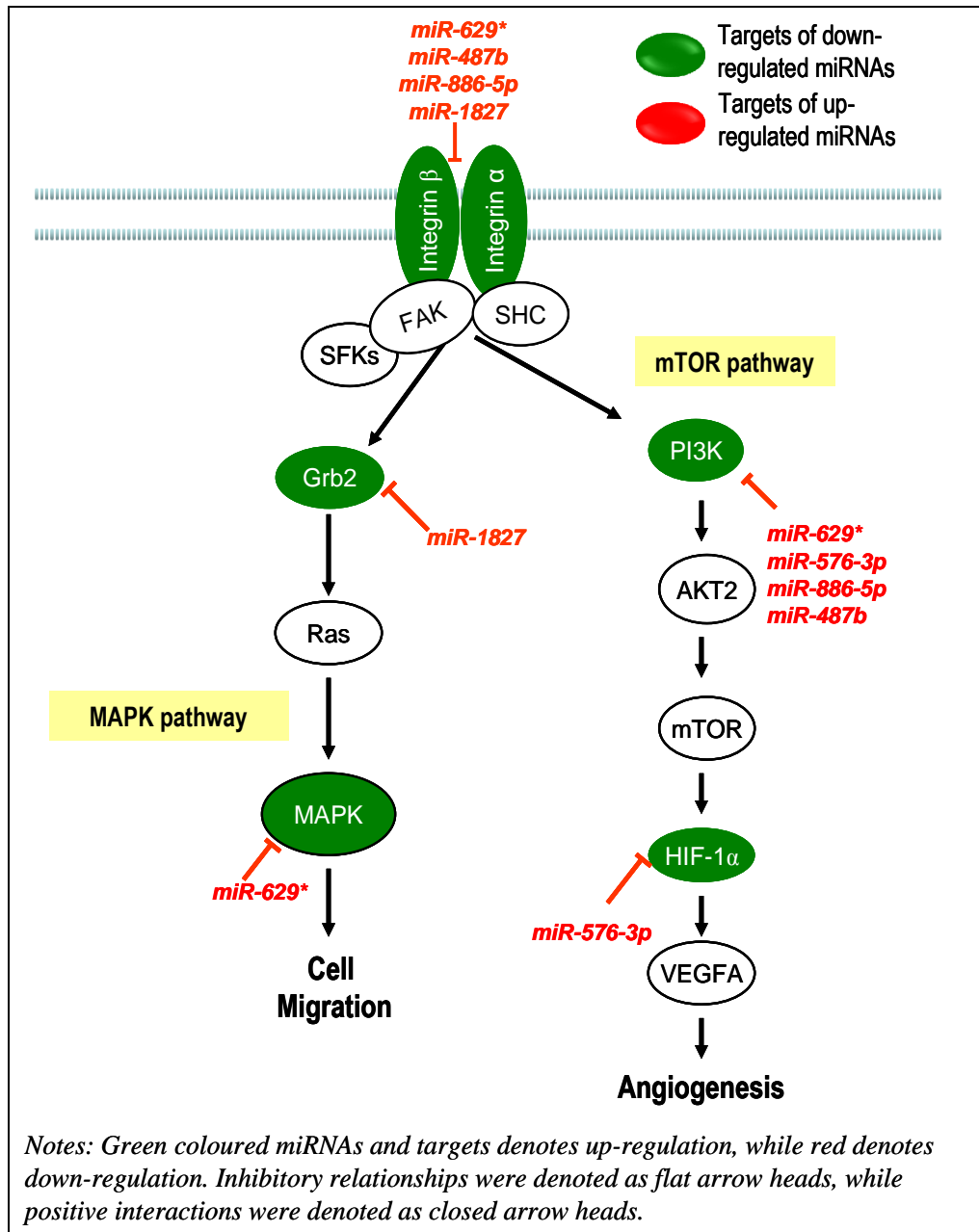


Figure 5.4: Illustration of hypothetical MAPK and mTOR signalling pathways as regulated by a list of significantly expressed miRNAs.

Past reports have shown that integrin together with FAK cross-talk with other signalling pathways to promote cancer cell migration, invasion and metastasis (Eliceiri, 2001). Integrin binding can induce FAK auto-phosphorylation and creates a binding site to recruit Src family kinases (SFKs), the largest of the non-receptor-tyrosine-kinase. Additionally, SFK can also phosphorylate additional sites in FAK, leading to the recruitment of the Grb2 adaptor molecule, which in turn activates multiple downstream signalling pathways including the MAPK pathway (Schlaepfer *et al.*, 1994; Guo *et al.*, 2004). In our study, down-regulated miR-1827 and miR-629* were predicted to target Grb-2 and MAPK expression respectively, thus activating the MAPK pathway which functions to promote myosin light-chain kinase (MLCK) phosphorylation and enhance cell migration, which was consistent with the aggressive invasion and migration properties of A549-I7 (Figure 5.4) (Klemke *et al.*, 1997; Schlaepfer *et al.*, 1998).

Besides the MAPK pathway, Meng and colleagues (2009) also demonstrated FAK cross-talks with Src to regulate the PI3K/AKT pathway to promote A549 lung cancer cells migration and invasion (Meng *et al.*, 2009). PI3K was predicted to be targeted by miR-629*, miR-576-3p, miR-886-5p and miR-487b and thus up-regulation of PI3K was predicted to occur in A549-I7. Finally, the hypoxia-inducible factor 1 α (HIF-1 α) which is a downstream target of the mTOR pathway cascade, was also deduced as a putative target of miR-576-3p (Figure 5.4). An uninhibited expression of HIF-1 α was predicted which consequently leads to the activation of VEGF expression, a commonly known potent mediator of angiogenesis (reviewed by Karar and Maity, 2009).

In this study, only miRNAs that have inverse correlation expression level with their predicted targets that reported in past research were included in the hypothetical signalling network in Figure 4.32. miRNAs that have contradictory expression level with their putative targets DIANA-microT 4.0 and TargetScan 5.2 were omitted from the hypothetical pathway. For example, TargetScan 5.2 predicted both down-regulated miR-1827 with context score of -0.17 and up-regulated miR-671-5p with context score of -0.21 are targeting mRNA encoding Pak6 protein. Also, WAVE2 was the putative target of both miR-1827 with context score of -0.36 and miR-671-5p with context score of -0.10 [Appendix 9 (A)]. Since both Pak6 and WAVE2 were reported to be up-regulated in highly metastatic cells, hence only down-regulated miR-1827 was included into the hypothetical pathway regardless of the context score. Also, an up-regulated miR-671-5p (with miTG score of 0.377) and 2 down-regulated miRNAs of miR-576-3p (with miTG score of 0.214) and miR-1827 (with miTG score of 0.445) are predicted targeting mRNA encoding TGF- β -RII according to DIANA-microT 4.0 algorithm [Appendix 9 (B)]. Here, only miR-576-3p and miR-1827 were included in the hypothetical signalling network since up-regulation of TGF- β II was reported in aggressive cells.

5.2 Future Perspectives

Our results provide novel insights of these metastasis-related miRNAs work in concert to regulate signalling network for cancer metastasis. Target and pathway prediction analyses are helpful to narrow down targets and pathways. Based on this hypothetical signalling network, we can later select candidate miRNAs for further investigation and refine the miRNA functions via functional experiments.

Prior to functional studies, a few other popular target prediction algorithms such as miRanda and PicTar can be employed to further filter out the list of putative targets of candidate miRNAs from the proposed hypothetical signalling network. First, the expression of the selected candidate miRNAs will need to examine their expression pattern in lung cancer patients using Real-Time PCR analysis on clinical metastatic tumour tissues with normal tissues. Luciferase assay will be performed to examine whether a predicted target gene by target prediction algorithms is a functional target of candidate miRNA. Over-expression or inhibition of endogenous miRNAs by transfecting sub-cell lines with mimics and antagomiRs will be performed in order to examine if changing endogenous miRNA expression can change the abilities of invasion and migration. Real-Time PCR will then be performed to detect mature putative miRNA expression of transfected-cells to monitor transfection efficiency. Soon after, transwell invasion assay, wound healing assay and cell proliferation assay will be performed to assess invasion, migration and proliferation properties of cells transfected with the candidate miRNA between non-transfected cells. Western blotting will be performed to detect the proteins expression of putative target genes of a candidate miRNAs.

Pathway enrichment analysis predicted the involvement of miR-1827 in all three major pathways of Wnt/PCP, TGF- β and integrin-Fak-Src signalling. Also, miRNA microarray revealed miR-1827 was found to be differentially under-expressed in MCF7-I7. Taken together, it is interesting to investigate the function of miR-1827 among all down-regulated miRNAs as a candidate miRNA to perform functional study. However, miR-1827 was the lowest expression among the 4 validated miRNAs as it needed 30 ng as a starting material to perform Real-Time PCR in this study. This phenomenon can be explain when a slight decrease of the endogenous miR-1827 expression in cells can drastically change actin cytoskeleton distribution as well as activate EMT to gain metastatic properties.

On the other hand, miR-487b is another potential anti-metastatic miRNAs for both lung and prostate cancer where miRNA microarray also revealed miR-487b expression was down-regulated in PC-3-I7. According to pathway enrichment analysis, miR-487b mainly targeting TGF- β and integrin signalling cascade in regulate EMT and actin polymerization. Therefore, it is interested to find out the actual functional role of miR-487b in lung and prostate cancer invasion and migration by carried out functional studies in future.

The miRNA* of miR-629* was also shown to be a potential anti-metastatic miRNA according to pathway enrichment analysis. MiR-629* expression has the highest fold change among down-regulated miRNAs. Pathway enrichment analysis revealed miR-629* might potentially act on all three major signalling pathways of non-canonical Wnt/PCP, TGF- β and integrin signalling cascades predicted by algorithm to regulate actin polymerization and cell motility. Thus, miR-629* is another potential candidate miRNA to perform further studies on.

Among the up-regulated miRNAs, miR-92b was found to be most potential pro-metastatic miRNAs as it was predicted to targeting many important molecule components of TGF- β and non-canonical Wnt/PCP signalling pathways. Thus, miR-92b is a potential candidate of up-regulated miRNA to perform functional studies in future.

MiR-25* and miR-106b* are among 11 differentially expressed miRNAs that do not have any putative targets in the hypothetical signalling network of Figure 4.32. This two miRNAs can be omitted from functional studies in future since both TargetScan 5.2 and DIANA-microT 4.0 did not predicted both miR-25* and miR-106b* in the proposed hypothetical signalling network.

Besides studying the mechanism of miRNAs in regulating cancer invasion and migration, the establishment of high and low invasiveness sub-cell lines also provides an excellent platform to investigate the other molecular aspects of migration and invasion in lung, breast and prostate cancer. Also, miRNAs microarray expression validation will need to perform on the differentially expressed miRNAs of PC-3 and MCF7 using Real-Time PCR in future. Later, pathway enrichment analysis, candidate miRNAs selection and functional studies will be performed on PC-3 and MCF7 respectively.

CHAPTER 6: CONCLUSION

In this study, we have identified a list of differentially expressed miRNAs between high and low invasiveness sub-cell lines of A549, PC-3 and MCF7. A hypothetical pathway network was proposed for A549 lung adenocarcinoma cell line, which provided novel insights of how these metastasis-related miRNAs work in concert to regulate the metastasis signalling network for lung cancer metastasis. Overall, data in this study provided valuable information not only with regards to the development of therapies involving miRNA control elements to stop tumor invasion and metastasis, but also for the development of potential candidate metastatic markers for lung cancer classification and prognosis as well. Pathway enrichment analysis was helpful to narrow down putative targets and pathways, and candidate miRNAs can be selected for further studies of experiments verifications to investigate the mechanism of miRNAs with its downstream targets in contribution to A549 lung cancer invasion and metastasis particularly in pathways such as the TGF- β , non-canonical Wnt/PCP and integrin-FAK-Src intracellular signalling cascade.

REFERENCES

- Ananthkrishnan, R., & Ehrlicher, A. (2007). The forces behind cell movement. *International Journal of Biological Sciences*, 3(5), 303-317.
- Araki, K., Shimura, T., Suzuki, H., Tsutsumi, S., Wada, W., Yajima, T., Kobayahi, T., Kubo, N. & Kuwano, H. (2011). E/N-cadherin switch mediates cancer progression via TGF- β -induced epithelial-to-mesenchymal transition in extrahepatic cholangiocarcinoma. *British Journal of Cancer*, 105(12), 1885-1893.
- Asangani, I. A., Rasheed, S. A., Nikolova, D. A., Leupold, J. H., Colburn, N. H., Post, S. & Allgayer, H. (2008). MicroRNA-21 (miR-21) post-transcriptionally downregulates tumor suppressor Pcd4 and stimulates invasion, intravasation and metastasis in colorectal cancer. *Oncogene*, 27(15), 2128-2136.
- Azuma, H., Ehata, S., Miyazaki, H., Watabe, T., Maruyama, O., Imamura, T., Sakamoto, T., Kiyama, S., Kiyama, Y., Ubai, T., Inamoto, T., Takahara, S., Itoh, Y., Otsuki, Y., Katsuoka, Y., Miyazono, K. & Horie, S. (2005). Effect of Smad7 expression on metastasis of mouse mammary carcinoma JyMC(A) cells. *Journal of the National Cancer Institute*, 97(23), 1734-1746.
- Bagheri-Yarmand, R., Mazumdar, A., Sahin, A. A. & Kumar, R. (2006). LIM kinase 1 increases tumor metastasis of human breast cancer cells via regulation of the urokinase-type plasminogen activator system. *International Journal of Cancer*, 118(11), 2703-2710.
- Baldi, E., Bonaccorsi, L. & Forti, G. (2003). Androgen receptor: good guy or bad guy in prostate cancer invasion? *Endocrinology*, 144(5), 1653-1655.
- Bandyopadhyay, A., Agyin, J. K., Wang, L., Tang, Y., Lei, X., Story, B. M., Cornell, J. E., Pollock, B. H., Mundy, G. R. & Sun, L. Z. (2006). Inhibition of pulmonary and skeletal metastasis by a transforming growth factor-beta type I receptor kinase inhibitor. *Cancer Research*, 66(13), 6714-6721.
- Baranwal, S., & Alahari, S. K. (2010). miRNA control of tumor cell invasion and metastasis. *International Journal of Cancer*, 126(6), 1283-1290.
- Bhaumik, D., Scott, G. K., Schokrpur, S., Patil, C. K., Campisi, J. & Benz, C. C. (2008). Expression of microRNA-146 suppresses NF-kappaB activity with reduction of metastatic potential in breast cancer cells. *Oncogene*, 27(42), 5643-5647.
- Bengochea, A., de Souza, M. M., Lefrançois, L., Le Roux, E., Galy, O., Chemin, I., Kim, M., Wands, J. R., Trepo, C., Hainaut, P., Scoazec, J. Y., Vitvitski, L. & Merle, P. (2008). Common dysregulation of Wnt/Frizzled receptor elements in human hepatocellular carcinoma. *British Journal of Cancer*, 99(1), 143-150.
- Berghmans, T., Paesmans, M. & Sculier, J. P. (2011). Prognostic factors in stage III non-small cell lung cancer: a review of conventional, metabolic and new biological variables. *Therapeutic Advances in Medical Oncology*, 3(3), 127-138.

- Bernard, O. (2007). Lim kinases, regulators of actin dynamics. *The International Journal of Biochemistry & Cell Biology*, 39(6), 1071-1076.
- Bhaumik, D., Scott, G. K., Schokrpur, S., Patil, C. K., Campisi, J. & Benz, C. C. (2008). Expression of microRNA-146 suppresses NF-kappaB activity with reduction of metastatic potential in breast cancer cells. *Oncogene*, 27(42), 5643-5647.
- Bhat, R. A., Stauffer, B., Komm, B. S. & Bodine, P. V. (2007). Structure-function analysis of secreted frizzled-related protein-1 for its Wnt antagonist function. *Journal of Cellular Biochemistry*, 102(6), 1519-1528.
- Biswas, S., Guix, M., Rinehart, C., Dugger, T. C., Chytil, A., Moses, H. L., Freeman, M. L. & Arteaga, C. L. (2007). Inhibition of TGF-beta with neutralizing antibodies prevents radiation-induced acceleration of metastatic cancer progression. *The Journal of Clinical Investigation*, 117(5), 1305-1313.
- Bokoch, G. M. (2003). Biology of the p21-activated kinases. *Annual Review of Biochemistry*, 72, 743-781.
- Bozzuto, G., Ruggieri, P. & Molinari, A. (2010). Molecular aspects of tumor cell migration and invasion. *Annali dell'Istituto Superiore di Sanita*, 46(1), 66-80.
- Bracken, C. P., Gregory, P. A., Khew-Goodall, Y. & Goodall, G. J. (2009). The role of microRNAs in metastasis and epithelial-mesenchymal transition. *Cellular and Molecular Life Sciences*, 66(10), 1682-1699.
- Bubendorf, L., Schöpfer, A., Wagner, U., Sauter, G., Moch, H., Willi, N., Gasser, T. C. & Mihatsch, M. J. (2000). Metastatic patterns of prostate cancer: an autopsy study of 1,589 patients. *Human Pathology*, 31(5), 578-583.
- Calin, G. A., & Croce C. M. (2006). MicroRNA signatures in human cancers. *Nature Reviews Cancer*, 6(11), 857-866.
- Cance, W. G., Harris, J. E., Iacocca, M. V., Roche, E., Yang, X., Chang, J., Simkins, S. & Xu, L. (2000). Immunohistochemical analyses of focal adhesion kinase expression in benign and malignant human breast and colon tissues: correlation with preinvasive and invasive phenotypes. *Clinical Cancer Research*, 6(6), 2417-2423.
- Cao, P., Deng, Z., Wan, M., Huang, W., Cramer, S. D., Xu, J., Lei, M. & Sui, G. (2010). MicroRNA-101 negatively regulates Ezh2 and its expression is modulated by androgen receptor and HIF-1alpha/HIF-1beta. *Molecular Cancer*, 9, 108.
- Chen, L. T., Xu, S. D., Xu, H., Zhang, J. F., Ning, J.F. & Wang, S. F. (2011). MicroRNA-378 is associated with non-small cell lung cancer brain metastasis by promoting cell migration, invasion and tumor angiogenesis. *Medical Oncology*, DOI: 10.1007/s12032-011-0083-x.
- Chuah, C. H., Mok, J. S. L., Liew, S. L., Ong, H. C., Yong, H. S. & Goh, S. H. (2006). *101 Plants to Fight Cancer*. An SBC Publication. ISBN 978-983-40638-2-5.

- Cunnick, G. H., Jiang, W. G., Douglas-Jones, T., Watkins, G., Gomez, K. F., Morgan, M. J., Subramanian, A., Mokbel, K. & Mansel, R. E. (2008). Lymphangiogenesis and lymph node metastasis in breast cancer. *Molecular Cancer*, 7, 23.
- Davila, M., Frost, A. R., Grizzle, W. E. & Chakrabarti, R. (2003). LIM kinase 1 is essential for the invasive growth of prostate epithelial cells: implications in prostate cancer. *The Journal of Biological Chemistry*, 278(38), 36868-36875.
- Derynck, R., & Zhang, Y. E. (2003). Smad-dependent and Smad-independent pathways in TGF-beta family signalling. *Nature*, 425(6958), 577-584.
- Dews, M., Homayouni, A., Yu, D., Murphy, D., Seignani, C., Wentzel, E., Furth, E. E., Lee, W. M., Enders, G. H., Mendell, J. T. & Thomas-Tikhonenko, A. (2006). Augmentation of tumor angiogenesis by a Myc-activated microRNA cluster. *Nature Genetics*, 38(9), 1060-1065.
- Ding, Y., Milosavljevic, T. & Alahari, S. K. (2008). Nischarin inhibits LIM Kinase to regulate cofilin phosphorylation and cell invasion. *Molecular and Cellular Biology*, 28(11), 3742-3756.
- Dombkowski, A. A., Sultana, Z., Craig, D. B. & Jamil, H. (2011). In silico analysis of combinatorial microRNA activity reveals target genes and pathways associated with breast cancer metastasis. *Cancer Informatics*, 10, 13-29.
- Du, L., & Pertsemlidis, A. (2010). MicroRNAs and lung cancer: tumors and 22-mers. *Cancer and Metastasis Reviews*, 29(1), 109-122.
- Ebisawa, T., Fukuchi, M., Murakami, G., Chiba, T., Tanaka, K., Imamura, T. & Miyazono, K. (2001). Smurf1 interacts with transforming growth factor-beta type I receptor through Smad7 and induces receptor degradation. *The Journal of Biological Chemistry*, 276(16), 12477-12480.
- Eliceiri, B. P. (2001). Integrin and growth factor receptor crosstalk. *Circ Res*, 89(12):1104-1110.
- Er, O., Frye, D. K., Kau, S. W., Broglio, K., Valero, V., Hortobagyi, G. N. & Arun, B. (2008). Clinical course of breast cancer patients with metastases limited to the liver treated with chemotherapy. *The Cancer Journal*, 14(1), 62-68.
- Espina, C., Céspedes, M. V., García-Cabezas, M. A., Gómez del Pulgar, M. T., Boluda, A., Oroz, L. G., Benitah, S. A., Cejas, P., Nistal, M., Manges, R., Lacal, J. C.. A critical role for Rac1 in tumor progression of human colorectal adenocarcinoma cells. *The American Journal of Pathology*, 172(1), 156-166.
- Esquela-Kerscher, A., & Slack, F. J. (2006). Oncomirs - microRNAs with a role in cancer. *Nature Reviews Cancer*, 6(4), 259-269.
- Filardo, E. J., Brooks, P. C., Deming, S. L., Damsky, C. & Cheresch, D. A. (1995). Requirement of the NPXY motif in the integrin beta 3 subunit cytoplasmic tail for melanoma cell migration in vitro and in vivo. *The Journal of Cell Biology*, 130(2), 441-450.

- Fish, J. E., Santoro, M. M., Morton, S. U., Yu, S., Yeh, R. F., Wythe, J. D., Ivey, K. N., Bruneau, B. G., Stainier, D. Y. & Srivastava, D. (2008). miR-126 regulates angiogenic signaling and vascular integrity. *Developmental Cell*, 15(2), 272-284.
- Frankel, L. B., Christoffersen, N. R., Jacobsen, A., Lindow, M., Krogh, A. & Lund, A. H. (2008). Programmed cell death 4 (PDCD4) is an important functional target of the microRNA miR-21 in breast cancer cells. *The Journal of Biological Chemistry*, 283(2), 1026-1033.
- Friedl, P., & Bröcker, E. B. (2000). The biology of cell locomotion within three-dimensional extracellular matrix. *Cellular and Molecular Life Sciences*, 57(1), 41-64.
- Fritz, G., Just, I. & Kaina, B. (1999). Rho GTPases are over-expressed in human tumors. *International Journal of Cancer*, 81(5), 682-687.
- Fukui, T., Kondo, M., Ito, G., Maeda, O., Sato, N., Yoshioka, H., Yokoi, K., Ueda, Y., Shimokata, K. & Sekido, Y. (2005). Transcriptional silencing of secreted frizzled related protein 1 (SFRP 1) by promoter hypermethylation in non-small-cell lung cancer. *Oncogene*, 24(41), 6323-6327.
- Gabriely, G., Wurdinger, T., Kesari, S., Esau, C. C., Burchard, J., Linsley, P. S. & Krichevsky, A. M. (2008). MicroRNA 21 promotes glioma invasion by targeting matrix metalloproteinase regulators. *Molecular and Cellular Biology*, 28(17), 5369-5380.
- Gattolliat, C. H., Thomas, L., Ciafrè, S. A., Meurice, G., Le Teuff, G., Job, B., Richon, C., Combaret, V., Dessen, P., Valteau-Couanet, D., May, E., Busson, P., Douc-Rasy, S. & Bénard, J. (2011). Expression of miR-487b and miR-410 encoded by 14q32.31 locus is a prognostic marker in neuroblastoma. *British Journal of Cancer*, 105(9), 1352-1361.
- Gebäck, T., Schulz, M. M., Koumoutsakos, P. & Detmar, M. (2009). TScratch: a novel and simple software tool for automated analysis of monolayer wound healing assays. *Biotechniques*, 46(4), 265-274.
- Gehlsen, K. R., Davis, G. E. & Sriramarao, P. (1992). Integrin expression in human melanoma cells with differing invasive and metastatic properties. *Clinical and Experimental Metastasis*, 10(2), 111-120.
- Gregory, R. I., & Shiekhattar, R. (2005). MicroRNA biogenesis and cancer. *Cancer Research*, 65(9), 3509-3512.
- Gregory, P. A., Bert, A. G., Paterson, E. L., Barry, S. C., Tsykin, A., Farshid, G., Vadas, M. A., Khew-Goodall, Y., Goodall, G. J. (2008). The miR-200 family and miR-205 regulate epithelial to mesenchymal transition by targeting ZEB1 and SIP1. *Nature Cell Biology*, 10(5), 593-601.
- Guo, W., & Giancotti, F. G. (2004). Integrin signalling during tumour progression. *Nat Rev Molecular and Cellular Biology*, 5(10), 816-826.

- Guo, L., & Lu, Z. (2010). The fate of miRNA* strand through evolutionary analysis: implication for degradation as merely carrier strand or potential regulatory molecule? *PLoS One*, 5(6), e11387.
- Gupta, G. P., & Massagué, J. (2006). Cancer Metastasis: Building a Framework. *Cell*, 127(4), 679-685.
- Habas, R., Kato, Y. & He, X. (2001). Wnt/Frizzled activation of Rho regulates vertebrate gastrulation and requires a novel Formin homology protein Daam1. *Cell*, 107(7), 843-854.
- Habas, R., Dawid, I. B. & He, X. (2003). Coactivation of Rac and Rho by Wnt/Frizzled signaling is required for vertebrate gastrulation. *Genes & Development*, 17(2), 295-309.
- Habas, R., & Dawid, I. B. (2005). Dishevelled and Wnt signaling: is the nucleus the final frontier? *Journal of Biology*, 4(1), 2.
- Halbleib, J. M., & Nelson, W. J. (2006). Cadherins in development: cell adhesion, sorting, and tissue morphogenesis. *Genes & Development*, 20(23), 3199-3214.
- Hanahan, D., & Weinberg, R. A. (2000). The hallmarks of cancer. *Cell*, 100(1), 57-70.
- Hayashi, H., Abdollah, S., Qiu, Y., Cai, J., Xu, Y. Y., Grinnell, B. W., Richardson, M. A., Topper, J. N., Gimbrone, M. A. Jr., Wrana, J. L. & Falb, D. (1997). The MAD-related protein Smad7 associates with the TGFbeta receptor and functions as an antagonist of TGFbeta signaling. *Cell*, 89(7), 1165-1173.
- Heasman, S. J. & Ridley, A. J. (2008). Mammalian Rho GTPases: new insights into their functions from in vivo studies. *Nature Review Molecular Cell Biology*, 9(9), 690-701.
- Heneghan, H. M., Miller, N., Lowery, A. J., Sweeney, K. J. & Kerin, M. J. (2009). MicroRNAs as Novel Biomarkers for Breast Cancer. *Journal of Oncology*, doi:10.1155/2010/950201.
- Hood, J. D., & Cheresch, D. A. (2002). Role of integrins in cell invasion and migration. *Nature Review Cancer*, 2(2):91-100.
- Hrzenjak, A., Timpl, M., Kremser, M. L., Strohmeier, B., Guelly, C., Neumeister, D., Lax, S., Moinfar, F., Tabrizi, A. D., Isadi-Moud, N., Zatloukal, K. & Denk, H. (2004). Inverse correlation of secreted frizzled-related protein 4 and beta-catenin expression in endometrial stromal sarcomas. *The Journal of Pathology*, 204(1), 19-27.
- Huang, Q., Gumireddy, K., Schrier, M., le Sage, C., Nagel, R., Nair, S., Egan, D. A., Li, A., Huang, G., Klein-Szanto, A. J., Gimotty, P. A., Katsaros, D., Coukos, G., Zhang, L., Puré, E. & Agami, R. (2008). The microRNAs miR-373 and miR-520c promote tumour invasion and metastasis. *Nature Cell Biology*, 10(2), 202-210.

- Huang, T. H., Wu, F., Loeb, G. B., Hsu, R., Heidersbach, A., Brincat, A., Horiuchi, D., Lebbink, R. J., Mo, Y. Y., Goga, A. & McManus, M. T. (2009). Up-regulation of miR-21 by HER2/neu signaling promotes cell invasion. *The Journal of Biological Chemistry*, 284(27), 18515-18524.
- Hurst, D. R., Edmonds, M. D., Scott, G. K., Benz, C. C., Vaidya, K. S. & Welch, D. R. (2009). Breast cancer metastasis suppressor 1 up-regulates miR-146, which suppresses breast cancer metastasis. *Cancer Research*, 69(4), 1279-1283.
- Hwang, H. W., & Mendell, J. T. (2006). MicroRNAs in cell proliferation, cell death, and tumorigenesis. *British Journal of Cancer*, 96(6), 776-780.
- Imamura, T., Takase, M., Nishihara, A., Oeda, E., Hanai, J., Kawabata, M. & Miyazono, K. (1997). Smad6 inhibits signalling by the TGF-beta superfamily. *Nature*, 389(6651), 622-626.
- Isaka, T., Nestor, A. L., Takada, T. & Allison, D. C. (2003). Chromosomal variations within aneuploid cancer lines. *Journal of Histochemistry and Cytochemistry*, 51(10), 1343-1353.
- Javelaud, D., Delmas, V., Möller, M., Sextius, P., André, J., Menashi, S., Larue, L. & Mauviel, A. (2005). Stable overexpression of Smad7 in human melanoma cells inhibits their tumorigenicity in vitro and in vivo. *Oncogene*, 24(51), 7624-7629.
- Jemal A, Bray F, Center MM, Ferlay J, Ward E, Forman D. (2011). Global cancer statistics. *CA: A Cancer Journal for Clinicians* 61(2), 69-90.
- Jeon, H. S., & Jen, J. (2010). TGF-beta signaling and the role of inhibitory Smads in non-small cell lung cancer. *Journal of Thoracic Oncology*, 5(4), 417-419.
- Jing, Y., Han, Z., Zhang, S., Liu, Y. & Wei, L. (2011). Epithelial-Mesenchymal Transition in tumor microenvironment. *Cell & Bioscience*, 1, 29.
- Kalluri, R., & Weinberg, R. A. (2009). The basics of epithelial-mesenchymal transition. *The Journal of Clinical Investigation*, 119(6), 1420-1428.
- Kamangar, F., Dores, G. M. & Anderson, W. F. (2006). Patterns of cancer incidence, mortality, and prevalence across five continents: defining priorities to reduce cancer disparities in different geographic regions of the world. *Journal of Clinical Oncology*, 24(14), 2137-2150.
- Karar, J., & Maity, A. (2009). Modulating the tumor microenvironment to increase radiation responsiveness. *Cancer Biology & Therapy*, 8(21), 1994-2001.
- Kato, Y., Habas, R., Katsuyama, Y., Näär, A. M. & He, X. (2002). A component of the ARC/Mediator complex required for TGF beta/Nodal signalling. *Nature*, 418(6898), 641-646.
- Katoh, M. (2005). WNT/PCP signaling pathway and human cancer (review). *Oncology Reports*, 14(6), 1583-1588.

- Kho, D. H., Bae, J. A., Lee, J. H., Cho, H. J., Cho, S. H., Lee, J. H., Seo, Y. W., Ahn, K. Y., Chung, I. J. & Kim, K. K. (2009). KITENIN recruits Dishevelled/PKC delta to form a functional complex and controls the migration and invasiveness of colorectal cancer cells. *Gut*, 58(4), 509-519.
- Klemke, R. L., Cai, S., Giannini, A. L., Gallagher, P. J., de Lanerolle, P., Cheresch, D. A. (1997). Regulation of cell motility by mitogen-activated protein kinase. *The Journal of Cell Biology*, 137(2), 481-492.
- Komiya, Y., & Habas, R. (2008). Wnt signal transduction pathways. *Organogenesis*, 4(2), 68-75.
- Koparal, A. T., & Zeytinoglu, M. (2003). Effects of Carvacrol on a Human Non-Small Cell Lung Cancer (NSCLC) Cell Line, A549. *Cytotechnology*, 43(1-3), 149-154.
- Korpala, M., Lee, E. S., Hu, G. & Kang, Y. (2008). The miR-200 family inhibits epithelial-mesenchymal transition and cancer cell migration by direct targeting of E-cadherin transcriptional repressors ZEB1 and ZEB2. *The Journal of Biological Chemistry*, 283(22), 14910-14914.
- Krichevsky, A. M., & Gabriely, G. (2009). miR-21: a small multi-faceted RNA. *Journal of Cellular and Molecular Medicine*, 13(1), 39-53.
- Kumar, R., Gururaj, A. E. & Barnes, C. J. (2006). p21-activated kinases in cancer. *Nature Reviews Cancer*, 6(6), 459-471.
- Kurayoshi, M., Oue, N., Yamamoto, H., Kishida, M., Inoue, A., Asahara, T., Yasui, W. & Kikuchi, A. (2006). Expression of Wnt-5a is correlated with aggressiveness of gastric cancer by stimulating cell migration and invasion. *Cancer Research*, 66(21), 10439-10448.
- Kurusu, S., Suetsugu, S., Yamazaki, D., Yamaguchi, H., Takenawa, T. (2005). Rac-WAVE2 signaling is involved in the invasive and metastatic phenotypes of murine melanoma cells. *Oncogene*, 24(8), 1309-1319.
- Lagerwaard, F. J., Levendag, P. C., Nowak, P. J., Eijkenboom, W. M., Hanssens, P. E. & Schmitz, P. I. (1999). Identification of prognostic factors in patients with brain metastases: a review of 1292 patients. *International Journal Radiation Oncology *Biology* Physics*, 43(4), 795-803.
- Lai, S. L., Chien, A. J. & Moon, R. T. (2009). Wnt/Fz signaling and the cytoskeleton: potential roles in tumorigenesis. *Cell Research*, 19(5), 532-545.
- Larue, L., & Bellacosa, A. (2005). Epithelial-mesenchymal transition in development and cancer: role of phosphatidylinositol 3' kinase/AKT pathways. *Oncogene*, 24(50), 7443-7454.
- Le Clainche, C., & Carlier, M. F. (2008). Regulation of actin assembly associated with protrusion and adhesion in cell migration. *Physiological Reviews*, 88(2), 489-513.

- Lee, A. Y., He, B., You, L., Dadfarmay, S., Xu, Z., Mazieres, J., Mikami, I., McCormick, F. & Jablons, D. M. (2004). Expression of the secreted frizzled-related protein gene family is downregulated in human mesothelioma. *Oncogene*, 23(39), 6672-6676.
- Lee, J. H., Cho, E. S., Kim, M. Y., Seo, Y. W., Kho, D. H., Chung, I. J., Kook, H., Kim, N. S., Ahn, K. Y. & Kim, K. K. (2005). Suppression of progression and metastasis of established colon tumors in mice by intravenous delivery of short interfering RNA targeting KITENIN, a metastasis-enhancing protein. *Cancer Research*, 65(19), 8993-9003.
- Lee, J. K., Bae, J. A., Sun, E. G., Kim, H. D., Yoon, T. M., Kim, K., Lee, J. H., Lim, S. C. & Kim, K. K. (2009). KITENIN increases invasion and migration of mouse squamous cancer cells and promotes pulmonary metastasis in a mouse squamous tumor model. *FEBS Letters*, 583(4), 711-717.
- Lee, E. H., Chari, R., Lam, A., Ng, R. T., Yee, J., English, J., Evans, K. G., Macaulay, C., Lam, S. & Lam, W. L. (2008). Disruption of the non-canonical WNT pathway in lung squamous cell carcinoma. *Clinical Medicine: Oncology*, 2008(2), 169-179.
- Leivonen, S. K., & Kähäri, V. M. (2007). Transforming growth factor-beta signaling in cancer invasion and metastasis. *International Journal of Cancer*, 121(10), 2119-2124.
- Levy, L., & Hill, C. S. (2006). Alterations in components of the TGF-beta superfamily signaling pathways in human cancer. *Cytokine & Growth Factor Reviews*, 17(1-2), 41-58.
- Lewis, B. P., Burge, C. B. & Bartel, D. P. (2005). Conserved seed pairing, often flanked by adenosines, indicates that thousands of human genes are microRNA targets. *Cell*, 20(1), 15-20.
- Li, D., Hallett, M. A., Zhu, W., Rubart, M., Liu, Y., Yang, Z., Chen, H., Haneline, L. S., Chan, R. J., Schwartz, R. J., Field, L. J., Atkinson, S. J. & Shou, W. (2011). Dishevelled-associated activator of morphogenesis 1 (Daam1) is required for heart morphogenesis. *Development*, 138(2), 303-315.
- Liang, S. H., Li, J., Al-beit, M., Zhang, J., Ma, D. & Lu, X. (2010). Screening and identification of potential miRNA involved in ovarian cancer invasion and metastasis. *Zhonghua Zhong Liu Za Zhi*, 32(9), 650-654.
- Liu, S., Kumar, S. M., Lu, H., Liu, A., Yang, R., Pushparajan, A., Guo, W. & Xu, X. (2012). MicroRNA-9 up-regulates E-cadherin through inhibition of NF- κ B1-Snail1 pathway in melanoma. *The Journal of Pathology*, 226(1), 61-72.
- Lorenz, M., Yamaguchi, H., Wang, Y., Singer, R. H. & Condeelis, J. (2004). Imaging sites of N-wasp activity in lamellipodia and invadopodia of carcinoma cells. *Current Biology*, 14(8), 697-703.

- Lu, Z., Liu, M., Stribinskis, V., Klinge, C. M., Ramos, K. S., Colburn, N. H. & Li, Y. (2008). MicroRNA-21 promotes cell transformation by targeting the programmed cell death 4 gene. *Oncogene*, 27(31), 4373-4379.
- Ma, M., Shen, J., Jiang, L., Han, B., Bai, H., Ji, H., Zhao, Y., Jin, B., Yu, Y., Pei, J. & Zhang, W. (2006). Prognostic factors in patients with stage IV non-small cell lung cancer. *The Chinese-German Journal Clinical Oncology*, 5(5), 319-323.
- Ma, L., Teruya-Feldstein, J. & Weinberg, R. A. (2007). Tumour invasion and metastasis initiated by microRNA-10b in breast cancer. *Nature*, 449(7163), 682-688.
- Ma, L., & Weinberg, R. A. (2008). Micromanagers of malignancy: role of microRNAs in regulating metastasis. *Trends in Genetics*, 24(9), 448-456.
- Ma, L., Young, J., Prabhala, H., Pan, E., Mestdagh, P., Muth, D., Teruya-Feldstein, J., Reinhardt, F., Onder, T. T., Valastyan, S., Westermann, F., Speleman, F., Vandesompele, J. & Weinberg, R. A. (2010). miR-9, a MYC/MYCN-activated microRNA, regulates E-cadherin and cancer metastasis. *Nature Cell Biology*, 12(3), 247-256.
- Maragkakis, M., Vergoulis, T., Alexiou, P., Reczko, M., Plomaritou, K., Gousis, M., Kourtis, K., Koziris, N., Dalamagas, T. & Hatzigeorgiou, A. G. (2011). DIANA-microT Web server upgrade supports Fly and Worm miRNA target prediction and bibliographic miRNA to disease association. *Nucleic Acids Research*, 39, W145-148.
- Mizejewski, G. J. (1999). Role of integrins in cancer: survey of expression patterns. *Proceedings of the Society for Experimental Biology and Medicine*, 222(2), 124-138.
- McCarty, S. K., Saji, M., Zhang, X., Jarjoura, D., Fusco, A., Vasko, V. V. & Ringel, M. D. (2010). Group I p21-activated kinases regulate thyroid cancer cell migration and are overexpressed and activated in thyroid cancer invasion. *Endocrine-Related Cancer*, 17(4), 989-999.
- Meng, F., Henson, R., Wehbe-Janek, H., Ghoshal, K., Jacob, S. T. & Patel, T. (2007). MicroRNA-21 regulates expression of the PTEN tumor suppressor gene in human hepatocellular cancer. *Gastroenterology*, 133(2), 647-658.
- Meng, X. N., Jin, Y., Yu, Y., Bai, J., Liu, G. Y., Zhu, J., Zhao, Y. Z., Wang, Z., Chen, F., Lee, K. Y. & Fu, S. B. (2009). Characterisation of fibronectin-mediated FAK signalling pathways in lung cancer cell migration and invasion. *British Journal of Cancer*, 101(2), 327-334.
- Moul, J. W. (2000). Prostate specific antigen only progression of prostate cancer. *Journal of Urology*, 163(6), 1632-1642.
- Muraoka-Cook, R. S., Kurokawa, H., Koh, Y., Forbes, J. T., Roebuck, L. R., Barcellos-Hoff, M. H., Moody, S. E., Chodosh, L. A. & Arteaga, C. L. (2004). Conditional overexpression of active transforming growth factor beta1 in vivo accelerates metastases of transgenic mammary tumors. *Cancer Research*, 64(24), 9002-9011.

- Neto, D. S., Pantaleão, L., de Sá, B. C. & Landman, G. (2007). Alpha-v-beta3 integrin expression in melanocytic nevi and cutaneous melanoma. *Journal of Cutaneous Pathology*, 34(11), 851-856.
- Nicoloso, M. S., Spizzo, R., Shimizu, M., Rossi, S. & Calin, G. A. (2009). MicroRNAs-the micro steering wheel of tumour metastases. *Nature Reviews Cancer*, 9(4), 293-302.
- Nobes, C. D., & Hall, A. (1995). Rho, rac, and cdc42 GTPases regulate the assembly of multimolecular focal complexes associated with actin stress fibers, lamellipodia, and filopodia. *Cell*, 81(1), 53-62.
- Otsuka, M., Zheng, M., Hayashi, M., Lee, J. D., Yoshino, O., Lin, S. & Han, J. (2008). Impaired microRNA processing causes corpus luteum insufficiency and infertility in mice. *The Journal of Clinical Investigation*, 118(5), 1944-1954.
- Ouyang, G., Wang, Z., Fang, X., Liu, J. & Yang, C. J. (2010). Molecular signaling of the epithelial to mesenchymal transition in generating and maintaining cancer stem cells. *Cellular and Molecular Life Sciences*, 67(15), 2605-2618.
- Papadopoulos, G. L., Alexiou, P., Maragkakis, M., Reczko, M. & Hatzigeorgiou, A. G. (2009). DIANA-mirPath: Integrating human and mouse microRNAs in pathways. *Bioinformatics*, 25, 1991-1993.
- Park, S. M., Gaur, A. B., Lengyel, E. & Peter, M. E. (2008). The miR-200 family determines the epithelial phenotype of cancer cells by targeting the E-cadherin repressors ZEB1 and ZEB2. *Genes & Development*, 22(7), 894-907.
- Parkin, D. M., Bray, F., Ferlay, J. & Pisani, P. (2005). Global cancer statistics, 2002. *CA: Cancer Journal for Clinicians*, 55(2), 74-108.
- Pentheroudakis, G., Fountzilas, G., Bafaloukos, D., Koutsoukou, V., Pectasides, D., Skarlos, D., Samantas, E., Kalofonos, H. P., Gogas, H. & Pavlidis, N. (2006). Metastatic breast cancer with liver metastases: a registry analysis of clinicopathologic, management and outcome characteristics of 500 women. *Breast Cancer Research and Treatment*, 97(3), 237-244.
- Poliseno, L., Tuccoli, A., Mariani, L., Evangelista, M., Citti, L., Woods, K., Mercatanti, A., Hammond, S. & Rainaldi, G. (2006). MicroRNAs modulate the angiogenic properties of HUVECs. *Blood*, 108(9), 3068-3071.
- Pollard, T. D., & Borisy, G. G. (2003). Cellular motility driven by assembly and disassembly of actin filaments. *Cell*, 112(4), 453-465.
- Price, L. S., Leng, J., Schwartz, M. A. & Bokoch, G. M. (1998). Activation of Rac and Cdc42 by integrins mediates cell spreading. *Molecular Biology of the Cell*, 9(7), 1863-1871.
- Pukrop, T., Klemm, F., Hagemann, T., Gradl, D., Schulz, M., Siemes, S., Trümper, L. & Binder, C. (2006). Wnt 5a signaling is critical for macrophage-induced invasion of breast cancer cell lines. *Proceeding of the National Academy Sciences of the United States of America*, 103(14), 5454-5459.

- Pukrop, T., & Binder, C. (2008). The complex pathways of Wnt 5a in cancer progression. *Journal of Molecular Medicine*, 86(3), 259-266.
- Ramis-Conde, I., Chaplain, M. A., Anderson, A. R. & Drasdo, D. (2009). Multi-scale modelling of cancer cell intravasation: the role of cadherins in metastasis. *Physical Biology*, 6(1), 016008.
- Reka, A. K., Kurapati, H., Narala, V. R., Bommer, G., Chen, J., Standiford, T. J. & Keshamouni, V. G. (2010). Peroxisome proliferator-activated receptor-gamma activation inhibits tumor metastasis by antagonizing Smad3-mediated epithelial-mesenchymal transition. *Molecular Cancer Therapeutics*, 9(12), 3221-3232.
- Ridley, A. J., Schwartz, M. A., Burridge, K., Firtel, R. A., Ginsberg, M. H., Borisy, G., Parsons, J. T. & Horwitz, A. R. (2003). Cell migration: integrating signals from front to back. *Science*, 302(5651), 1704-1709.
- Ridley, A. J. (2006). Rho GTPases and actin dynamics in membrane protrusions and vesicle trafficking. *Trends in Cell Biology*, 16(10), 522-529.
- Ritchie, W., Rajasekhar, M., Flamant, S. & Rasko, J. E. (2009). Conserved expression patterns predict microRNA targets. *PLoS Computational Biology*, 5(9), e1000513.
- Saad, F., Clarke, N. & Colombel, M. (2006). Natural history and treatment of bone complications in prostate cancer. *European Urology*, 49(3), 429-440.
- Sahai, E., & Marshall, C. J. (2002). RHO-GTPases and cancer. *Nature Reviews Cancer*, 2(2), 133-142.
- Sassen, S., Miska, E. A. & Caldas, C. (2008). MicroRNA: implications for cancer. *Virchows Archiv*, 452(1), 1-10.
- Sato, A., Khadka, D. K., Liu, W., Bharti, R., Runnels, L. W., Dawid, I. B. & Habas, R. (2006). Profilin is an effector for Daam1 in non-canonical Wnt signaling and is required for vertebrate gastrulation. *Development*, 133(21), 4219-4231.
- Scheel, C., Eaton, E. N., Li, S. H., Chaffer, C. L., Reinhardt, F., Kah, K. J., Bell, G., Guo, W., Rubin, J., Richardson, A. L. & Weinberg, R. A. (2011). Paracrine and autocrine signals induce and maintain mesenchymal and stem cell states in the breast. *Cell*, 145(6), 926-940.
- Schlaepfer, D. D., Hanks, S. K., Hunter, T. & van der Geer, P. (1994). Integrin-mediated signal transduction linked to Ras pathway by GRB2 binding to focal adhesion kinase. *Nature*, 372(6508), 786-791.
- Schlaepfer, D. D., Jones, K. C. & Hunter, T. (1998). Multiple Grb2-mediated integrin-stimulated signaling pathways to ERK2/mitogen-activated protein kinase: summation of both c-Src- and focal adhesion kinase-initiated tyrosine phosphorylation events. *Molecular and Cellular Biology*, 18(5), 2571-2785.

- Schneider, S., Weydig, C. & Wessler, S. (2008). Targeting focal adhesions: Helicobacter pylori-host communication in cell migration. *Cell Communication and Signaling*, 6, 2.
- Segura, M. F., Hanniford, D., Menendez, S., Reavie, L., Zou, X., Alvarez-Diaz, S., Zakrzewski, J., Blochin, E., Rose, A., Bogunovic, D., Polsky, D., Wei, J., Lee, P., Belitskaya-Levy, I., Bhardwaj, N., Osman, I. & Hernando, E. (2009). Aberrant miR-182 expression promotes melanoma metastasis by repressing FOXO3 and microphthalmia-associated transcription factor. *Proceeding of the National Academy Sciences of the United States of America*, 106(6), 1814-1819.
- Sells, M. A., Knaus, U. G., Bagrodia, S., Ambrose, D. M., Bokoch, G. M. & Chernoff, J. (1997). Human p21-activated kinase (Pak1) regulates actin organization in mammalian cells. *Current Biology*, 7(3), 202-210.
- Siddiqui, E., Mumtaz, F. H. & Gelister, J. (2004). Understanding prostate cancer. *The Journal of the Royal Society for the Promotion of Health*, 124(5), 219-221.
- Siegel, P. M., Shu, W., Cardiff, R. D., Muller, W. J. & Massagué, J. (2003). Transforming growth factor beta signaling impairs Neu-induced mammary tumorigenesis while promoting pulmonary metastasis. *Proceeding of the National Academy Sciences of the United States of America*, 100(14), 8430-8435.
- Sossey-Alaoui, K., Safina, A., Li, X., Vaughan, M. M., Hicks, D. G., Bakin, A. V. & Cowell, J. K. (2007). Down-regulation of WAVE3, a metastasis promoter gene, inhibits invasion and metastasis of breast cancer cells. *The American Journal of Pathology*, 170(6), 2112-2121.
- Sossey-Alaoui, K., Bialkowska, K. & Plow, E. F. (2009). The miR200 family of microRNAs regulates WAVE3-dependent cancer cell invasion. *The Journal of Biological Chemistry*, 284(48), 33019-33029.
- Sossey-Alaoui, K., Downs-Kelly, E., Das, M., Izem, L., Tubbs, R. & Plow, E. F. (2011). WAVE3, an actin remodeling protein, is regulated by the metastasis suppressor microRNA, miR-31, during the invasion-metastasis cascade. *International Journal of Cancer*, 129(6), 1331-1343.
- Spremulli, E. N., & Dexter, D. L. (1983). Human tumor cell heterogeneity and metastasis. *Journal of Clinical Oncology*, 1(8), 496-509.
- Stetler-Stevenson, W. G., Aznavoorian, S. & Liotta, L. A. (1993). Tumor cell interactions with the extracellular matrix during invasion and metastasis. *Annual Review of Cell and Developmental Biology*, 9, 541-573.
- Strutt, D. I., Weber, U. & Mlodzik, M. (1997). The role of RhoA in tissue polarity and Frizzled signalling. *Nature*, 387(6630), 292-295.
- Suárez, Y., Fernández-Hernando, C., Pober, J. S. & Sessa, W. C. (2007). Dicer dependent microRNAs regulate gene expression and functions in human endothelial cells. *Circulation Research*, 100(8), 1164-1173.

- Suetsugu, S., Miki, H. & Takenawa, T. (2002). Spatial and temporal regulation of actin polymerization for cytoskeleton formation through Arp2/3 complex and WASP/WAVE proteins. *Cell Motility and Cytoskeleton*, 51(3), 113-122.
- Takenawa, T., & Miki, H. (2001). WASP and WAVE family proteins: key molecules for rapid rearrangement of cortical actin filaments and cell movement. *Journal of Cell Science*, 114(Pt 10), 1801-1809.
- Tavazoie, S. F., Alarcón, C., Oskarsson, T., Padua, D., Wang, Q., Bos, P. D., Gerald, W. L. & Massagué, J. (2008). Endogenous human microRNAs that suppress breast cancer metastasis. *Nature*, 451(7175), 147-152.
- ten Klooster, J. P., Jaffer, Z. M., Chernoff, J. & Hordijk, P. L. (2006). Targeting and activation of Rac1 are mediated by the exchange factor beta-Pix. *The Journal of Cell Biology*, 172(5), 759-769.
- Tian, F., DaCosta Byfield, S., Parks, W. T., Yoo, S., Felici, A., Tang, B., Piek, E., Wakefield, L. M. & Roberts, A. B. (2003). Reduction in Smad2/3 signaling enhances tumorigenesis but suppresses metastasis of breast cancer cell lines. *Cancer Research*, 63(23), 8284-8292.
- Tian, F., Byfield, S. D., Parks, W. T., Stuelten, C. H., Nemani, D., Zhang, Y. E. & Roberts, A. B. (2004). Smad-binding defective mutant of transforming growth factor beta type I receptor enhances tumorigenesis but suppresses metastasis of breast cancer cell lines. *Cancer Research*, 64(13), 4523-4530.
- Tlsty, T. D., & Coussens, L. M. (2006). Tumor stroma and regulation of cancer development. *Annual Review of Pathology*, 1, 119-150.
- Uematsu, K., He, B., You, L., Xu, Z., McCormick, F. & Jablons, D. M. (2003). Activation of the Wnt pathway in non small cell lung cancer: evidence of dishevelled overexpression. *Oncogene*, 22(46), 7218-7221.
- Ueno, K., Hazama, S., Mitomori, S., Nishioka, M., Suehiro, Y., Hirata, H., Oka, M., Imai, K., Dahiya, R. & Hinoda, Y. (2009). Down-regulation of frizzled-7 expression decreases survival, invasion and metastatic capabilities of colon cancer cells. *British Journal of Cancer*, 101(8), 1374-1381.
- Valastyan, S., Reinhardt, F., Benaich, N., Calogrias, D., Szász, A. M., Wang, Z. C., Brock, J. E., Richardson, A. L. & Weinberg, R. A. (2009). A pleiotropically acting microRNA, miR-31, inhibits breast cancer metastasis. *Cell*, 137(6), 1032-1046.
- Ventura, A., & Jacks, T. (2009). MicroRNAs and cancer: short RNAs go a long way. *Cell*, 136(4), 586-591.
- Voorhoeve, P. M., le Sage, C., Schrier, M., Gillis, A. J., Stoop, H., Nagel, R., Liu, Y. P., van Duijse, J., Drost, J., Griekspoor, A., Zlotorynski, E., Yabuta, N., De Vita, G., Nojima, H., Looijenga, L. H. & Agami, R. (2006). A genetic screen implicates miRNA-372 and miRNA-373 as oncogenes in testicular germ cell tumors. *Cell*, 124(6), 1169-1181.

- Wang, S., Aurora, A. B., Johnson, B. A., Qi, X., McAnally, J., Hill, J. A., Richardson, J. A., Bassel-Duby, R. & Olson, E. N. (2008). The endothelial-specific microRNA miR-126 governs vascular integrity and angiogenesis. *Developmental Cell*, 15(2), 261-271.
- Wang, G., Mao, W. & Zheng, S. (2008). MicroRNA-183 regulates Ezrin expression in lung cancer cells. *FEBS Letters*, 582(25-26), 3663-3668.
- Wang, Y. (2009). Wnt/Planar cell polarity signaling: a new paradigm for cancer therapy. *Molecular Cancer Therapeutics*, 8(8), 2103-2109.
- Wang, X., Ling, C., Bai, Y. & Zhao, J. (2011). MicroRNA-206 is associated with invasion and metastasis of lung cancer. *Anatomical Record (Hoboken)*, 294(1), 88-92.
- Weeraratna, A. T., Jiang, Y., Hostetter, G., Rosenblatt, K., Duray, P., Bittner, M. & Trent, J. M. (2002). Wnt5a signaling directly affects cell motility and invasion of metastatic melanoma. *Cancer Cell*, 1(3), 279-288.
- Wentz-Hunter, K. K., & Potashkin, J. A. (2011). The Role of miRNAs as Key Regulators in the Neoplastic Microenvironment. *Molecular Biology International*, 2011, 839872.
- Wu, W., Sun, M., Zou, G. M. & Chen, J. (2007). MicroRNA and cancer: Current status and prospective. *International Journal of Cancer*, 120(5), 953-960.
- Wu, F., Yang, Z. & Li, G. (2009). Role of specific microRNAs for endothelial function and angiogenesis. *Biochemical and Biophysical Research Communications*, 386(4), 549-553.
- Wu, H., Zhu, S. & Mo, Y. Y. (2009). Suppression of cell growth and invasion by miR-205 in breast cancer. *Cell Research*, 19(4), 439-448.
- Wu, H., & Mo, Y. Y. (2009). Targeting miR-205 in breast cancer. *Expert Opinion on Therapeutic Targets*, 13(12), 1439-1448.
- Würdinger, T., Tannous, B. A., Saydam, O., Skog, J., Grau, S., Soutschek, J., Weissleder, R., Breakefield, X. O. & Krichevsky, A. M. (2008). miR-296 regulates growth factor receptor overexpression in angiogenic endothelial cells. *Cancer Cell*, 14(5), 382-393.
- Xia, M., & Hu, M. (2010). The role of microRNA in tumor invasion and metastasis. *Journal of Cancer Molecules*, 5, 33-39.
- Xiong, F., Wu, C., Chang, J., Yu, D., Xu, B., Yuan, P., Zhai, K., Xu, J., Tan, W. & Lin, D. (2011). Genetic variation in an miRNA-1827 binding site in MYCL1 alters susceptibility to small-cell lung cancer. *Cancer Research*, 71(15), 5175-5181.
- Xu, J., Lamouille, S. & Derynck, R. (2009). TGF-beta-induced epithelial to mesenchymal transition. *Cell Research*, 19(2), 156-172.

- Xu, C. C., Wu, L. M., Sun, W., Zhang, N., Chen, W. S. & Fu, X. N. (2011). Effects of TGF- β signaling blockade on human A549 lung adenocarcinoma cell lines. *Molecular Medicine Report*, 4(5), 1007-1015.
- Yamaguchi, H., Lorenz, M., Kempiak, S., Sarmiento, C., Coniglio, S., Symons, M., Segall, J., Eddy, R., Miki, H., Takenawa, T. & Condeelis, J. (2005). Molecular mechanisms of invadopodium formation: the role of the N-WASP-Arp2/3 complex pathway and cofilin. *The Journal of Cell Biology*, 168(3), 441-452.
- Yang, K., Handorean, A. M. & Iczkowski, K. A. (2009). MicroRNAs 373 and 520c are downregulated in prostate cancer, suppress CD44 translation and enhance invasion of prostate cancer cells in vitro. *International Journal of Clinical and Experimental Pathology*, 2(4), 361-369.
- Yang, L. H., Xu, H. T., Han, Y., Li, Q. C., Liu, Y., Zhao, Y., Yang, Z. Q., Dong, Q. Z., Miao, Y., Dai, S. D. & Wang, E. H. (2010). Axin downregulates TCF-4 transcription via beta-catenin, but not p53, and inhibits the proliferation and invasion of lung cancer cells. *Molecular Cancer*, 9, 25.
- Yang, J. S., Phillips, M. D., Betel, D., Mu, P., Ventura, A., Siepel, A. C., Chen, K. C. & Lai, E. C. (2011). Widespread regulatory activity of vertebrate microRNA* species. *RNA*, 17(2), 312-326.
- Yilmaz, M., & Christofori, G. (2009). EMT, the cytoskeleton, and cancer cell invasion. *Cancer and Metastasis Reviews*, 28(1-2), 15-33.
- Yoshioka, K., Foletta, V., Bernard, O. & Itoh, K. (2003). A role for LIM kinase in cancer invasion. *Proceeding of the National Academy Sciences of the United States of America*, 100(12), 7247-7252.
- Yu, S. L., Chen, H. Y., Yang, P. C. & Chen, J. J. (2007). Unique MicroRNA signature and clinical outcome of cancers. *DNA and Cell Biology*, 26(5), 283-292.
- Zainal, A. O., Zainudin, M. A., Saleha, N. I. T. (2006). *Malaysia Cancer Statistics-Data and figure Peninsular Malaysia 2006*. Kuala Lumpur: National Cancer Registry, Ministry of Health Malaysia.
- Zhang, Y., Chang, C., Gehling, D. J., Hemmati-Brivanlou, A. & Derynck, R. (2001). Regulation of Smad degradation and activity by Smurf2, an E3 ubiquitin ligase. *Proceeding of the National Academy Sciences of the United States of America*, 98(3), 974-979.
- Zhang, S., Fei, T., Zhang, L., Zhang, R., Chen, F., Ning, Y., Han, Y., Feng, X. H., Meng, A. & Chen, Y. G. (2007). Smad7 antagonizes transforming growth factor beta signaling in the nucleus by interfering with functional Smad-DNA complex formation. *Molecular and Cellular Biology*, 27(12), 4488-4499.
- Zhang, Y. E. (2009). Non-Smad pathways in TGF-beta signaling. *Cell Research*, 19(1), 128-139.
- Zhang, H., Li, Y. & Lai, M. (2010). The microRNA network and tumor metastasis. *Oncogene*, 29(7), 937-948.

- Zhu, J., Motejlek, K., Wang, D., Zang, K., Schmidt, A. & Reichardt, L. F. (2002). beta8 integrins are required for vascular morphogenesis in mouse embryos. *Development*, 129(12), 2891-2903.
- Zhu, S., Wu, H., Wu, F., Nie, D., Sheng, S. & Mo, Y. Y. (2008). MicroRNA-21 targets tumour suppressor genes in invasion and metastasis. *Cell Research*, 18(3), 350-359.
- Zhu, L., Chen, H., Zhou, D., Li, D., Bai, R., Zheng, S. & Ge, W. (2011). MicroRNA-9 up-regulation is involved in colorectal cancer metastasis via promoting cell motility. *Medical Oncology*, DOI: 10.1007/s12032-011-9975-z.

APPENDICES

Appendix 1: Solutions and Formulations

Appendix 1.1: Cell Culture

(A) Culture Media

To prepare 250.0 ml of complete Dulbecco's Modified Eagle Medium (DMEM) culture media supplemented with 10.0 % (v/v) fetal bovine serum (FBS) (JR Scientific Inc, USA), 25.0 ml of FBS was added into a sterile autoclaved bottle and mixed with 225.0 ml of sterile DMEM (Thermo Scientific Hyclone, USA), then was stored at 4°C. Same procedure for Roswell Park Memorial Institute 1640 (RPMI 1640) (Thermo Scientific Hyclone, USA) supplemented with 10.0 % (v/v) FBS. Culture media were also supplemented with 100.0 U/ml penicillin and 100.0 µg/ml streptomycin (Lonza, USA).

(B) 1X PBS

1.0 L of 1X concentration of Phosphate Buffered Saline (PBS) solution with pH at 7.4 was prepared by mixing 100.0 ml of pre-mixed 10X calcium- and magnesium-free PBS (Mediatech Cellgro®, USA) with pH 7.4 and topped up with distilled water to 1.0 L. The 1X PBS was autoclaved at 121°C, 15 psi for 15 min and stored at room temperature.

(C) 0.1 % (v/v) Trypsin-0.53 mM EDTA

98.0 mg of ethylenediaminetetraacetic acid (EDTA) (GibcoBRL, USA) was dissolved in 500.0 ml of 1X PBS to prepare 1X PBS-0.53 mM EDTA, followed by sterile autoclaved at 121°C, 15 psi for 15 min and was stored at room temperature. 100.0 ml of 0.1% (v/v) of trypsin solution was prepared by mixing 4.0 ml of 2.5% (v/v) trypsin-EDTA (Sigma-Aldrich, USA) with 96.0 ml of sterile 1X PBS-0.53 mM EDTA and was stored at room temperature.

(D) 0.04 % (w/v) Trypan Blue Dye

10.0 ml of 0.04 % (w/v) of trypan blue solution was prepared by dissolving 4.0 mg of trypan blue (Sigma-Aldrich, USA) in 10.0 ml of 1X PBS, incubated at 60°C to ensure complete dissolving. The solution was then stored at room temperature.

Appendix 1.2: Transwell Invasion Assay

(A) Matrigel

Stock Matrigel (BD Biosciences, USA) was thawed on ice at 4°C overnight. To prepare 1.5 mg/ml of Matrigel, 100.0 µl of 8.9 mg/ml of Matrigel (from lot number: A0952) was diluted with 593.0 µl of cold serum free media on ice. Diluted Matrigel was stored at -20°C.

(B) 1.0 % (w/v) Methylene Blue

100.0 ml of 1.0 % (w/v) of Methylene blue was prepared by dissolving 1.0 g of methylene blue powder (Sigma, USA) in distilled water, incubated at 60°C to ensure complete dissolving. The solution was then stored at room temperature.

Appendix 1.3: Wound Healing Assay

(A) Mitomycin C Stock Solution

Stock solution of 1.0 mg/ml of mitomycin C was prepared by mixing 2.0 mg of Mitomycin C, *Streptomyces caespitosus* (Merck Calbiochem[®], Germany) with 20.0 ml of sterile 1X PBS and sterile filtered using 0.45 µm syringe filter (Sartorius, USA). The dissolved stock solution was then aliquoted and freeze at -20°C up to 3 months and protected from light.

Appendix 1.4: MiRNA Microarray

(A) DEPC-Treated Water

1.0 L of 0.1 % (v/v) diethyl pyrocarbonate (DEPC)-treated water was prepared by adding 1.0 ml of DEPC (Merck, Germany) to 1.0 L of distilled water. The solution was mixed well by shaking and left at room temperature for overnight prior to being autoclaved at 121°C, 15 psi for 15 min and was stored at room temperature.

(B) 1.0 mM Tris Solution

50.0 ml nuclease-free water (Qiagen, Germany) was transferred to a 50.0 ml DEPC-treated bottle. 50.0 µl of nuclease-free water was discarded and 50.0 µl of 1 M Tris-HCl, pH 8 (Ambion, USA) was added without adjusting pH reading. The diluted 1.0 mM Tris solution was stored at room temperature up to 3 months.

(C) 1X PBS, 0.02 % (v/v) Tween-20

100.0 ml of 10X PBS pH 7.4 and 0.2 ml Tween-20 (Promega, USA) were added into a 1.0 L bottle, then was topped up with distilled water to 1.0 L. The solution was kept at room temperature up to 3 months.

(D) 5 % (w/v) BSA

2.0 g powdered bovine serum albumin (BSA) (Merck Calbiochem[®], Germany) was dissolved with 40.0 µl of 1X PBS in a 50.0 ml conical tube by vortex to mix. 8 aliquots of 5.0 ml of 5.0 % BSA was made and stored at -20°C up to 6 months. An aliquot can be stored at 4°C for a week once thawed and do not freeze/thaw more than 4 times.

(E) 5X SSC, 0.05 % (v/v) SDS, 0.005 % (v/v) BSA

2.5 ml of 20X SSC (Applied Biosystems, USA), 0.05 ml 10.0 % (v/v) sodium dodecyl sulfate polyacrylamide (SDS) (Applied Biosystems, USA) and 0.01 ml of 5.0 % (w/v) BSA in 1X PBS were added together with water to a final volume of 10.0 ml. 10.0 ml of the mixture was aliquoted and each aliquot was stored at -20°C up to 6 months. An aliquot can be stored at 4°C for a week once thawed with not freeze/thaw more than 4 times.

Appendix 2: Commercial Kits

Commercial kits used in this study were:

1. Qiagen miRNeasy mini kit (Qiagen, Germany)
2. Agilent RNA 6000 Nano Kit (Agilent Technologies, USA)
3. FlashTag[™] Biotin RNA Labelling Kit for Affymetrix[®] GeneChip[®] miRNA Arrays (Genisphere, USA)
4. GeneChip[®] miRNA Array (Affymetrix, USA)
5. TaqMan[®] microRNA assay (Applied Biosystems, USA)
6. TaqMan[®] MicroRNA Reverse Transcription Kit (Applied Biosystems, USA)
7. TaqMan[®] Fast Advanced Master Mix Product (Applied Biosystems, USA)

Appendix 3: Transwell Invasion Assay Data

(A) A549 Transwell Invasion Assay Data

Sub-cell lines	Invaded cells per field					
	Replicates			Average	Std dev	SEM
	1	2	3			
A549-I7	68	38	74	60	19.3	11.14
A549-NI7	15	15	32	21	9.8	5.67

(B) PC-3 Transwell Invasion Assay Data

Sub-cell lines	Invaded cells per field					
	Replicates			Average	Std dev	SEM
	1	2	3			
PC-3-I7	90	99	80	90	9.5	5.49
PC-3-NI7	38	14	27	26	12.0	6.94

(C) MCF7 Transwell Invasion Assay Data

Sub-cell lines	Invaded cells per field					
	Replicates			Average	Std dev	SEM
	1	2	3			
MCF7-I7	63	115	80	86	26.5	15.31
MCF7-NI7	24	31	32	29	4.4	2.52

(D) MDA-MB-231 Transwell Invasion Assay Data

Sub-cell lines	Invaded cells per field					
	Replicates			Average	Std dev	SEM
	1	2	3			
MDA-MB-231-I7	40	105	98	81	35.7	20.60
MDA-MB-231-NI7	19	25	28	24	4.6	2.65

Appendix 4: Wound Healing Assay Data

(A) A549 Wound Healing Assay Data

Sample	Replicate				Average	Std Dev	SEM
	1	2	3	4			
Open image area of A549-I7 0 h	0.3604	0.4832	0.4809	0.4324			
Open image area of A549-I7 28 h	0.0830	0.1816	0.2494	0.1761			
Area migrated of A549-I7	0.2774	0.3015	0.2314	0.2564			
Wound healing of A549-I7 (%)	77.0	62.4	48.1	59.3	61.7	14.42	7.211
Open image area of A549-NI7 0 h	0.3876	0.4930	0.5044	0.5330			
Open image area of A549-NI7 28 h	0.2436	0.4222	0.3808	0.4715			
Area migrated by A549-NI7	0.1440	0.0708	0.1237	0.0615			
Wound healing of A549-NI7 (%)	37.2	14.4	24.5	11.5	21.9	11.42	5.710

(B) PC-3 Wound Healing Assay Data

Sample	Replicate				Average	Std Dev	SEM
	1	2	3	4			
Open image area of PC-3-I7 0 h	0.3855	0.4095	0.4754	0.3554			
Open image area of PC-3-I7 28 h	0.2363	0.1412	0.1657	0.0577			
Area migrated of PC-3-I7	0.1492	0.2683	0.3098	0.2978			
Wound healing of PC-3-I7 (%)	38.7	65.5	65.2	83.8	63.3	15.38	7.69
Open image area of PC-3-NI7 0 h	0.4005	0.4837	0.4292	0.2986			
Open image area of PC-3-NI7 28 h	0.3195	0.3173	0.2933	0.1408			
Area migrated by PC-3-NI7	0.0810	0.1664	0.1359	0.1577			
Wound healing of PC-3-NI7 (%)	20.2	34.4	31.7	52.8	34.8	7.52	3.76

(C) MCF7 Wound Healing Assay Data

Sample	Replicate				Average	Std Dev	SEM
	1	2	3	4			
Open image area of MCF7-I7 0 h	0.3298	0.3928	0.4050	0.3377			
Open image area of MCF7-I7 23 h	0.0284	0.1100	0.0899	0.0000			
Area migrated by MCF7-I7	0.3014	0.2828	0.3151	0.3377			
Wound healing of MCF7-I7 (%)	91.4	72.0	77.8	100.0	85.3	9.95	4.977
Open image area of MCF7-NI7 0 h	0.3318	0.3999	0.3808	0.3887			
Open image area of MCF7-NI7 23 h	0.1967	0.2078	0.2408	0.1975			
Area migrated by MCF7-NI7	0.1351	0.1921	0.1400	0.1912			
Wound healing of MCF7-NI7 (%)	40.7	48.0	36.8	49.2	43.7	5.72	2.860

(D) MDA-MB-231 Wound Healing Assay

Sample	Replicate				Average	Std Dev	SEM
	1	2	3	4			
Open image area of MDA-MB-231-I7 0 h	0.4174	0.5239	0.5478	0.4878			
Open image area of MDA-MB-231-I7 28 h	0.2726	0.2365	0.2198	0.2777			
Area migrated by MDA-MB-231-I7	0.1447	0.2874	0.3279	0.2101			
Wound healing of MDA-MB-231-I7 (%)	34.7	54.9	59.9	43.1	48.1	13.34	6.668
Open image area of MDA-MB-231-NI7 0 h	0.4399	0.5459	0.5642	0.5459			
Open image area of MDA-MB-231-NI7 28 h	0.3689	0.3614	0.4396	0.3399			
Area migrated by MDA-MB-231-NI7	0.0709	0.1845	0.1246	0.2060			
Wound healing of MDA-MB-231-NI7 (%)	16.1	33.8	22.1	37.7	27.4	8.99	4.494

Appendix 5: Cell Proliferation Assay Data
Appendix 5.1: Number of Viable Cells Data

(A) Number of Viable Cells Data of A549

Day	number of viable cells (x 1,000)																	
	A549-I7						A549-NI7						A549					
	Replicate			Avg	Std Dev	SEM	Replicate			Avg	Std Dev	SEM	Replicate			Avg	Std Dev	SEM
	1	2	3				1	2	3				1	2	3			
0	20	20	20	20	-	-	20	20	20	20	-	-	20	20	20	20	-	-
1	35	40	40	38	2.9	1.67	30	40	40	37	5.8	3.33	30	50	50	43	11.5	6.67
2	100	80	80	87	11.5	6.67	110	80	100	97	15.3	8.82	100	120	90	103	15.3	8.82
3	500	220	250	323	153.7	88.76	420	360	310	363	55.1	31.80	570	200	180	317	219.6	126.80
4	670	800	520	663	140.1	80.90	660	840	860	787	110.2	63.60	630	800	740	723	86.2	49.78
5	1150	900	1360	1137	230.3	132.96	910	1560	1800	1423	460.5	265.85	1450	1100	1350	1300	180.3	104.08
6	1550	1440	1720	1570	141.1	81.45	1110	1680	1780	1523	361.4	208.67	1670	1480	1890	1680	205.2	118.46
7	2420	1930	2210	2187	245.8	141.93	2200	2480	2200	2293	161.7	93.33	1920	2190	2020	2043	136.5	78.81

(B) Number of Viable Cells Data of PC-3

Day	number of viable cells (x 1,000)																	
	PC-3-I7						PC-3-NI7						PC-3					
	Replicate			Avg	Std Dev	SEM	Replicate			Avg	Std Dev	SEM	Replicate			Avg	Std Dev	SEM
	1	2	3				1	2	3				1	2	3			
0	20	20	20	20	-	-	20	20	20	20	-	-	20	20	20	20	-	-
1	50	70	40	53	15.3	8.82	60	40	40	47	11.5	6.67	40	50	40	43	5.8	3.33
2	80	100	110	97	15.3	8.82	60	90	110	87	25.2	14.53	98	130	90	106	21.2	12.22
3	420	380	310	370	55.7	32.15	210	360	260	277	76.4	44.10	380	480	530	463	76.4	44.10
4	950	1180	1220	1117	145.7	84.13	800	600	830	743	40.4	23.33	1080	820	830	910	147.3	85.05
5	1560	1830	1360	1583	235.9	136.18	1120	1560	1630	1437	276.5	159.62	1450	2000	1820	1757	280.4	161.90
6	2100	2400	2210	2237	151.8	87.62	2380	2590	1960	2310	320.8	185.20	2300	2410	2140	2283	135.8	78.39
7	2990	2500	2850	2780	252.4	145.72	2610	2460	2840	2637	191.4	110.50	3100	2740	2230	2690	437.1	252.39

(C) Number of Viable Cells Data of MCF7

Day	number of viable cells (x 1,000)																	
	MCF7-I7						MCF7-NI7						MCF7					
	Replicate			Avg	Std Dev	SEM	Replicate			Avg	Std Dev	SEM	Replicate			Avg	Std Dev	SEM
	1	2	3				1	2	3				1	2	3			
0	20	20	20	20	-	-	20	20	20	20	-	-	20	20	20	20	-	-
1	30	30	40	33	5.8	3.33	20	40	40	33	11.5	6.67	30	20	40	30	10.0	5.77
2	130	100	110	113	15.3	8.82	70	110	70	83	23.1	13.33	160	180	130	157	25.2	14.53
3	490	380	270	380	110.0	63.51	380	360	240	327	75.7	43.72	450	390	460	433	37.9	21.86
4	900	1360	1220	1160	235.8	136.14	790	920	1100	937	155.7	89.88	1210	906	778	965	221.9	128.11
5	1960	1730	1970	1887	135.8	78.39	1740	1560	1630	1643	90.7	52.39	1840	2010	1820	1890	104.4	60.28
6	2230	2400	2210	2280	104.4	60.28	2150	2010	1980	2047	90.7	52.39	2370	1970	2190	2177	200.3	115.66
7	2580	2800	2450	2610	176.9	102.14	2320	2330	2630	2427	176.2	101.71	2500	2470	2810	2593	188.2	108.68

(D) Number of Viable Cells Data of MDA-MB-231

Day	number of viable cells (x 1,000)																	
	MDA-MB-231-I7						MDA-MB-231-NI7						MDA-MB-231					
	Replicate			Avg	Std Dev	SEM	Replicate			Avg	Std Dev	SEM	Replicate			Avg	Std Dev	SEM
	1	2	3				1	2	3				1	2	3			
0	20	20	20	20	-	-	20	20	20	20	-	-	20	20	20	20	-	-
1	50	30	40	40	10.0	5.77	40	20	30	30	10.0	5.77	30	20	20	23	5.8	3.33
2	50	100	70	73	25.2	14.53	90	110	60	87	25.2	14.53	90	120	130	113	20.8	12.02
3	190	300	270	253	56.9	32.83	200	360	240	267	83.3	48.07	450	390	460	433	37.9	21.86
4	800	550	770	707	136.5	78.81	460	920	1110	830	334.2	192.96	1010	860	790	887	112.4	64.89
5	1330	990	1,540	1287	277.5	160.24	820	1410	1680	1303	439.8	253.92	1340	1480	1610	1477	135.0	77.96
6	1830	1640	1440	1637	195.0	112.60	1330	2010	1980	1773	384.2	221.84	2170	1860	2000	2010	155.2	89.63
7	2150	1840	2350	2113	257.0	148.36	2430	2330	1990	2250	230.7	133.17	2550	2210	1970	2243	291.4	168.26

Appendix 5.2: Doubling Time Data

(A) A549 Doubling Time Data

Day 4	A549-I7				A549-NI7				A549			
	Replicate			Average	Replicate			Average	Replicate			Average
	1	2	3		1	2	3		1	2	3	
number of viable cells (x1,000)	670	800	520	663	660	840	860	787	630	800	740	723
Ratio	33.5	40.0	26.0	33.2	33.0	42.0	43.0	39.3	31.5	40.0	37.0	36.2
Doubling time (days)	0.79	0.75	0.85	0.79	0.79	0.74	0.74	0.76	0.80	0.75	0.77	0.77
Doubling time (h)	18.9	18.0	20.4	19.0	19.0	17.8	17.7	18.1	19.3	18.0	18.4	18.5
Std Dev	1.20				0.74				0.64			
SEM of doubling time (h)	0.695				0.429				0.369			

(B) PC-3 Doubling Time Data

Day 4	PC-3-I7				PC-3-NI7				PC-3			
	Replicate			Average	Replicate			Average	Replicate			Average
	1	2	3		1	2	3		1	2	3	
number of viable cells (x1,000)	950	1180	1220	840	800	600	830	743	1080	820	830	910
Ratio	47.5	59.0	61.0	42.0	40.0	30.0	41.5	37.2	54.0	41.0	41.5	45.5
Doubling time (days)	0.72	0.68	0.67	0.74	0.75	0.82	0.74	0.77	0.70	0.75	0.74	0.73
Doubling time (h)	17.2	16.3	16.2	17.8	18.0	19.6	17.9	18.4	16.7	17.9	17.9	17.4
Std Dev (h)	0.57				0.94				0.70			
SEM of doubling time (h)	0.330				0.541				0.403			

(C) MCF7 Doubling Time Data

Day 4	MCF7-I7				MCF7-NI7				MCF7			
	Replicate			Average	Replicate			Average	Replicate			Average
	1	2	3		1	2	3		1	2	3	
number of viable cells (x1,000)	900	1360	1220	1160	790	920	1100	937	1210	906	778	965
Ratio	45.0	68.0	61.0	58.0	39.5	46.0	55.0	46.8	60.5	45.3	38.9	48.5
Doubling time (days)	0.73	0.66	0.67	0.68	0.75	0.72	0.69	0.72	0.68	0.73	0.76	0.72
Doubling time (h)	17.5	15.8	16.2	16.4	18.1	17.4	16.6	17.3	16.2	17.4	18.2	17.2
Std Dev (h)	0.89				0.75				0.99			
SEM of doubling time (h)	0.515				0.432				0.571			

(D) MDA-MB-231 Doubling Time Data

Day 4	MDA-MB-231-I7				MDA-MB-231-NI7				MDA-MB-231			
	Replicate			Average	Replicate			Average	Replicate			Average
	1	2	3		1	2	3		1	2	3	
number of viable cells (x1,000)	800	550	770	840	460	920	1110	830	1010	860	790	887
Ratio	40.0	27.5	38.5	42.0	23.0	46.0	55.5	41.5	50.5	43.0	39.5	44.3
Doubling time (days)	0.75	0.84	0.76	0.74	0.88	0.72	0.69	0.74	0.71	0.74	0.75	0.73
Doubling time (h)	18.0	20.1	18.2	17.8	21.2	17.4	16.6	17.9	17.0	17.7	18.1	17.5
Std Dev (h)	1.13				2.49				0.57			
SEM of doubling time (h)	0.651				1.435				0.332			

Appendix 6: Agilent Bioanalyzer Data

Sub-cell line	Replicate	RNA concentration (ng/μl)	28S/18S rRNA Ratio	RNA area
PC-3-I7	1	518	2.3	92.1
	2	501	2.3	89.2
	3	367	2.1	63.5
	4	446	2.3	79.4
PC-3-NI7	1	1132	2.0	201.3
	2	1220	2.0	217.0
	3	1322	2.1	235.1
	4	1240	1.7	220.6
A549-I7	1	588	2.1	104.5
	2	559	2.1	99.4
	3	611	2.1	108.7
	4	643	2.1	114.3
A549-NI7	1	919	1.7	428.2
	2	1023	2.0	476.7
	3	740	2.0	345.0
	4	1053	2.0	490.6
MCF7-I7	1	1053	2.1	490.8
	2	1215	1.9	566.5
	3	1406	2.2	655.2
	4	1077	2.2	501.8
MCF7-NI7	1	1110	2.1	517.5
	2	1095	2.2	510.5
	3	977	2.2	455.5
	4	1091	2.1	508.5

Appendix 7: MiRNA Microarray Data

(A) A549 MiRNA Microarray Data

miRNA	Mature miRNA ID	miRBase Accession Number	Sequence
miR-378	hsa-miR-378a-3p	MIMAT0000732	ACUGGACUUGGAGU CAGAAGG
miR-671-5p	hsa-miR-671-5p	MIMAT0003880	AGGAAGCCCUGGAG GGGCUGGAG
miR-25*	hsa-miR-25-5p	MIMAT0004498	AGGCGGAGACUUGG GCAAUUG
miR-92b	hsa-miR-92b-3p	MIMAT0003218	UAUUGCACUCGUCC CGGCCUCC
miR-106b*	hsa-miR-106b-3p	MIMAT0004672	CCGCACUGUGGGUA CUUGCUGC
miR-550*	hsa-miR-550a-3p	MIMAT0003257	UGUCUACUCCCUC AGGCACAU
miR-629*	hsa-miR-629-3p	MIMAT0003298	GUUCUCCCAACGUA AGCCAGC
miR-576-3p	hsa-miR-576-3p	MIMAT0004796	AAGAUGUGGAAAAA UUGGAAUC
miR-886	hsa-miR-886	MI0005527	CGGGUCGGAGUUAG CUCAAGCGG
miR-487b	hsa-miR-487b	MIMAT0003180	AAUCGUACAGGGUC AUCCACUU
miR-1827	hsa-miR-1827	MIMAT0006767	UGAGGCAGUAGAUU GAAU

(B) PC3 MicroRNA Microarray Data

miRNA	Mature miRNA ID	miRBase Accession Number	Sequence
miR-129-1*	hsa-miR-129-1-3p	MIMAT0004548	AAGCCCUUACCCCA AAAAGUAU
miR-606	hsa-miR-606	MIMAT0003274	AAACUACUGAAAUA CAAAGAU
miR-34b*	hsa-miR-34b-5p	MIMAT0000685	UAGGCAGUGUCAUU AGCUGAUUG
miR-19b-1	hsa-miR-19b-3p	MIMAT0000074	UGUGCAAUCCAUG CAAACUGA
miR-320a	hsa-miR-320a	MIMAT0000510	AAAAGCUGGGUUGA GAGGGCGA
miR-132*	hsa-miR-132-5p	MIMAT0004594	ACCGUGGCUUUCGA UUGUUACU
miR-744	hsa-miR-744-5p	MIMAT0004945	UGC GGGGCUAGGGC UACAGCA
miR-654	hsa-miR-654-5p	MIMAT0003330	UGGUGGGCCGCAGA ACAUGUGC
miR-409	hsa-miR-409-5p	MIMAT0001638	AGGUUACCCGAGCA ACUUUGCAU
miR-1180	hsa-miR-1180	MIMAT0005825	UUUCCGGCUCGCGU GGGUGUGU
miR-503	hsa-miR-503	MIMAT0002874	UAGCAGCGGGAACA GUUCUGCAG
miR-423	hsa-miR-423-5p	MIMAT0004748	UGAGGGGCAGAGAG CGAGACUUU
miR-382	hsa-miR-382	MIMAT0000737	GAAGUUGUUCGUGG UGGAUUCG
miR-487b	hsa-miR-487b	MIMAT0003180	AAUCGUACAGGGUC AUCCACUU
miR-409	hsa-miR-409-3p	MIMAT0001639	GAAUGUUGCUCGGU GAACCCCU
miR-210	hsa-miR-210	MIMAT0000267	CUGUGCGUGUGACA GCGGCUGA
miR-342	hsa-miR-342-3p	MIMAT0000753	UCUCACACAGAAAU CGCACCCGU
miR-134	hsa-miR-134	MIMAT0000447	UGUGACUGGUUGAC CAGAGGGG
miR-379	hsa-miR-379-5p	MIMAT0000733	UGGUAGACUAUGGA ACGUAGG
miR-708	hsa-miR-708-5p	MIMAT0004926	AAGGAGCUUACAAU CUAGCUGGG

(C) MCF7 MicroRNA Microarray Data

miRNA	Mature miRNA ID	miRBase Accession Number	Sequence
miR-302c*	hsa-miR-302c-5p	MIMAT0000716	UUUAACAUGGGGGUACC UGCUG
miR-496	hsa-miR-496	MIMAT0002818	UGAGUAUUACAUGGCCA AUCUC
miR-135b	hsa-miR-135b-5p	MIMAT0000758	UAUGGCUUUUCAUCCU AUGUGA
miR-324	hsa-miR-324-3p	MIMAT0000762	ACUGCCCCAGGUGCUGC UGG
miR-181d	hsa-miR-181d	MIMAT0002821	AACAUUCAUUGUUGUCG GUGGGU
miR-1252	hsa-miR-1252	MIMAT0005944	AGAAGGAAAUUGAAUUC AUUUA
miR-93	hsa-miR-93-3p	MIMAT0004509	ACUGCUGAGCUAGCACU UCCCG
miR-376c	hsa-miR-376c	MIMAT0000720	AACAUAGAGGAAAUUCC ACGU
miR-30b*	hsa-miR-30b-3p	MIMAT0004589	CUGGGAGGUGGAUGUUU ACUUC
miR-616	hsa-miR-616-3p	MIMAT0004805	AGUCAUUGGAGGGUUUG AGCAG
miR-664	hsa-miR-664	MIMAT0005949	UAUUCAUUUAUCCCCAG CCUACA
miR-891b	hsa-miR-891b	MIMAT0004913	UGCAACUUACCUGAGUC AUUGA
miR-448	hsa-miR-448	MIMAT0001532	UUGCAUAUGUAGGAUGU CCCAU
miR-543	hsa-miR-543	MIMAT0004954	AAACAUUCGCGGUGCAC UUCUU
miR-624	hsa-miR-624	MIMAT0004807	CACAAGGUAUUGGUAUU ACCU
miR-624*	hsa-miR-624-star	MIMAT0003293	UAGUACCAGUACCUUGU GUUCA
miR-1234	hsa-miR-1234	MIMAT0005589	UCGGCCUGACCACCACC CCAC
miR-199a-1	hsa-miR-199a-5p	MIMAT0000231	CCCAGUGUUCAGACUAC CUGUUC
miR-578	hsa-miR-578	MIMAT0003243	CUUCUUGUGCUCUAGGA UUGU
miR-513a-1	hsa-miR-513a-3p	MIMAT0004777	UAAAUUUCACCUUUCUG AGAAGG
miR-603	hsa-miR-603	MIMAT0003271	CACACACUGCAAUUACU UUUGC
miR-1231	hsa-miR-1231	MIMAT0005586	GUGUCUGGGCGGACAGC UGC
miR-183	hsa-miR-183	MIMAT0000261	UAUGGCACUGGUAGAAU UCACU
miR-1827	hsa-miR-1827	MIMAT0006767	UGAGGCAGUAGAUUGAA

			U
miR-129-2	hsa-miR-129-2-3p	MIMAT0004605	AAGCCCUUACCCCAAAA AGCAU
miR-1246	hsa-miR-1246	MIMAT0005898	AAUGGAUUUUUGGAGCA GG
miR-519e*	hsa-miR-519e-5p	MIMAT0002828	UUCUCCAAAAGGGAGCA CUUUC
miR-1247	hsa-miR-1247	MIMAT0005899	ACCCGUCCCGUUCGUCCC CGGA
miR-365a	hsa-miR-365a-3p	MIMAT0000710	UAAUGCCCCUAAAAAUC CUUAU
miR-503	hsa-miR-503	MIMAT0002874	UAGCAGCGGGAACAGUU CUGCAG
miR-152	hsa-miR-152	MIMAT0000438	UCAGUGCAUGACAGAAC UUGG
miR-10a	hsa-miR-10a-5p	MIMAT0000253	UACCCUGUAGAUCCGAA UUUGUG

Appendix 8: Real-Time PCR Data

(A) 4 MiRNA Taqman MiRNA Assay Details

Assay Name	miRBase ID	miRBase Accessions	AB Assay	Target Sequence
has-miR-378	hsa-miR-378	MIMAT0000732	2243	ACUGGACUUGGAGUCAGAAGG
has-miR-92b	hsa-miR-92b	MIMAT0003218	007028_mat	UAUUGCACUCGUCCCGGCCUCC
hsa-miR-671-5p	hsa-miR-671-5p	MIMAT0003880	197646_mat	AGGAAGCCCUGGAGGGGCUGG AG
hsa-miR-1827	hsa-miR-1827	MIMAT0006767	2814	UGAGGCAGUAGAUUGAAU

(B) miR-92b of Real-Time PCR Data

Invasiveness		miR-92b Ct	RNU6 Ct	ΔCt (miR-92b Ct - RNU6 Ct)	$\Delta\Delta Ct$ (high ΔCt - low ΔCt)	Fold change (A549-I7/A549-NI7)	std dev of ΔCt	SEM	P-value
high	rep1	25.07	28.30	-3.23			0.392	0.226	0.014
	rep2	25.12	28.09	-2.97					
	rep3	25.24	28.98	-3.74					
	mean	25.14	28.46	-3.31					
low	rep1	25.5	28.14	-2.64	-0.59	1.505	0.159	0.092	
	rep2	25.48	28.09	-2.61	-0.36	1.283			
	rep3	25.57	28.64	-3.07	-0.67	1.591			
	mean	25.52	28.29	-2.77	-0.54	1.460			

(C) miR-378 of Real-Time PCR Data

Invasiveness		miR-378 Ct	RNU6 Ct	ΔCt (miR-378 Ct - RNU6 Ct)	$\Delta\Delta Ct$ (high ΔCt - low ΔCt)	Fold change (A549-I7/A549-NI7)	std dev of ΔCt	SEM	P-value
high	rep1	27.59	28.30	-0.71			0.345	0.199	0.001
	rep2	27.31	28.09	-0.78					
	rep3	27.64	28.98	-1.34					
	mean	27.51	28.46	-0.94					
low	rep1	28.27	28.14	0.13	-0.84	1.790	0.099	0.057	
	rep2	28.21	28.09	0.12	-0.90	1.866			
	rep3	28.29	28.64	-0.35	-0.99	1.986			
	mean	28.26	28.29	-0.03	-0.91	1.881			

(D) miR-671-5p of Real-Time PCR Data

Invasiveness		miR-671-5p Ct	RNU6 Ct	ΔCt (miR-671-5p Ct - RNU6 Ct)	$\Delta\Delta Ct$ (high ΔCt - low ΔCt)	Fold change (A549-I7/A549-NI7)	std dev of ΔCt	SEM	P-value
high	rep1	31.79	28.30	3.49			0.626	0.361	0.028
	rep2	31.68	28.09	3.59					
	rep3	31.44	28.98	2.46					
	mean	31.64	28.46	3.18					
low	rep1	32.06	28.14	3.92	-0.43	1.347	0.297	0.172	
	rep2	32.18	28.09	4.09	-0.50	1.414			
	rep3	32.02	28.64	3.38	-0.92	1.892			
	mean	32.09	28.29	3.80	-0.62	1.551			

(E) miR-1827 of Real-Time PCR Data

Invasiveness		miR-1827 Ct	RNU6 Ct	$\Delta\text{Ct} = (\text{miR-1827 Ct} - \text{RNU6 Ct})$	$\Delta\Delta\text{Ct} = (\text{high } \Delta\text{Ct} - \text{low } \Delta\text{Ct})$	Fold change (A549-I7/A549-NI7)	std dev of ΔCt	SEM	P-value
high	rep1	35.75	28.30	7.45			0.727	0.420	0.012
	rep2	36.96	28.09	8.87					
	rep3	36.87	28.98	7.89					
	mean	36.53	28.46	8.07					
low	rep1	33.74	28.14	5.6	1.85	0.277	0.095	0.055	
	rep2	33.83	28.09	5.74	3.13	0.114			
	rep3	33.35	28.64	4.71	3.18	0.110			
	mean	33.64	28.29	5.35	2.72	0.167			

Appendix 9: Target Prediction Data

(A) Putative Gene Targets of miRNAs using TargetScan 5.2 Algorithm

Target gene	Total context score (≤ 0.10)										
	miR-378	miR-671-5p	miR-25* †	miR-92b	miR-106b* †	miR-550* †	miR-629* †	miR-576-3p	miR-886-5p	miR-487b	miR-1827
TGFB1	-	-	N/A	-	N/A	N/A	N/A	-	-	-	-0.14
TGFB3	-	-	N/A	-	N/A	N/A	N/A	-0.14	-	-	-
TGFBR2	-	-	N/A	-	N/A	N/A	N/A	-	-	-	-0.34
SMAD2	-	-	N/A	-0.17	N/A	N/A	N/A	-	-	-0.38	-0.31
SMAD3	-	-0.26	N/A	-	N/A	N/A	N/A	-	-	-	-0.12
SMAD7	-	-0.11	N/A	-0.34	N/A	N/A	N/A	-	-	-	-
SMURF1	-	-	N/A	-0.16	N/A	N/A	N/A	-	-	-	-0.17
CDH1	-	-0.23	N/A	-0.10	N/A	N/A	N/A	-	-	-	-
WNT5A	-	-	N/A	-	N/A	N/A	N/A	-0.27	-	-	-0.20
FZD3	-	-0.27	N/A	-	N/A	N/A	N/A	-	-	-	-
VANGL1	-0.37	-	N/A	-0.59	N/A	N/A	N/A	-0.33	-	-	-0.10
DVL3	-	-0.56	N/A	-	N/A	N/A	N/A	-	-	-	-0.25
SFRP4	-	-	N/A	-	N/A	N/A	N/A	-0.22	-	-	-0.25
PRICKLE2	-	-	N/A	-0.12	N/A	N/A	N/A	-	-	-	-
PRICKLE4	-	-0.27	N/A	-	N/A	N/A	N/A	-	-	-	-
ITGB3	-	-	N/A	-	N/A	N/A	N/A	-	-	-	-0.12
ITGB8	-	-	N/A	-	N/A	N/A	N/A	-	-	-	-0.41
ARHGEF7	-	-	N/A	-	N/A	N/A	N/A	-	-	-	-0.11
PAK1	-	-	N/A	-	N/A	N/A	N/A	-	-	-	-0.22
PAK6	-	-0.21	N/A	-	N/A	N/A	N/A	-	-	-	-0.17
PAK7	-	-	N/A	-	N/A	N/A	N/A	-	-	-0.44	-
CDC42	-	-	N/A	-0.16	N/A	N/A	N/A	-	-	-	-0.18
WASF2	-	-0.10	N/A	-	N/A	N/A	N/A	-	-	-	-0.36

WASF3	-	-	N/A	-	N/A	N/A	N/A	-0.23	-	-	-
ARPC5	-	-	N/A	-	N/A	N/A	N/A	-	-	-	-0.17
LIMK1	-	-	N/A	-	N/A	N/A	N/A	-	-	-	-0.11
GRB2	-0.17	-0.21	N/A	-	N/A	N/A	N/A	-	-	-	-0.35
HIF1A	-	-	N/A	-	N/A	N/A	N/A	-0.24	-	-	-
SUFU	-0.14	-	N/A	-	N/A	N/A	N/A	-	-	-	-0.22

[†]TargetScan 5.2 algorithm do not predicts miRNA* (miR-25*, miR-106b*, miR-550* and miR-629*).

(B) Putative Gene Targets of miRNAs using DIANA-microT 4.0 algorithm

Target gene	miTG score (≥ 0.10)										
	miR-378	miR-671-5p	miR-25*	miR-92b	miR-106b*	miR-550*	miR-629*	miR-576-3p	miR-886-5p	miR-487b	miR-1827
TGFB3	-	-	-	-	-	0.212	0.291	-	-	-	-
TGFBR2	-	0.377	-	-	-	-	-	0.214	-	-	0.445
SMAD2	-	-	-	-	-	0.217	0.230	-	-	-	0.365
SMAD3	-	0.409	-	-	-	-	-	-	-	-	-
SMAD7	-	0.431	-	-	-	-	-	-	-	-	-
SMURF2	-	-	-	-	-	0.218	-	-	-	-	-
CDH1	0.220	-	-	0.224	-	-	-	-	-	-	-
WNT5A	0.287	0.206	-	0.415	-	-	-	0.381	-	-	-
FZD3	-	-	-	-	-	-	0.226	0.248	-	-	-
VANGL1	0.416	-	-	-	-	0.208	0.362	0.292	-	-	-
DVL3	-	0.493	-	-	-	-	-	-	-	-	0.311
DAAM1	-	-	-	0.472	-	-	0.205	0.539	-	-	-
SFRP4	-	0.238	-	-	-	-	-	0.419	-	-	-
PRICKLE2	-	0.244	-	0.203	-	0.216	0.284	0.203	-	-	-
ITGA3	-	-	-	-	-	-	-	-	0.233	-	-
ITGA6	-	-	-	-	-	-	-	-	-	0.471	-
ITGB3	-	-	-	0.348	-	-	-	-	-	-	-
ITGB8	-	0.225	-	0.235	-	0.214	0.235	-	-	-	0.378
PAK1	-	0.316	-	-	-	-	0.386	-	-	-	0.430
PAK6	-	-	-	-	-	-	-	0.231	-	-	0.419
PAK7	-	-	-	-	-	-	0.326	0.215	-	0.429	-
CDC42	-	-	-	-	-	-	0.362	-	-	-	0.324
WASF3	-	0.212	-	-	-	-	-	0.224	-	-	-
LIMK1	-	-	-	-	-	-	-	-	-	-	0.326
GRB2	0.414	0.338	-	-	-	-	-	-	-	-	-

MAPK14	-	-	-	-	-	-	0.579	-	-	-	-
MAPK13	-	-	-	-	-	-	0.346	-	-	-	-
PIK3R5	-	-	-	-	-	-	0.334	-	-	-	-
PIK3R2	-	-	-	-	-	-	-	-	0.247	-	-
PIK3C2A	-	-	-	-	-	-	-	-	-	0.332	-
HIF1A	-	-	-	-	-	-	-	0.434	-	-	-